

This Page Is Inserted by IFW Operations  
and is not a part of the Official Record

## **BEST AVAILABLE IMAGES**

Defective images within this document are accurate representations of the original documents submitted by the applicant.

Defects in the images may include (but are not limited to):

- BLACK BORDERS
- TEXT CUT OFF AT TOP, BOTTOM OR SIDES
- FADED TEXT
- ILLEGIBLE TEXT
- SKEWED/SLANTED IMAGES
- COLORED PHOTOS
- BLACK OR VERY BLACK AND WHITE DARK PHOTOS
- GRAY SCALE DOCUMENTS

IMAGES ARE BEST AVAILABLE COPY.

**As rescanning documents *will not* correct images,  
please do not report the images to the  
Image Problems Mailbox.**



PATENT APPLICATION

1657  
RECEIVED  
JUL 02 2002  
TECH CENTER 1600/2800

IN THE UNITED STATES PATENT AND TRADEMARK OFFICE

In re Application of : Alexandre MARTI, Norbert LANGE, Matthieu  
ZELLWEGER, Georges WAGNIERES, Hubert  
VAN DEN BERGH, Patrice JICHLINSKI and  
Pavel KUCERA  
Serial no. : 09/673,871  
Filed : with an effective filing date April 22, 1999  
For : SOLUTION FOR DIAGNOSING OR TREATING  
TISSUE PATHOLOGIES  
Group Art Unit : 1617  
Examiner : Shahnam JI Sharareh  
Docket : NITROS P146US

#10  
HKO  
10/17/02

The Commissioner of Patents and Trademarks  
Washington, D.C. 20231

**SUPPLEMENTAL RESPONSE**

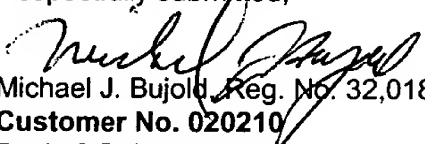
Dear Sir:

[XXX] NO FEES ARE PAYABLE WITH RESPECT TO THIS RESPONSE.

Further in response to the official action mailed March 27, 2002 and the response filed June 27, 2002, enclosed please find a copy of the references 1-8 which are referred to in the previously filed response.

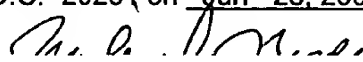
In the event that there are any fee deficiencies or additional fees are payable, please charge the same or credit any overpayment to our Deposit Account (Account No. 04-0213).

Respectfully submitted,

  
Michael J. Bujold, Reg. No. 32,018  
Customer No. 020210  
Davis & Bujold, P.L.L.C.  
Fourth Floor  
500 North Commercial Street  
Manchester NH 03101-1151  
Telephone 603-624-9220  
Facsimile 603-624-9229  
E-mail: [patent@davisandbujold.com](mailto:patent@davisandbujold.com)

**CERTIFICATE OF MAILING**

I hereby certify that this correspondence is being deposited with the United States Postal Service, with sufficient postage, as First-Class Mail in an envelope addressed to: Commissioner of Patents and Trademarks, Washington, D.C. 20231 on Jun 28, 2002.



# OPTIMISATION OF THE FORMATION AND DISTRIBUTION OF PROTOPORPHYRIN IX IN THE UROTHELIUM: AN IN VITRO APPROACH

A. MARTI, N. LANGE, H. VAN DEN BERGH, D. SEDMERA, P. JICHLINSKI AND P. CHANCEK\*

From the Institute of Physiology, Faculty of Medicine, University of Lausanne, the Federal Institute of Technology, and the Service of Urology, University Hospital, Lausanne, Switzerland

## ABSTRACT

**Purpose:** To optimize conditions for photodynamic detection (PDD) and photodynamic therapy (PDT) of bladder carcinoma, urothelial accumulation of protoporphyrin IX (PpIX) and conditions leading to cell photodestruction were studied.

**Materials and Methods:** Porcine and human bladder mucosae were superfused with derivatives of 5-aminolevulinic acid (ALA). PpIX accumulation and distribution across the mucosa was studied by microspectrofluorometry. Cell viability and structural integrity were assessed by using vital dyes and microscopy.

**Results:** ALA esters, especially hexyl-ALA, accelerated and regularized urothelial PpIX accumulation and allowed for necrosis upon illumination.

**Conclusions:** hexyl-ALA used at micromolar concentrations is the most efficient PpIX precursor for PDD and PDT.

**KEY WORDS:** aminolevulinic acid, photodynamic detection, photodynamic therapy, urinary bladder, cancer, in vitro

Urinary bladder tumors show an increasing incidence in man after the sixth decade. They consist mainly of superficial transitional carcinomas and are characterized by frequent recurrence and/or risk to progress toward invasive tumors.<sup>1</sup> This is linked to their frequent multifocal character and concomitant presence of high grade dysplasia (DYS) centers and/or carcinomas in situ (CIS).<sup>2</sup>

The treatment of superficial bladder tumors is based mainly on endoscopic resections combined with chemo- or immunotherapy by intravesical installation. While the use of BCG is likely to modify the recurrence profile of the illness, reduce the risk of progression and improve the survival,<sup>3</sup> the resistance to BCG of certain tumoral bladders and decrease of vesical compliance resulting from repetitive treatments remain therapeutic problems.

As an alternative, photodynamic therapy (PDT) aims at destroying malignant cells by inducing cytotoxic reactions which result from interaction of light with photosensitive endo- or exogenous compounds, often preferentially accumulating in the target tissues. This concept led to development of several oncological treatments, for example, in dermatology, otorhinolaryngology, gastrology, ophthalmology and gynaecology.

In urology, where the main indication for PDT is multi-recurrent superficial bladder cancer resistant to BCG treatment, PDT has received only marginal interest because the first generation photosensitizers did not localize with sufficient selectivity in neoplastic tissues and induced skin photosensitivity after systemic administration. Recently, interest in PDT of bladder cancers has been renewed by demonstration of the selectivity of protoporphyrin IX (PpIX) induced after instillation of 5-aminolevulinic acid (ALA). PpIX is an intermediate of the cycle of heme synthesis (fig. 1) and its intracellular content can be significantly increased when the regulatory step of the cycle is bypassed by exposing the tissue to a precursor, for instance 5-aminolevulinic acid (ALA).<sup>4</sup> In addition, PpIX accumulates at much higher con-

centrations in malignant than in normal cells due to the reduction of ferrochelatase and iron deficiency in tumors.<sup>5</sup>

The results obtained by PDT in skin tumors<sup>6</sup> suggested that a similar approach might be used in urology. While the diagnosis of CIS and DYS is difficult or impossible during cystoscopy using white light, fluorescence cystoscopy after intravesical administration of 3% ALA solution often allows us to detect and define with precision the limits of DYS and CIS.<sup>7,8</sup> The sensitivity and specificity of photodynamic detection (PDD) approach 80%. The preferential accumulation of PpIX in the transformed urothelium,<sup>9</sup> the intravesical tolerance of ALA solutions adjusted to physiological pH values, and the absence of systemic effects reinforce the interest of such an approach.

A complete destruction of a tumor by PDT critically depends on a sufficiently high concentration and homogeneous distribution of PpIX in the malignant cell layers.<sup>10</sup> Although relatively high ALA concentrations were instilled into the bladder for many hours, fluorescence microscopy showed a rather irregular distribution of PpIX within superficial tumors of the bladder.<sup>11</sup> Also, the conditions for reaching the threshold of phototoxicity in the urothelium are not exactly known. This is not surprising as a double charged molecule like ALA is not expected to penetrate with ease across cell membranes and interstitial spaces. More lipophilic derivatives of ALA are expected to be more favored from this point of view. After traversing the cellular membrane non-specific esterases will reduce such compounds to 5-ALA. Dimethylsulfoxide (DMSO) and desferrioxamine (DES) have been

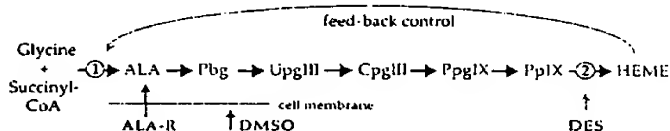


**FIG. 1.** Simplified scheme of heme biosynthesis and interventions used. ALA: 5-aminolevulinic acid; ALA-R: esters of ALA; Pbg: porphobilinogen; UpgIII: uroporphyrinogen III; CpgIII: coproporphyrinogen III; PpgIX: protoporphyrinogen IX; PpIX: protoporphyrin IX. 1: ALA synthase; 2: ferrochelatase + Fe<sup>++</sup>. DMSO: dimethylsulfoxide; DES: desferrioxamine. Gray arrows: inhibitory effects.

Accepted for publication November 8, 1998.

\* Requests for reprints: Institut de Physiologie, Université de Lausanne, Rue Bugnon 7, 1005 Lausanne, Switzerland.

Supported by grant 17 from the Geneva-Vaud Foundation and the Deutsche Forschungsgemeinschaft (DFG), Bonn, Germany.

# UROTHELIAL ACCUMULATION OF PROTOPORPHYRIN IX

and to enhance PpIX accumulation. DMSO increases the transmembrane passage of small molecules.<sup>12</sup> DES, chelates the intracellular iron and hence inhibits the ferrochelatase activity. Consequently, PpIX is not converted into heme (fig. 1) and accumulates in cells.<sup>5</sup>

Thus, to define standardized and optimal conditions for PDD and PDT, a systematic study of the penetration of ALA derivatives into cells, the kinetics of PpIX accumulation, intra-urothelial PpIX distribution and mechanisms of cell photodestruction is mandatory. As a first approach to this problem, we developed an experimental setup allowing us to answer some of these questions by using bladder mucosae explanted in vitro. Here we present the kinetics and tissue profiles of intracellular PpIX accumulation, and data about phototoxicity obtained in pig or human urothelium exposed to ALA, its esters, and ALA with DMSO or DES.

## MATERIALS AND METHODS

**Preparation of bladder mucosa.** The study required living urothelium obtained under controlled conditions. Porcine urothelium resembles human urothelium structurally<sup>13</sup> and can be obtained easily and reproducibly. Porcine bladders were excised from slaughtered animals. Pieces of human bladder wall were obtained from patients undergoing radical

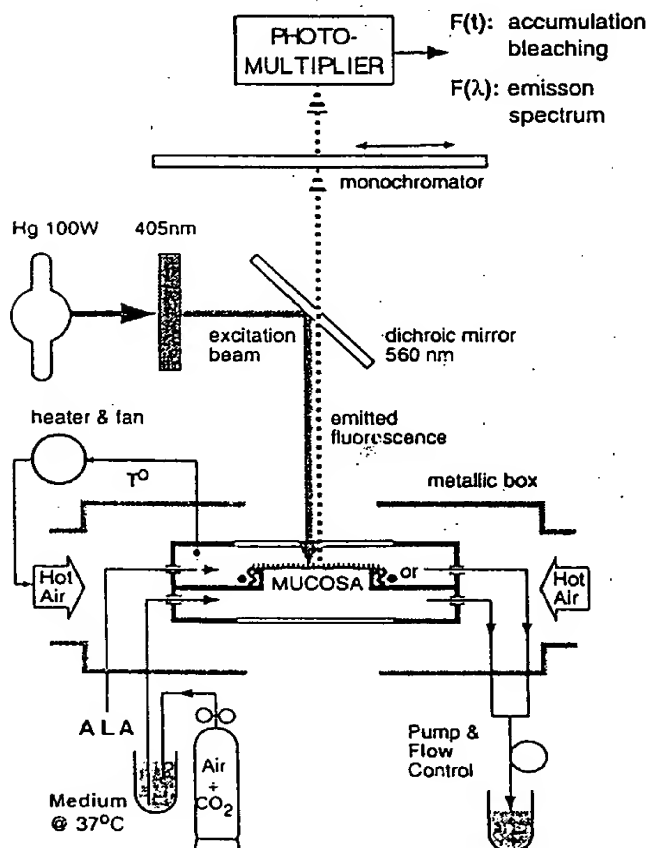


FIG. 2. Microspectrophotometry of protoporphyrin IX in bladder mucosa. Bladder mucosa is placed over and around circular rim of perspex plate and fixed with thin silicone O-ring (or). Preparation is mounted into transparent chamber and incubated in presence of ALA derivatives. Mucosa is periodically excited (100W mercury lamp, Eppendorf filter 405 nm (FWHM: 12 nm), 200 msec exposure,  $45 \pm 5 \mu\text{W}/(0.05 \text{ mm}^2)$ ) and fluorescence emitted by cells is recorded by using EMI 20 photomultiplier. Motorized monochromator (continuous interference filter Veril, Leitz) allows analysis of emission spectrum.

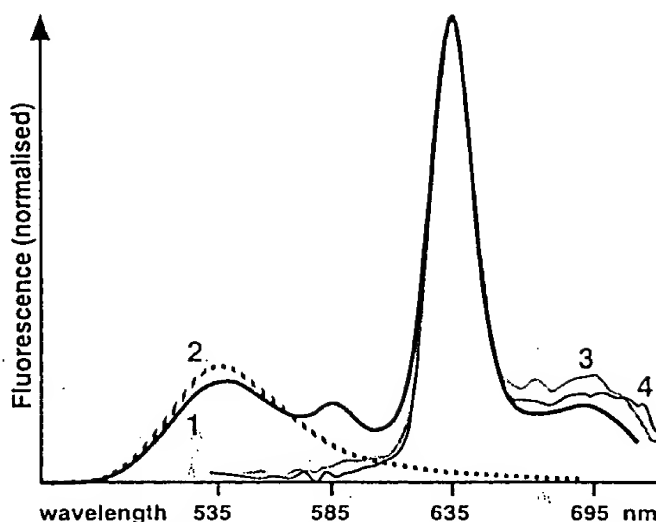


FIG. 3. Specificity of fluorescence signal. Four emission spectra as obtained from living mucosae and from frozen sections of urothelium. 1, living mucosa preincubated for 2 hours with ALA. 2, same mucosa after 10 minutes illumination. 3 and 4, urothelial sections incubated with ALA+DES and H-ALA, respectively. Spectra 1, 3 and 4 show identical peaks around 635 and 690 nm corresponding to PpIX accumulated in urothelium. In spectrum 2, PpIX signals disappeared leaving only tissue autofluorescence. Note that emission peak at 670 nm of curve 3 is due to photooxidation products of PpIX.

cystectomy for advanced carcinoma (3 males, 1 female; average age  $73 \pm 6$  years). Resected bladders were opened and de visu normal and flat areas were taken for experiments. All these manipulations took about 45 minutes. Normality was confirmed by histology. The protocols were approved by the state commissions controlling animal experiments and clinical research.

The tissues were stored at 4°C in Tyrode solution. The urothelium was microdissected from the bladder wall using fine scissors. The plane of cleavage passed as near as possible to the basal membrane so that thin sheets of urothelium with remnants of lamina propria connective tissue were obtained.

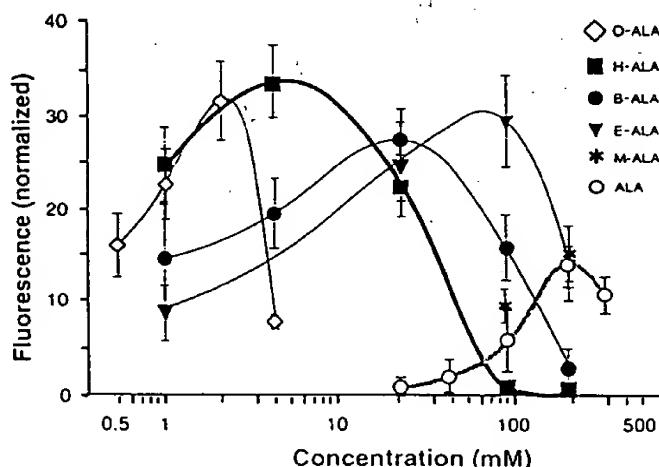


FIG. 4. PpIX kinetics for different precursors. O-ALA and H-ALA are most efficient precursors tested: at concentration 100 times lower than that of ALA, they induce 2 to 3 times higher PpIX accumulation. Determinations are made after 1 hour of incubation. Values are means  $\pm$  S.D. from 20 measurements (4 mucosae per condition, 5 measurements in each mucosa). Values for M-ALA, determined at 90 and 180 mM only, were  $9.4 \pm 1.8$  and  $15 \pm 3$  respectively.

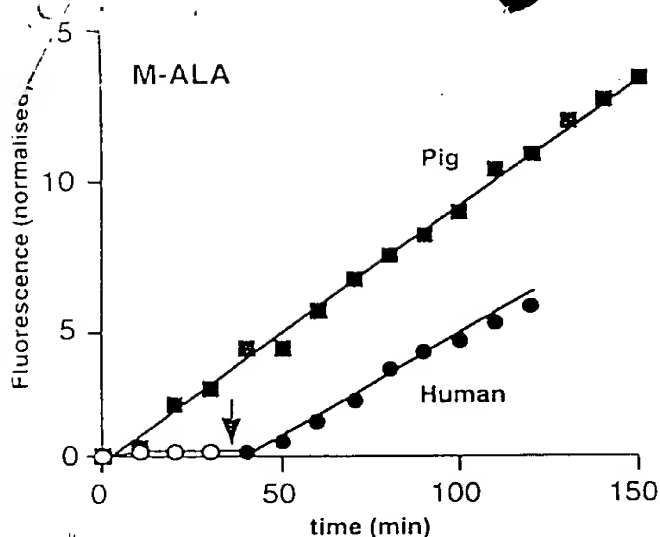


FIG. 5. Comparison of PpIX fluorescence in pig and human mucosae. During first 3 hours of incubation fluorescence increase is nearly linear in pig mucosa. Pig mucosa accumulates PpIX faster ( $F = 0.082 \text{ min}^{-1}$ ,  $r^2 = 0.99$ ) than human mucosa ( $F = 0.062 \text{ min}^{-1}$ ,  $r^2 = 0.98$ ). PpIX fluorescence is only observed when human mucosa is warmed up. M-ALA was administered at time 0. Arrow: warming of human mucosa; empty circles: human mucosa at 23°C; full symbols: mucosae at 36°C.

These were cut into  $7 \times 7 \text{ mm}$ . fragments which were mounted (urothelium up) in a transparent culture chamber designed for epithelia<sup>14</sup> as illustrated in fig. 1. The mucosa divided the chamber into superior and inferior compartments (diameter 20 mm., height 3 mm.) and the area exposed to exchanges was  $0.125 \text{ cm}^2$ . The chamber was fixed onto the plate of an epi-illumination microscope (Leitz Orthoplan) and thermostabilised at  $36 \pm 0.5^\circ\text{C}$ . The inferior compartment was continuously perfused by oxygenated Tyrode solution. Solutions of ALA derivatives were injected as a single dose into the superior compartment.

**Media.** The Tyrode solution contained (in mmol/l.):  $143.0 \text{ Na}^+$ ,  $2.0 \text{ K}^+$ ,  $0.8 \text{ Mg}^{++}$ ,  $1.4 \text{ Ca}^{++}$ ,  $122 \text{ Cl}^-$ ,  $20.0 \text{ HCO}_3^-$ ,  $3 \text{ H}_2\text{PO}_4^-$ ,  $1.2 \text{ SO}_4^{--}$ , 8 glucose (osmolarity 290 mOsm/l.) and was saturated with air enriched with 5%  $\text{CO}_2$  (pH 7.5). ALA and some of its derivatives were dissolved in phosphate buffer saline at 4°C, and the pH was adjusted to  $5.2 \pm 0.5$ . Dimethylsulfoxide (DMSO) ( $17.5 \mu\text{M}$ ) and desferrioxamine mesylate (DES) ( $15 \mu\text{M}$ ) were added to some solutions. All solutions were colorless. They were stored on ice and used within one hour.

ALA was from Merck (Dietikon, Switzerland), methyl-ester

(M-ALA) and DES were from Fluka (Buchs, Switzerland). Ethyl-(E-ALA), butyl-(B-ALA) hexyl-ester (H-ALA) and octyl-ester (O-ALA) were synthesized.<sup>15</sup> Their purity was superior to 95%.

**Spectrofluorometry.** The kinetics of urothelial PpIX accumulation with respect to precursor concentration and to time of administration were characterized as follows (fig. 1). The urothelium, incubated with a given precursor, was excited by violet light ( $405 \text{ nm}$ ,  $45 \pm 5 \mu\text{W}/0.05 \text{ mm}^2$ , 200 ms) each 10 minutes or each hour and the fluorescence emitted by the cells, which is taken to be proportional to the cell PpIX concentration, was passed through a low pass filter ( $>610 \text{ nm}$ ) and recorded by a photomultiplier. The specificity of the fluorescence signal was systematically checked by analyzing the emission spectra.

The spatial distribution of PpIX across the mucosa was determined at selected time intervals in serial  $25 \mu\text{m}$ . thick frozen sections. To avoid strong photobleaching due to light exposure, the samples were prepared in the dark. The profiles of PpIX fluorescence within the mucosa were determined by scanning the fluorescence signal across the section.

**Cell viability.** At the end of experiments, the urothelium was exposed to acridine orange (dissolved in Tyrode 1:10000) which stains nuclei of living cells only. The proportion of labeled nuclei was evaluated by fluorescence microscopy (excitation at  $405 \text{ nm}$ , emission  $> 560 \text{ nm}$ ). In some cases, the time-course of PpIX photodestruction (photobleaching) was determined and the consequent phototoxicity effects on urothelial cell were studied by using electron microscopy. Two hours after the exposure to light, the mucosae were fixed in paraformaldehyde/glutaraldehyde and embedded in Epon. Sections of  $700 \text{ \AA}$  were analyzed by transmission microscopy (Zeiss, Germany). Some mucosae were dehydrated and dried (CPD 030 critical point dryer, Balzers, Liechtenstein), coated with  $300 \text{ nm}$  gold (S150 sputter coater, Edwards, Zivvy, Basle) and studied by using scanning electron microscope (JEOL, Tokyo).

**Statistical analysis.** Supposing that the photobleaching of endogeneous chromophores is small, fluorescence values were normalized, that is, corrected for the tissue autofluorescence [ $I_n(t) = (I_n(t) - AF)/AF$ ]. The data are presented as arithmetical means and standard deviations. A paired bilateral  $t$  test was used to compare the results and values of  $p \leq 0.05$  were considered as significant.

## RESULTS

**Nature of the fluorescence signal.** The spectral analysis of the light emitted by the mucosa shows that, in the absence of PpIX precursors, the tissue emits weak autofluorescence giving a very small signal in the red domain ( $\geq 610 \text{ nm}$ ). This signal serves to normalize the specific PpIX fluorescence. The latter appears in presence of PpIX precursors as one major

Pp IX accumulation in urothelium in response to ALA derivatives

Precursor	Hours of Administration						
	1	2	3	4	5	6	7
ALA	$17 \pm 7$	$31 \pm 7$	$41 \pm 6$	$54 \pm 9$	$64 \pm 7$	$67 \pm 10$	$65 \pm 12$
ALA+DMSO	$14 \pm 3$	$36 \pm 8$	$57 \pm 17$	$75 \pm 17$	$90 \pm 18$	$90 \pm 18$	$87 \pm 31$
M-ALA	$15 \pm 3$	$35 \pm 5$	$53 \pm 5$	$69 \pm 9$	$82 \pm 13$	$94 \pm 14$	$91 \pm 20$
M-ALA+DMSO	$18 \pm 3$	$42 \pm 5$	$63 \pm 9$	$79 \pm 11$	$97 \pm 14$	$115 \pm 13$	$114 \pm 17$
ALA+DES	$21 \pm 2$	$48 \pm 11$	$81 \pm 13$	$117 \pm 14$	$157 \pm 36$	$193 \pm 50$	$256 \pm 27$
B-ALA	$27 \pm 3$	$61 \pm 7$	$100 \pm 14$	$134 \pm 26$	$163 \pm 28$	$156 \pm 27$	$144 \pm 25$
H-ALA	$34 \pm 4$	$67 \pm 6$	$105 \pm 12$	$134 \pm 20$	$167 \pm 27$	$175 \pm 26$	$189 \pm 37$
H-ALA+DES	$32 \pm 3$	$62 \pm 5$	$98 \pm 4$	$126 \pm 10$	$153 \pm 7$	$172 \pm 8$	$170 \pm 16$

Ed: Table  
as wanted?

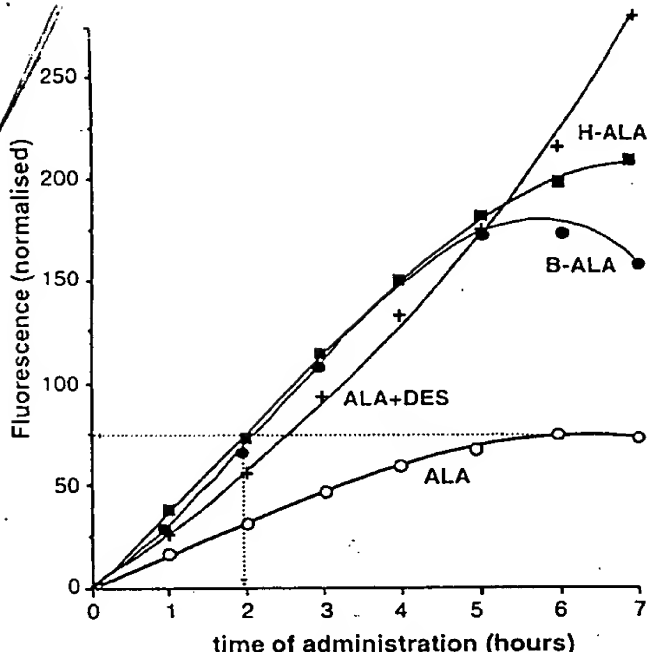


FIG. 6. PpIX accumulation with ALA, ALA+DES, B-ALA and H-ALA. H-ALA, although administered at much lower, and hence less toxic concentration, can considerably shorten time of administration (dotted lines), allowing both rapid and efficient PDD and PDT. (ALA and ALA+DES: 700 mOsm; H-ALA: 290 mOsm). Values are means extracted from table.

(635 nm) and one minor (690 nm) peak (fig. 3). No differences were observed between the emission spectra shape of pure ALA- and ALA-esters-induced PpIX. The PpIX peaks disappear after exposure of the mucosa to light.

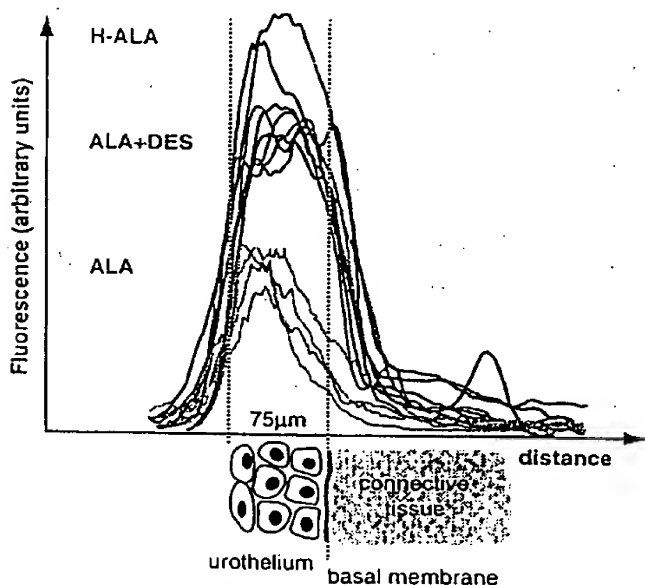


FIG. 7. Fluorescence intensity as measured across bladder mucosa. H-ALA allows highest and most homogeneously distributed PpIX accumulation in urothelium. Data from 12 fluorescence scans across mucosal sections were corrected to mean urothelial thickness. Scanning speed 100 mm/sec.; excitation at 405 nm.; width of illuminated slit 30 µm.; emission at 610 nm.

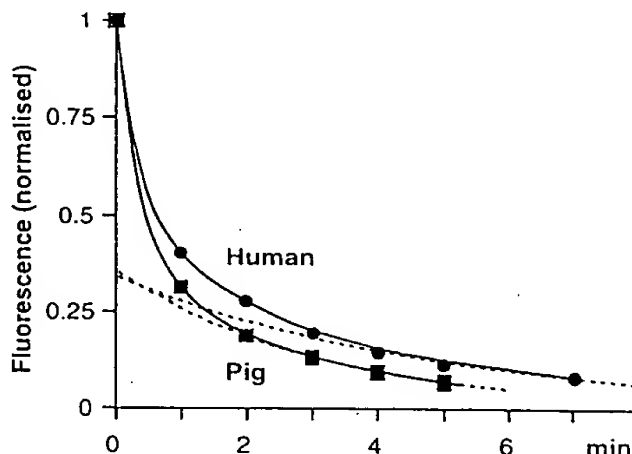


FIG. 8. Photosensitivity of fluorescence signal. Time-course of photobleaching of PpIX upon continuous illumination (405 nm, 4.75 J/cm²) of mucosa. Photobleaching appears to show fast and slow phases. Residual signal corresponds to autofluorescence.

*Effect of PpIX precursor concentration.* Fig. 4 illustrates the results obtained for ALA and its esters after 1 hour of incubation. All precursors show similar kinetics: with increasing concentration, the fluorescence intensity increases, reaches a maximum and then decreases sharply. As compared with ALA, the applied concentrations of E-ALA, B-ALA, H-ALA and O-ALA are respectively 2, 10, 45 and 90 times lower, but nevertheless result in 2 to 2.5 times higher fluorescence.

The reduction of fluorescence at high concentrations may indicate significant cytotoxicity of ALA esters which resulted in peeling of the mucosa (as with ALA at 180 mM), or even immediate cellular lysis (as with H- and B-ALA at 180 mM) (not shown). Due to its higher lipophilicity, precipitation of O-ALA in aqueous solutions at high concentrations may reduce the total drug content.

*Accumulation of PpIX in the mucosa.* Both the pig and human mucosae exposed to precursors accumulate PpIX, after warming to 37°C, that is, upon metabolic activation. This is illustrated in fig. 5 which shows an example of human mucosa with an accumulation ratio comparable to that of pig mucosa. However, on the average, the human mucosae (n = 4, 3 males, 1 female, mean age 52 years) accumulated PpIX 3.6 times less than the pig mucosae.

The table shows the results obtained in the pig mucosae with ALA derivatives used at their respective optimal concentrations. In all cases, the fluorescence increased nearly linearly up to four hours and saturated between the 6th and 7th hours. With ALA+DES, the fluorescence continued to increase exponentially up to 7 hours. ALA was the least efficient of the tested precursors. The other substances induced a significantly faster and greater (1.3 to 3 times) increase of PpIX fluorescence. H-ALA and ALA+DES were the most efficient, but H-ALA and B-ALA were shown to reach the highest fluorescence at the shortest administration times (table, fig. 6). No significant difference in PpIX formation was observed between H-ALA and B-ALA used at their optimal concentrations. This indicates that the biosynthetic pathway of heme was saturated by the more lipophilic esters, while PpIX production induced by pure ALA never reached sufficiently high intracellular drug contents.

Iso-osmolar replacement of sodium in the Tyrode solution by choline did not modify the accumulation kinetics of PpIX (not shown) indicating that the penetration of ALA derivatives into the cell does not involve a sodium-dependent co-transport.

At the end of each experiment (24 mucosae, 7 hours of

incubation, 8 precursors at their optimum concentration), on labeling with acridine orange, all preparations showed cells with bright nuclear fluorescence, indicating that the urothelium remained alive.

**Distribution of PpIX across the mucosa.** The fluorescence profiles across the mucosae were recorded after 2 hours of incubation with ALA, H-ALA and ALA+DES. As the thickness of urothelium varied (from 66 to 88  $\mu\text{m}$ ), the results are presented after a homothetic translation to 75  $\mu\text{m}$ . As shown in fig. 7, PpIX fluorescence induced by the 3 precursors is limited essentially to the urothelial cells. With ALA, the fluorescence is limited mostly to the superficial cells while with ALA+DES and especially H-ALA, the fluorescence is about twice as high and distributed in all urothelial layers.

**Phototoxicity.** If the mucosa accumulating PpIX is exposed to continuous violet illumination for 10 minutes, the urothelial fluorescence decays. Supposing an exponential decay with time, the two rate constants are of about 30 seconds and 3 minutes (fig. 8). This time dependence of the fluorescence signal may be due to more stable photoporphyrins formed by photodegradation of PpIX. After 10 minutes of illumination, the

specific fluorescence is no longer detectable which indicates that most fluorescing porphyrins were destroyed.

When the mucosae illuminated for 10 minutes were incubated for 2 additional hours, the cells that had been exposed to light died. This was documented by electron microscopy (fig. 9) which revealed damaged mitochondria, marginalisation of nuclear chromatin, vacuolised cytosol and fenestration of the plasma membrane. The superficial cells were rounded and lost contact with each other. In mucosae preincubated for shorter times (for example, ALA, 2 hours), the necrotic changes were found mostly in the superficial cells. In mucosae preincubated for longer times (for example, ALA, 6 hours) the urothelial necrosis was complete while the underlying connective tissue was not damaged. The necrosis induced by violet light was confined to the illuminated area and was surrounded by normal cells (fig. 9).

F9

#### DISCUSSION

The use of bladder mucosa explanted into a superfusion chamber is a powerful tool which, unlike cell cultures, per-

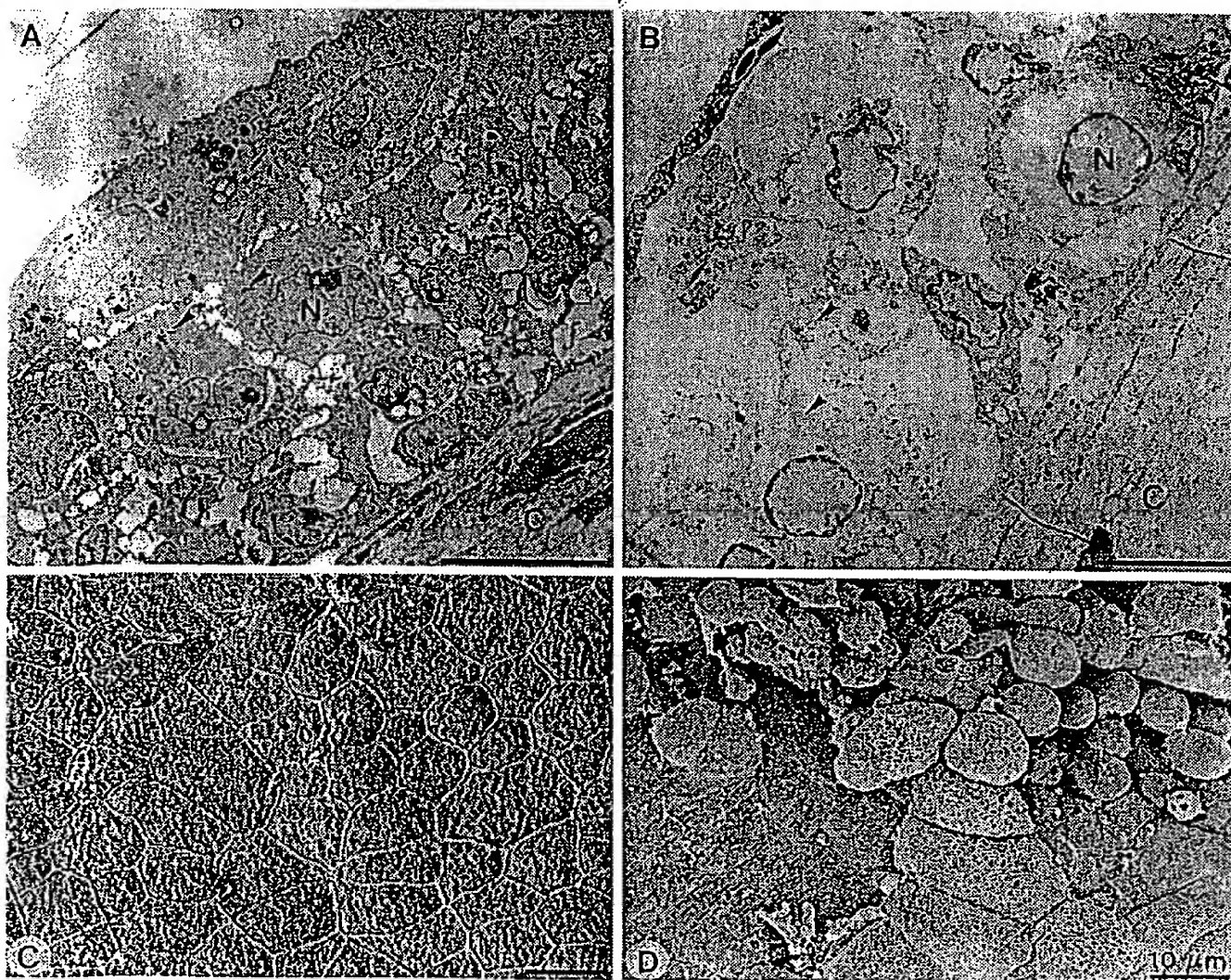


FIG. 9. Urothelial necrosis induced in bladder mucosae by exposure to light. Transmission (A, B) and scanning (C, D) electron micrographs of bladder mucosae incubated for 6 hours with ALA. A, C, control mucosae with normal intra- and intercellular structure. B, D, mucosae exposed to light (105 nm, 4.75 J/cm<sup>2</sup>, 10 minutes) and incubated for 2 additional hours, showing marginalized chromatin, swollen mitochondria, vacuolized cytoplasm, fenestrated plasma membrane and lost intercellular contacts. Arrows: mitochondria, N: nuclei, C: connective tissue. Bars: 10  $\mu\text{m}$ .



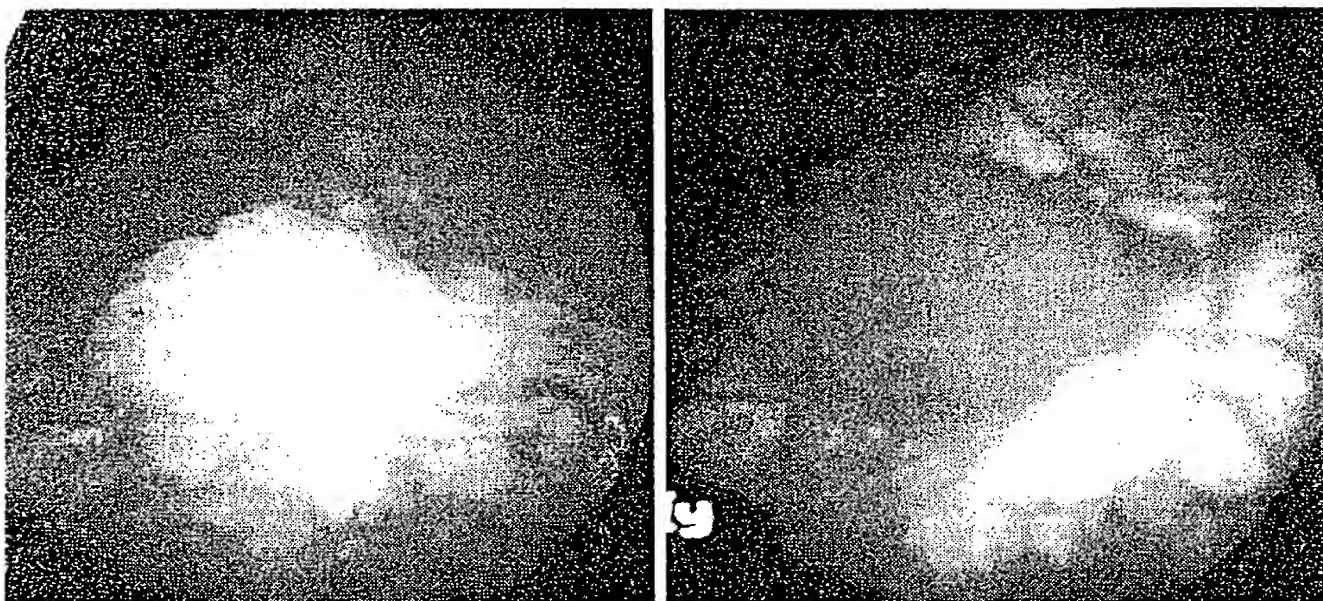


FIG. 10. Endoscopic view of human bladder papilloma. Left: image in white light. Dimension of tumor is  $4 \times 8$  mm. Right: image in the violet light after instillation of hexyl-ALA (8 mM) for 2 hours. Highly fluorescent tumoral cells (red) appearing on background of non-fluorescent (green) normal tissue. Histological diagnosis: pTaG1. (With permission.<sup>24</sup>)

ants the study of epithelia with intact architecture and functional polarity. This is especially valuable for evaluation of penetration of substances into the normal as well as pathological epithelia. Although the blood circulation is eliminated in this preparation, the renewal of submucosal medium secures the homeostasis and survival of urothelial cells.

Urothelium of pig and human origins has a very similar structure although surface proteoglycans are not identical and mucus cells are absent in the normal human bladder.<sup>13</sup> In our hands, both mucosae also show similar accumulation kinetics although the final fluorescence intensity in the human case is lower. This reflects possibly decreased cell viability due to unavoidable and long (about 2 hours) hypoxia resulting from early vascular ligation during the bladder preparations.

The synthesis of supplemental PpIX must be preceded by penetration of the precursor across the plasma membrane. Three results strongly suggest that the precursors penetrate into the cells by simple diffusion:<sup>1</sup> esters with the longer aliphatic moiety (hence more lipophilic) penetrate faster and to a greater extent,<sup>2</sup> similar kinetics of PpIX formation for L-ALA (4 mM) and D-ALA (20 mM) as well as comparable fluorescence levels under optimized concentrations suggesting a passive, concentration gradient driven uptake as predicted by simple diffusion laws,<sup>4</sup> and absence of sodium in the solutions does not decrease the PpIX accumulation as would be expected for a sodium-linked co-transport frequently operating for amino-acid cell transport. This is in agreement with results obtained in cell cultures.<sup>16</sup>

Once inside the cell, the esters of the ALA are hydrolyzed by non-specific cell esterases and free ALA appears in the cytoplasm.<sup>16</sup> The cell fluorescence will, however, increase only upon metabolic activation in the mitochondria, which confirms that PpIX synthesis is an energy-dependent process (Fig. 5).

Whatever the precursor used, the time profiles of accumulation are similar: with increased concentration, the synthesis of PpIX increases to a maximum and then decreases to zero. Similar results were obtained in cell cultures.<sup>16</sup> In our case, the final decrease is accompanied by a loss of cell fluorescence and presence of free cells floating in the superfu-

sate. This might be due to the hypertonicity of the solutions<sup>17</sup> (fig. 4) and/or to the toxicity of ALA itself. Indeed, the cells also peel off in presence of diluted but highly penetrant precursors such as H-ALA where the resulting high cytoplasmic ALA concentration might favor the production of oxygen reactive radicals<sup>18</sup> and subsequent cell injury.

PpIX fluorescence increases essentially linearly up to 4 hours and then attains a plateau value or even slightly decreases. Similar results were found in cell cultures from tumoral bladders and in rat urothelium *in vivo*.<sup>19-21</sup> It is possible that this plateau reflects not only the balance between PpIX synthesis and PpIX utilization, which should happen with all precursors, but also the penetration of precursors into deeper lying cells, which should increase with liposolubility of the ALA esters, and appears to be shown by the fluorescence profiles. The observed dependence of decreasing optimal concentration with increasing chain length of the ALA derivatives has been confirmed in cell cultures.<sup>16</sup> O-ALA at higher concentrations shows a tendency to precipitate at physiological pH values which limits its clinical use.

Clearly, DMSO, which is supposed to increase the membrane permeability, potentiates the PpIX accumulation under our conditions much less than the esterification of ALA. DES, a selective iron chelator, when combined with ALA, inhibited the conversion of PpIX to heme and thus potentiated PpIX accumulation to higher levels and before a plateau was reached. This suggests that the synthesis of PpIX in itself was not slowed down in any of the conditions used. Surprisingly, DES showed no potentiation when combined with H-ALA. The explanation of this result awaits new experiments.

The photobleaching curves show a fast and a slow component, which might result from the bleaching of fluorescent photooxidation products, originating in different intracellular compartments.<sup>22</sup> A mixture of isomeric chlorins resulting from the first photodegradation process of PpIX has been shown to be about 10 times more stable to photooxidation than PpIX.<sup>23</sup> Their appearance may be seen from the fluorescence emission peak at 670 nm (fig. 3, curve 3). Our results show that 10 minutes exposure to light is sufficient to induce cell necrosis in all layers of a normal urothelium. In



no records of photobleaching could help to dose the radiation energy necessary to destroy the tumoral tissue.

# CONCLUSIONS

The in vitro preparation of bladder mucosa developed in this work has brought additional valuable information on the dynamics of accumulation and destruction of photosensitive molecules used in the PDD and PDT of urothelial carcinoma. In the case of PpIX, H-ALA seems to be a good compromise between lipophilicity, solubility and performance with respect to high PpIX formation and low precursor concentration. In comparison with ALA, it increases and accelerates the PpIX synthesis, penetrates into all epithelial cell layers, and is efficient at low concentrations. At these low concentrations it preserves urothelial viability and allows effective cell photodestruction. The optimal time necessary for PDD and PDT at the conditions applied is shortened from near 6 to 1.5 hours. As shown in fig. 10, under these conditions applied on humans, PDD results confirm the predictions and show effective accumulation of PpIX in urothelial carcinoma.

**Acknowledgments.** We thank C. Verdan for help with electron micrographs and Dr. G. Wagnières for valuable discussions.

# REFERENCES

1. Abel, P. D.: Follow-up of patient with superficial transitional cell carcinoma of the bladder: the case for a change in policy. *Br. J. Urol.*, 72: 135, 1993.
2. Raghavan, D., Shipley, W. U., Garnick, M. B., Russell, P. J. and Richie, J. P.: Biology and management of bladder cancer. *N. Engl. J. Med.*, 322: 1129, 1990.
3. Lamm, D. L.: BCG in perspectives: advances in the treatment of superficial bladder cancer. *Eur. Urol.*, 27: 2, 1995.
4. Kennedy, J. C. and Pottier, R. H.: Endogenous protoporphyrin IX, a clinical useful photosensitizer for photodynamic therapy. *J. Photochem. Photobiol. B: Biol.*, 14: 275, 1992.
5. Berg, K., Anholt, H., Beech, Ø. and Moan, J.: The influence of iron chelators on the accumulation of protoporphyrin IX in 5-aminolevulinic acid-treated cells. *Brit. J. Cancer*, 74: 688, 1996.
6. Kennedy, J. C., Pottier, R. H. and Pross, D. C.: Photodynamic therapy with endogenous protoporphyrin IX; basic principles and present clinical experience. *J. Photochem. Photobiol. B: Biol.*, 6: 143, 1990.
7. Kriegmair, M., Baumgartner, R., Knüchel, R., Stepp, H. and Hofstädter, A.: Detection of early bladder cancer by 5-aminolevulinic acid induced Protoporphyrin fluorescence. *J. Urol.*, 155: 105, 1996.
8. Jichlinski, P., Forrer, M., Mizeret, J., Glanzmann, T., Braichotte, G., Wagnière, G., Zimmer, G., Guillou, L., Schmidlin, F., Graber, P. and Leisinger, H. J.: Clinical evaluation of a method for detecting superficial transitional cell carcinoma of the bladder by light induced fluorescence of protoporphyrin IX following topical application of 5-aminolevulinic acid. Preliminary results. *Lasers Surg. Med.*, 20: 402, 1997.
9. Steinbach, P., Kriegmair, M., Baumgartner, R., Hofstädter, F. and Knüchel, R.: Intravesical instillation of 5-aminolevulinic acid: the fluorescence metabolite is limited to the urothelial cells. *Urology*, 44: 676, 1994.
10. Potter, W. R., Mang, T. S. and Dougherty, T. J.: The theory of photodynamic therapy dosimetry: consequences of photodestruction of sensitizer. *Photochem. Photobiol. B: Biol.*, 46: 97, 1987.
11. Steinbach, P., Weingandt, H., Baumgartner, R., Kriegmair, M., Hofstädter, F. and Knüchel, R.: Cellular fluorescence of the endogenous photosensitizer protoporphyrin IX following exposure to 5-aminolevulinic acid. *Photochem. Photobiol. B: Biol.*, 62: 887, 1995.
12. Jacob, W. J., Herschler, R. J. and Rosenbaum, E. E.: Dimethylsulfoxide (DMSO); laboratory and clinical evaluation. *JAMA*, 147: 1350, 1965.
13. Desgrandchamps, P., Moulinier, F., Cochand-Priollet, B., Wasserf, M., Teillac, P. and Le Duc, A.: Microscopic study of the pig ureteral urothelium. *J. Urol.*, 157: 1926, 1997.
14. Kucera, P., Abriel, H. and Katz, U.: Ion transport across the early chick embryo: I. electrical measurements, ionic fluxes and regional heterogeneity. *J. Membr. Biol.*, 141: 149, 1994.
15. de Kloek, J. and Beijersbergen van Henegouwen, G.: Prodrugs of 5-aminolevulinic acid for photodynamic therapy. *Photochem. Photobiol. B: Biol.*, 64: 1996.
16. Gaullier, J. M., Berg, K., Peng, Q., Anholt, H., Selbo, P. K., Ma, L. W. and Moan, J.: Use of 5-aminolevulinic acid esters to improve photodynamic therapy on cells in culture. *Cancer Res.*, 57: 1481, 1997.
17. Haller, C., Schick, C. S., Zorn, M. and Kübler, W.: Cytotoxicity of radiocontrast agents on polarized renal epithelial cell monolayers. *Cardiovasc. Res.*, 33: 655, 1996.
18. Hermes-Lima, M.: How do Ca<sup>2+</sup> and 5-aminolevulinic acid-derived oxyradicals promote injury to isolated mitochondria? *Free Radic. Biol. Med.*, 19: 381, 1995.
19. Chang, S.-C., Mac Robert, A. and Bown, S.: Biodistribution of protoporphyrin IX in rat urinary bladder after intravesical instillation of 5-aminolevulinic acid. *J. Urol.*, 155: 1744, 1996.
20. Bachor, R., Reich, E., Rück, A. and Hautmann, R.: Aminolevulinic acid for photodynamic therapy of bladder carcinoma. *Urol. Res.*, 24: 285, 1996.
21. Iinuma, S., Bachor, R., Flotte, T. and Hasan, T.: Biodistribution and phototoxicity of 5-aminolevulinic acid-induced PPIX in an orthotopic rat bladder tumor model. *J. Urol.*, 153: 802, 1995.
22. Rück, A., Köllner, H., Schneckenburger, H. and Steiner, R.: Competition between photobleaching and fluorescence increase of photosensitizing porphyrin and tetrasulphonated chloroaluminiumphthalocyanine. *J. Photochem. Photobiol. B: Biol.*, 5: 311, 1990.
23. Cox, G. S., Bobillier, C. and Whitten, D. G.: Photo-oxidation and singlet oxygen sensitization by protoporphyrin IX and its photo-oxidation products. *Photochem. Photobiol. B: Biol.*, 36: 401, 1982.
24. Lange, N., Jichlinski, P., Zellweger, M., Forrer, M., Marti, A., Kucera, P., Guillou, L., Wagnières, G. and Van den Bergh, H.: Photodetection of early human bladder cancer based on the fluorescence of 5-aminolevulinic acid hexylester-induced protoporphyrin IX: a pilot study. *British J. Canc.*, in press.

## Photodetection of early human bladder cancer based on the fluorescence of 5-aminolaevulinic acid hexylester-induced protoporphyrin IX: a pilot study

N Lange<sup>1</sup>, P Jichlinski<sup>2</sup>, M Zellweger<sup>1</sup>, M Forrer<sup>1</sup>, A Marti<sup>2</sup>, L Guillou<sup>4</sup>, P Kucera<sup>3</sup>, G Wagnières<sup>1</sup> and H van den Bergh<sup>1</sup>

<sup>1</sup>Institute of Environmental Engineering, Swiss Federal Institute of Technology (EPFL), CH-1015 Lausanne, Switzerland; <sup>2</sup>Department of Urology, CHUV Hospital, CH-1011 Lausanne, Switzerland; <sup>3</sup>Institute of Physiology, University of Lausanne, CH-1005 Lausanne, Switzerland; <sup>4</sup>Department of Pathology, CHUV Hospital, CH-1011 Lausanne, Switzerland

**Summary** Exogenous administration of 5-aminolaevulinic acid (ALA) is becoming widely used to enhance the endogenous synthesis of protoporphyrin IX (PpIX) in photodynamic therapy (PDT) and fluorescence photodetection (PD). Recently, results have shown that the chemical modification of ALA into its more lipophilic esters circumvents limitations of ALA-induced PpIX like shallow penetration depth into deep tissue layers and inhomogeneous biodistribution and enhances the total PpIX formation. The present clinical pilot study assesses the feasibility and the advantages of a topical ALA ester-based fluorescence photodetection in the human bladder. In this preliminary study 5-aminolaevulinic acid hexylester (h-ALA) solutions, containing concentrations ranging from 4 to 16 mM, were applied intravesically to 25 patients. Effects of time and drug dose on the resulting PpIX fluorescence level were determined in vivo with an optical fibre-based spectrofluorometer. Neither local nor systemic side-effects were observed for the applied conditions. All conditions used yielded a preferential PpIX accumulation in the neoplastic tissue. Our clinical investigations indicate that with h-ALA a twofold increase of PpIX fluorescence intensity can be observed using 20-fold lower concentrations as compared to ALA.

**Keywords:** 5-aminolaevulinic acid; 5-aminolaevulinic acid hexylester; photodynamic therapy; fluorescence; protoporphyrin IX; human bladder cancer

Fluorescence photodetection (PD) and photodynamic therapy (PDT) are techniques currently under clinical assessment for both visualization and local destruction of malignant tumours and premalignant lesions. One drawback of these methods found with some photosensitizers is a more or less long-term cutaneous photosensitivity (Wagnières et al, 1998; Dougherty et al, 1990). A more recent strategy for administering photosensitizers involves the application of 5-aminolaevulinic acid (ALA) in order to stimulate the formation of protoporphyrin IX (PpIX) in situ. The exogenous ALA bypasses the negative feedback control from haem to ALA synthase that catalyses the condensation of glycine and succinyl-coenzyme A (CoA). Given in excess, exogenous ALA thus can result in a temporary accumulation of PpIX, in particular, in cells with higher metabolic turnover. Since PpIX has fairly good photosensitizing properties (Cox et al, 1982; Kennedy et al, 1990) proposed ALA as a possible photodynamic agent. Following this pioneering work, this treatment modality has been widely studied for various cancers (Kennedy et al, 1992; Peng et al, 1992; Svanberg et al, 1994).

As well as for the PDT of malignant or premalignant lesions, ALA-induced PpIX is now being used for the detection of such lesions. This technique has been shown to work, among other applications, in urology, where easy instillation in the bladder, combined with the fact that this organ is readily accessible endoscopically, makes it an ideal object. Alongside classical techniques

such as cytology or white light examination, fluorescence PD by ALA-induced PpIX provides some advantages (Leveckis et al, 1994; Kriegmair et al, 1996; Jichlinski et al, 1997). This inspection modality allows an exact mapping which pinpoints, with a high level of sensitivity and specificity, the locations of carcinoma in situ (CIS) as well as early stages of cancer-like dysplasias, which are normally difficult to recognize under white light examination.

However, when using topically instilled ALA for the PDT of CIS and precancerous lesions, this modality appears to be limited by the amount of ALA that enter the target cells or by the tissue penetration and the distribution of the resulting PpIX in the targeted tissue. Almost all of these possible disadvantages accompanying the use of ALA can be ascribed to the physical-chemical properties of the molecule itself. Applied under physiological conditions, ALA is a zwitterion (Novo et al, 1996). Because the lipid bilayer of biological membranes is relatively impermeable to charged molecules, the cellular uptake of ALA is shallow. Consequently, in order to increase the transport across cellular membranes, fairly high drug doses and increased administration times have to be used. This deficiency results in a low penetration depth (Warloë et al, 1992; Loh et al, 1993; Peng et al, 1995) and an ALA-induced PpIX distribution, which is not optimized for the PDT of the deep layers of nodular lesions in the urothelium (Iinuma et al, 1995; Chang et al, 1996) after topical ALA application.

Systematic studies have shown that the modification of a drug to an ester, an amide or a urethane by the addition of a long-chain hydrocarbon improves penetration through biological barriers (Bridges et al, 1979; Jain, 1987a, 1987b). After penetration into the cell, the ester derivative can then, for example, be hydrolysed back to the free ALA by non-specific esterases. Recently,

Received 24 July 1998

Revised 8 October 1998

Accepted 15 October 1998

Correspondence to: N Lange

promising results were obtained with different alkylesters of ALA *in vivo* and *in vitro* (Kloek et al, 1996; Peng et al, 1996; Gaullier et al, 1997; Marti et al, 1998). These groups demonstrated that the application of esterified ALA derivatives results in an up to 25-fold increase in PpIX fluorescence levels as compared to ALA.

This report covers initial clinical investigations with 5-aminolaevulinic acid hexylester hydrochloride (h-ALA)-induced fluorescence PD in the human bladder. Following our preclinical studies (Marti et al, 1999), we selected h-ALA from the multitude of possible ALA-alkylesters because it represents a good compromise between water–urine solubility and sufficient PpIX formation capacity at low doses. Furthermore, h-ALA has been shown to lead to a homogenous distribution of PpIX-related fluorescence over the entire urothelium in our pig bladder model (Marti et al, 1998). In addition, it can be synthesized simply from ALA and hexanol (Kloek et al, 1997). The goal of this clinical pilot study was to test h-ALA as a potential candidate for improving both the PD and PDT in the urinary bladder. Therefore, topical application of h-ALA should result in higher PpIX formation than is the case with the same amount of ALA. It should enable shorter times between instillation and examination and lower drug concentrations while retaining the outstanding selectivity of ALA. This work presents a preliminary optimization of h-ALA-induced PpIX in respect to the resulting fluorescence intensities. Both the influence of the

concentration and instillation time of h-ALA solutions on the total amount of PpIX were determined *in vivo* by the use of an optical fibre-based spectrofluorometer.

## MATERIALS AND METHODS

### Patients

Twenty-five patients (seven women and 18 men, four cases of ordinary ALA and 21 cases of h-ALA) have been involved in this first study conducted since August 1997. The mean age was 70 years, covering an age range of between 44 and 85. Local ethical committee approval was granted for this study, and written consent was obtained in each case.

### Preparation and administration of ALA and h-ALA

ALA (99%) was purchased from Merck (Darmstadt, Germany). Other chemicals (thionyl chloride 99% and 1-hexanol 99.9%) used for the synthesis of h-ALA were ordered from Fluka Chemie AG (Buchs, Switzerland) and were used without further purification.

The synthesis described here is a slight modification of the methods reported recently (Takeya, 1992; Kloek et al, 1996). In brief, 3.5 ml of thionyl chloride were added drop by drop under stirring to an excess (~ 10 ml) of 1-hexanol cooled on ice in an

**Table 1** Experimental instillation conditions used in the first clinical trials with h-ALA and normalized fluorescence levels on papillary tumours (pTa G2) obtained by normalization to reference cuvette

Patient no.	Concentration (mM)	Instillation time (h)	Resting time (h)	Fluorescence signal (r.u.)
1	4	2*	—	16.2
2	4	2	—	11.2
3	4	4	—	34.5
4	4	4	—	20.5
5 <sup>b</sup>	8	2	—	22.1
				38.4
6	8	2	—	36.2
7	8	2	—	46.7
8	8	2	—	—
9 <sup>b</sup>	8	2	2	151.1
				102.0
10	8	2	2	115.8
11	8	2	2	147.5
12	8	4	—	66.4
13	8	4	—	72.6
14	8	4	—	63.4
15	8	4	—	73.8
16	8	4	—	94.4
17	8	4	—	77.1
18	8	4	2	102.7
19	8	4	2	95.0
20	16	2	—	15.8
21	16	2	—	16.7
22	180 <sup>a</sup>	4	2	54.0
23	180 <sup>a</sup>	4	2	43.6
24	180 <sup>a</sup>	4	2	46.2
25	180 <sup>a</sup>	4	2	45.3

\*Instillation of the 180 mM solution of ALA. <sup>b</sup>Patient with two papillary tumours.

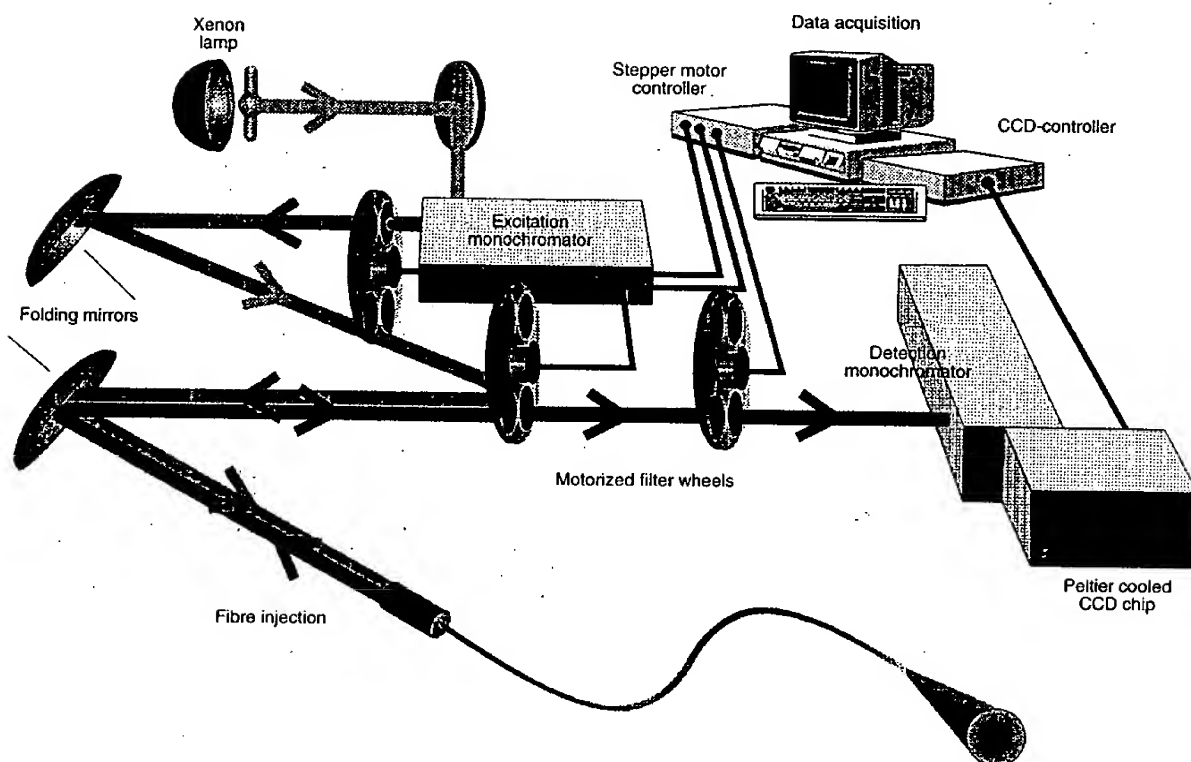


Figure 1 Schematic view of the optical fibre-based spectrofluorometer

argon atmosphere. The solution was stirred for a further 30 min to bring the reaction to completion; after warming up to room temperature, 2.5 g of ALA ( $M_r = 167.6 \text{ g mol}^{-1}$ ) were added to the solution. The suspension was then stirred overnight at room temperature under argon. The final phase of the reaction was controlled on-line by thin layer chromatography (TLC) (TLC foils; Schleicher & Schuell, Merck, Darmstadt, Germany) in  $\text{CH}_2\text{Cl}_2/\text{MeOH}$  (9:1) stained by  $\text{KMnO}_4$  ( $R_f = 0.6$ ). Once the reaction was complete, the solvent and hexylchloride were removed under reduced pressure ( $\sim 0.5$  torr). The viscous residue was dissolved in warm methanol. Then a small amount of methanol was evaporated until the first crystals of the reaction product appeared. A small quantity of diethylether was added and h-ALA was allowed to crystallize on ice. This dissolving and recrystallizing procedure was then subsequently repeated until only one spot was recognized on the TLC, yielding 80–90% of h-ALA ( $M_r = 251.8 \text{ g mol}^{-1}$ ) as a white powder. The product was characterized by proton nuclear magnetic resonance ( $^1\text{H-NMR}$ ) with a 400 MHz (Bruker, Germany) spectrometer and identified as 5-aminolaevulinic acid hexylester hydrochloride. The purity ( $> 95\%$ ) was further verified by high performance liquid chromatography (HPLC) with UV/VIS detection at 270 and 350 nm respectively (data not shown). No other products were observed.

The ALA solutions were administered in accordance with standard protocol used in Lausanne's CHUV Hospital (Jichlinski et al, 1997). In brief, 1500 mg of ALA were dissolved in 38 ml of sterile water. Five millilitres of phosphate-buffered saline (PBS) were added and the pH was adjusted with a further 7 ml of aqueous

sodium hydroxide (1N) to a value of pH 5.3. This solution with a concentration of 180 mM of ALA was sterilized by filtration through a Millipore filter (Millipore, Millex GS  $0.22 \mu$ ) and stored at  $-18^\circ\text{C}$  1 day before measurements were conducted. The solution was instilled into patients' bladders using a 16 French Foley catheter 6 h prior to photodetection. Patients were asked to retain the solution for 4 h. Their bladders were evacuated 2 h prior to treatment.

Depending on the prodrug concentration to be applied, 50–200 mg (i.e. 4–16 mM) of crystalline h-ALA were dissolved in 35 ml of water. Then 13 ml of PBS were added to the aqueous solution and adjusted with 0.1 N hydrochloric acid to give the same pH value of 5.3. The solutions were instilled as described above. Table 1 summarizes the different conditions under which ALA and h-ALA were applied. All patients treated with ALA (four cases) and some instilled with h-ALA (five cases) had a supplementary resting time of 2 h after being exposed to the drug solution.

## Procedure

### Bladder inspection under white light illumination

Prior to further treatment or measurement, the actual status of the bladder was documented under white light illumination. The frame accumulation colour CCD camera (Storz, Tuttlingen, Germany), connected to a video recorder (JVC, Japan) and an RGB monitor (Sony, Japan) was plugged directly into the ocular of a 23.5 French cystoscope (Storz PDD, Tuttlingen, Germany) to record the standard endoscopic colour image.

### Fluorescence spectroscopy

Fluorescence emission spectra were recorded with an optical fibre-based spectrofluorometer based on a Peltier-cooled CCD coupled to a spectrograph (Cromex 250, SI Instruments, Germany). The experimental setup is shown in Figure 1. Arranged on a trolley, the whole setup can be easily transported. Excitation light ( $\lambda_{ex} = 405$  nm) from a 75 W high-pressure Xenon lamp (UXL-75 XE, Ushio Inc., Japan) was spectrally resolved by a quarter meter monochromator (Chromex 250, SI Instruments, Germany) with a bandwidth of 5 nm and an excitation filter, SCHOTT BG3 (Schott AG, Mainz, Germany), mounted on a filter wheel. A stepper motor (SMC 100, Princeton Instruments Inc., USA) controlled this excitation filter wheel, which was equipped with different low-pass filters installed to purify the excitation light. Fully reflective mirrors and a dichroic mirror (Reynard DC 450; Reynard, USA), mounted on a second filter wheel, were used to feed the light into a 600  $\mu$ m core silicone-clad silica fibre with perpendicular polished end-faces. Excitation energy measured at the distal end of the fibre tip was determined with a calibrated power-meter (Optical Power Meter 840, Newport, USA). Fluorescence emitted by any sample was collected with the same fibre and separated from the excitation light by the dichroic optics described above. A long-pass filter (Reynard FG 455) mounted on a third filter wheel made further spectral separation, virtually eliminating all reflected excitation light prior to acquisition. This filter setup allows the acquisition of fluorescence emission spectra between 450 and 900 nm. Detection based on this combination enables fast data acquisition combined with a low level of noise. The whole setup and data acquisition was controlled by a 486 personal computer using CSMA software (SI Instruments GmbH, Germany).

An aqueous solution of Rhodamine B ( $c = 1 \times 10^{-6}$  mol l<sup>-1</sup>) in a 10 mm quartz cuvette was used as a reference. Emission spectra of the reference were recorded before and after each measurement. All measurements were normalized to the peak value of the reference to give comparable results corrected for day-to-day fluctuations of the excitation light energy or detection pathway alignment.

After inspection of the bladder under white light, the distal end of the fibre was introduced via the biopsy channel of the cystoscope. A background measurement was performed in the centre of the bladder to allow the correction of the spectra for parasitic light and fluorescence generated by the fibre itself. Then the physician brought the distal end of the fibre directly into contact with the bladder wall.

### Bladder inspection under violet light illumination

After measurement of the fluorescence spectra (see below) of healthy, cancerous and suspicious areas in the bladder, the camera was equipped with a long-pass filter ( $\lambda > 520$  nm; Wratten filter No. 12, Kodak, Rochester, USA), positioned between the ocular of the cystoscope and the CCD-Chip. A footswitch allows the physician to place a bandpass filter (380–450 nm) in front of the 300 W Xenon arc lamp (Storz, Tuttlingen, Germany) to give about 150 mW of violet light at the end of the cystoscope. Excitation with violet light generated a visible pale-green autofluorescence of the healthy mucosa. As a result of the absorption of autofluorescence, the blood vessels of the lamina propria appear somewhat darker. Filtration of the light below 520 nm allows these sites to be distinguishable from zones containing high PpIX concentrations, appearing in a clear, bright, fluorescing red. To improve the fluorescence images, the camera was switched into frame

accumulation mode for enhanced sensitivity. The integration times ranged from one-eighth to one-half of a second, depending on observation distance.

### Biopsy sampling and pathology

Prior to transurethral resection of the bladder wall (TURB), a total number of 109 biopsies from fluorescent and non-fluorescent areas (average 5.2 per patient; guided by light-induced fluorescence after excitation at 405 nm) were taken from the patients treated with h-ALA solutions. Macroscopic fluorescence findings and locations were documented for each biopsy. All samples were sent for histopathological examination. The urothelial carcinomas were graded and staged according to the World Health Organization (WHO) 1973 classification (Mostofio et al, 1973) and the UICC/AJC 1992 system (Hermanek and Subin 1992) respectively. Flat intra-epithelial neoplastic lesions were graded according to the criteria of Nagy et al (1982) and classified as grade 1 (mild dysplasia), grade 2 (moderate dysplasia), grade 3 (marked dysplasia) and carcinoma in situ.

## RESULTS

### Macroscopic findings

All aqueous solutions of h-ALA stayed clear and colourless until use. Neither systemic nor local reactions following the examination with both h-ALA and ALA were observed under the conditions used in this study. Even the highest drug dose administered (16 mm) of h-ALA was well tolerated. h-ALA-induced synthesis of PpIX was observed in each patient. All papillary and planar tumours, also visible under white light cystoscopy, showed bright red fluorescence. This red fluorescence was found to demarcate the outline of the urothelial lesions with high precision. Using the violet light of the filtered Xenon arc lamp, it was possible to perform both fluorescence-guided biopsies as well as accurate resections of targeted tissues. Qualitatively, all conditions tested resulted in a clearly visible contrast between healthy and diseased sites of the bladder wall.

Table 2 Correlation between histopathological finding and fluorescence diagnosis following h-ALA instillation

Histopathological findings	Total number of biopsies	Fluorescence positive	Fluorescence negative
Healthy mucosa	28	5	23
Metaplasia	1	1	—
Hyperplasia	3	3	—
Dysplasia G1	12	10	2
Dysplasia G2	5	3	2
Dysplasia G3	2	2	—
CIS	11	9	2
pTa G1	8	8	—
pTa G2	14	14	—
pTa G3	19	19	—
pT1 G2–G3	4	4	—
pT2a	2	2	—
Total	109	80	29

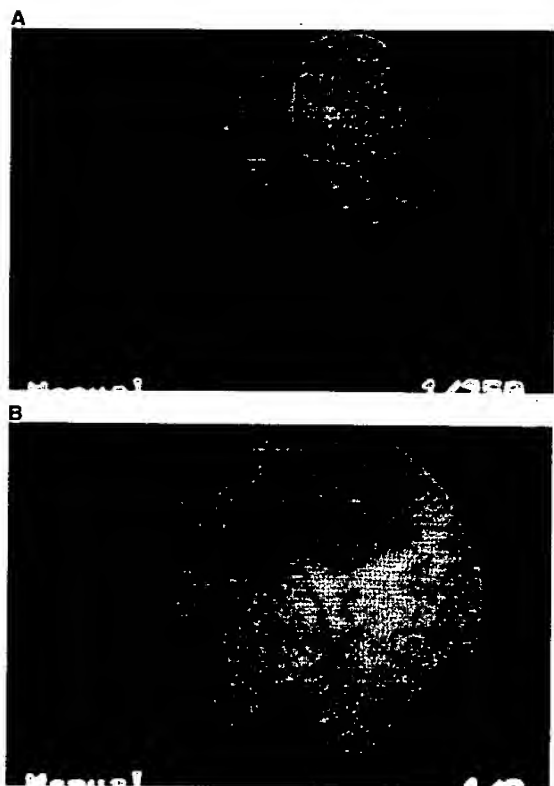


**Figure 2** Endoscopic view of a flat papillary tumour (pTa G2) after 2 h of h-ALA exposure (for description see text) under (A) white light, (B) violet light examination

Figure 2 demonstrates the advantageous use of h-ALA-induced PpIX for the fluorescence diagnosis of human bladder cancer. The two pictures show a sequence of a white light (Figure 2A) and a violet light (Figure 2B) examination after instillation of 8 mm of h-ALA over a period of 2 h (patient no. 10). White light illumination shows two papillary tumours (pTa G2) situated below the air bubble of the bladder under investigation. Fluorescence PD of the same area (Figure 2B) indicates a further lesion [flat papillary tumour (pTa G2)] which is barely detectable under white light.

### Fluorescence findings and histopathological diagnosis

A total of 109 biopsies were taken under light-induced fluorescence from patients after instillation with h-ALA solutions. The correlation between the fluorescence findings and the histopathological analysis is summarized in Table 2. Thirty-two tissue samples were excised from healthy areas of the bladders investigated, containing eight samples, which were considered to be fluorescent. Histopathological diagnosis of the latter samples indicates the reasons for these 'false positive' responses. All these specimens showed tissular structures known for a higher cellular turnover, e.g. metaplasias, hyperplasias, chronic inflammation, or scar formation. In total, only six of the 77 biopsies taken from malignant and premalignant sites were not fluorescing. Three of these 'false negative' responses can be explained by nonoptimized conditions with regard to the concentrations of h-ALA applied (two moderate dysplasias; patient no. 4) as well as non-optimal

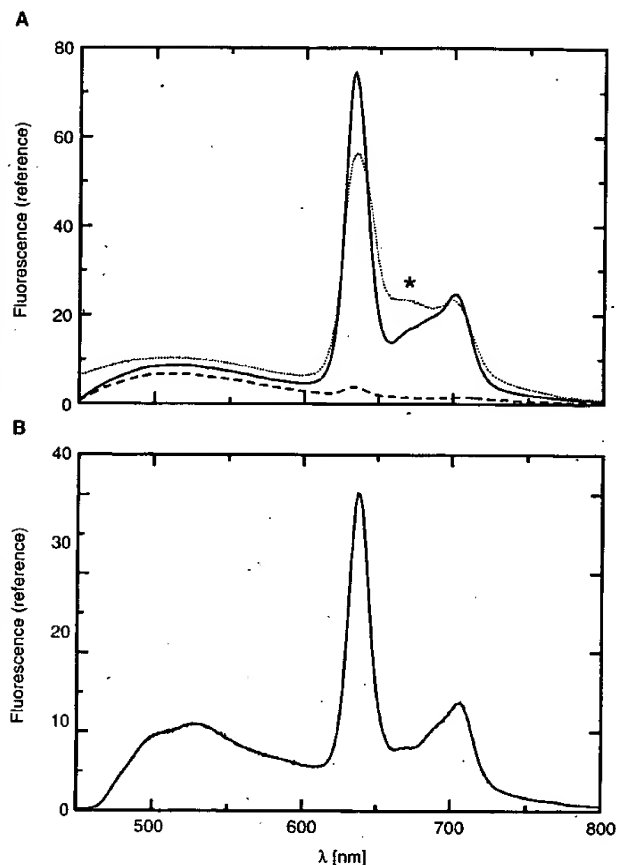


**Figure 3** (A) Fluorescence spectra of h-ALA-induced PpIX ( $\lambda_{ex} = 405$  nm) in normal mucosa (---) and a papillary tumour (pTa G2, —) after 4 h of instillation with 8 mm h-ALA (...): a fluorescence peak (\*) at 670 nm becomes visible due to photobleaching of PpIX. (B) Fluorescence spectra of ALA-induced PpIX ( $\lambda_{ex} = 405$  nm) in a papillary tumour (pTa G2, —) after 6 h of installation with 180 mm ALA

incubation times (CIS; patient no. 1). A further CIS was missed (patient no. 13) probably due to an unusually long period of white light illumination preceding photodetection, resulting in the photobleaching of PpIX. Without exception, histopathologically-staged pTa G1 or higher samples were found by fluorescence photodetection.

### Fluorescence spectroscopy

Fluorescence emission spectra were measured on a total number of 24 patients (20 h-ALA, four ALA) (Table 1). ALA- and h-ALA-induced porphyrins were excited at 405 nm on both healthy and malignant areas in the human bladder. The emission from the urothelial surface was spectrally resolved between 450 and 800 nm. A comparison of the emission spectra after ALA and h-ALA exposure is plotted in Figure 3. The total fluorescence intensity is normalized to the reference. As shown in this Figure, the characteristic emission bands of PpIX at  $\lambda = 635$  nm and  $\lambda = 708$  nm after excitation in the Soret Band are clearly visible. According to the spectral shape, the fluorescence is attributed to PpIX. In none of the spectra recorded in vivo, an indication of porphyrins other than PpIX could be found. Depending on the duration of white and violet light examinations before fluorescence



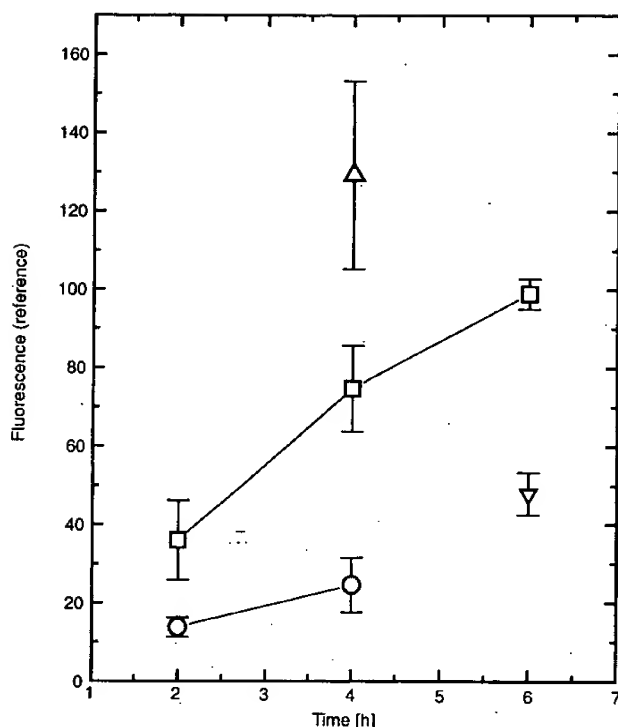


**Figure 4** Effect of instillation time on the relative PpIX fluorescence intensity at 636 nm in papillary tumours (pTa G2) (□: 8 mm h-ALA; ○: 4 mm h-ALA; △: 8 mm h-ALA (2 h of instillation + 2 h of resting time); ▽: 180 mm ALA)

measurements, a peak, attributed to a PpIX photobleaching product, of around 665–675 nm appeared (dotted line in Figure 3A). The appearance of this supplementary fluorescence peak results in a line broadening because of overlapping fluorescence emission peaks and may suggest some degree of heterogeneity. In addition to the fluorescence emission spectra recorded on a papillary tumour pTa G2 after 4 h of h-ALA exposure, the corresponding spectra obtained on a healthy area were plotted (dashed line in Figure 3A). From these spectra, it can be seen that the healthy mucosa's autofluorescence of around 513 nm exceeds the two typical fluorescence peaks of PpIX at 636 nm and 708 nm. All samples taken from sites with these fluorescence characteristics were confirmed as healthy after histopathological examination. Evaluation of all fluorescence data available reveals that papillary tumour had the highest emission intensities. Premalignant lesions, such as dysplasias and carcinoma in situ, generally showed lower PpIX fluorescence intensities compared to malignant lesions. However, no direct relationship has been discovered between histopathological grading and relative fluorescence values.

#### Effect of exposure time and concentration

Three different solutions containing 50 mg (4 mm, four patients), 100 mg (8 mm, 15 patients) and 200 mg (16 mm, two patients) of h-ALA in 50 ml of the solvent were instilled in human bladders between 2 and 6 h prior to the fluorescence measurements (Table 1). Increased red fluorescence due to enhanced PpIX formation in pre-malignant and malignant lesions compared to the surrounding healthy sites was observed at all applied conditions. In order to quantify the resulting PpIX fluorescence, emission

spectra were collected from different sites of the treated bladders. The fluorescence intensities of papillary tumours pTa graded G2 or G3 at 636 nm were chosen as standard in order to determine the influence of the different treatment conditions applied. This selection is based on the presence of this type of lesion in each bladder examined. Table 1 summarizes the influence of the different conditions on the relative fluorescence intensities of the PpIX emission band at 636 nm.

Analysis of the data available from patients exposed for 2 h (patient nos 1, 2, 5, 6, 7, 20 and 21) to different h-ALA concentrations indicates a strong concentration dependent on the PpIX fluorescence. It appears that, within 2 h, a solution of 8 mm h-ALA generates the highest fluorescence levels as compared to 4 mm and 16 mm of h-ALA. In Figure 4, the time course of the relative fluorescence intensity is plotted for h-ALA concentrations of 4 mm and 8 mm. An increase of fluorescence intensity with instillation time was observed in the two solutions. In addition, Figure 4 shows that, taking both the total fluorescence and the slope of the graphs into consideration, an instillation of 8 mm h-ALA solution is more efficient than that of a 4 mm solution.

In the course of our preliminary clinical study, a total of four patients (nos 8–11) were instilled under slightly different conditions. The patients' bladders were exposed to the solutions for 2 h. Following this exposure time, the bladders were emptied and the patients were allowed a supplementary resting time of 2 h. From Figure 4, it is clear that following this '(2+2)-concept' significantly enhanced fluorescence levels can be obtained compared to permanent exposure to the drug for 4 h.

The comparison of the relative fluorescence intensities of an 8 mm h-ALA solution and a 180 mm solution of ALA under similar conditions (4 h of instillation, 2 h of supplementary resting time) clearly demonstrates the advantage of using h-ALA. A treatment under these conditions with a topical 8 mm h-ALA solution resulted in a twofold increase of the fluorescence signal as compared to topical 180 mm ALA. After only 4 h of h-ALA exposure (8 mm), the relative fluorescence intensity already exceeded that induced by ALA (180 mm) 6 h after instillation.

#### DISCUSSION

Bladder cancer is a fairly common disease, appearing between the ages of 50 and 70 (Richie et al, 1989; Levi, 1993). This cancer, characterized by a high incidence (Levi, 1993), can appear in many distinct morphological forms, single or multiple, visible such as papillary or invisible such as 'flat' atypical lesions, mainly represented by low- or high-grade dysplasia or CIS. Bladder tumour multiplicity and the presence of these different forms of atypia are indicators of poor disease prognosis. Recognition of all visible or invisible lesions is therefore a prerequisite for any kind of treatment, with the aim of reducing the risk of progression or the rate of recurrence.

Although topical application of ALA has proved to be a helpful and reliable tool in fluorescence photodetection of invisible lesions in human bladder disease (Kriegsmair et al, 1994; Jichlinski et al, 1996), some problems remain due to ALA's poor bioavailability. A small hydrophilic amino acid like ALA does not penetrate into all tissue compartments with great ease. Hence its concentration in tissue may remain relatively low and its distribution somewhat heterogeneous. Consequently, high drug doses over long instillation periods have to be used.

Three different concepts have been proposed to enhance the ALA-induced PpIX formation in deeper layers of the target tissue. Two of them are based on the use of chemicals, given along with ALA, in order to enhance both its penetration into deeper tissue layers and/or the total PpIX accumulation. This transepithelial penetration enhancement can be achieved either by prior dimethyl sulphoxide exposure of the targeted area (Peng et al, 1995) or by encapsulation of ALA into liposomes (Fukuda et al, 1992). The second approach uses agents interfering directly with the biosynthetic pathway of haem. Tetrapyrrol modulators, such as 1,10-phenanthroline (Rebeiz et al, 1996) and allyl-isopropyl-acetamide (AIA) (Schoenfeld et al, 1994) stimulating the enzymatic activity associated with PpIX formation. Iron chelators (e.g. ethylenediaminetetraacetic acid (EDTA) (Hanania and Malik, 1992; Orenstein et al, 1995; Warloe et al, 1995), desferrioxamine (DFO) (Ortel et al, 1993) CP94 (Chang et al, 1997) have been shown to increase PpIX concentration by preventing the ferrochelatase-mediated insertion of iron into the tetrapyrrol ring. This study followed a third approach, based on the thesis that the transformation of the hydrophilic ALA into more lipophilic prodrugs will enhance drug uptake.

In view of the results obtained using esters of ALA in vitro (Kloek et al, 1996; Gaullier et al, 1997; Marti et al, 1999; Tyrrell et al, 1993) and in vivo (Kloek et al, 1996; Peng et al, 1996), it appeared reasonable to envisage developing such a substance for clinical tests in which superficial bladder carcinoma is detected by fluorescence and possibly even treated by PDT. From the variety of derivatives recently tested in our laboratory (Marti et al, 1999), we selected h-ALA as it represents a good compromise between water-urine solubility and lipophilicity. It also gave an excellent in-vitro dose drug response compared to ALA solutions. Furthermore, it can be synthesized with a fairly high yield and low cost. The goal of this first clinical study with h-ALA in urology was to evaluate the feasibility of fluorescence photodetection with this new agent and the advantages achieved by instillation of h-ALA as compared to ALA for use in the human bladder.

One criterion for the use of h-ALA as a potential candidate in replacing ALA, is the preservation of the outstanding selectivity of ALA-induced PpIX for malignant and pre-malignant tissues. Confirmed by histopathological examination, we have demonstrated that the fluorescence of PpIX in the urothelium induced by intravesically administered h-ALA correlated significantly with neoplastic lesions and was suitable for the detection of papillary tumours as well as for dysplasia and carcinoma in situ. The 7% rate of false negative responses found in the present study is comparable to the value given by Jichlinski et al in 1997 and slightly higher than that presented by the Munich group (Kriegmair et al, 1996). A total number of 28 biopsies were taken from areas proven to be benign. Only five of these samples revealed an enhanced red fluorescence under violet light irradiation, yielding a rate of falsely positive fluorescence findings of 17%. This result seems to be quite small compared to both the results of Kriegmair et al (1996) and Jichlinski et al (1997). But it may be explained by the small number of biopsies taken, or the fact that the fluorescence induced by the long-chain esters was found to be limited to the site of application (Peng et al, 1996), hence no supplementary PpIX build-up from systemic ALA uptake is observed.

Clinical fluorescence spectroscopy has been used for measuring the PpIX accumulation kinetics, indicating an increase of h-ALA-

induced PpIX with time in the human bladder within 6 h. A quantitative comparison of the fluorescence intensities at 636 nm following similar instillation conditions with solutions of 180 mM of ALA or 8 mM of h-ALA, respectively, clearly shows the advantages of h-ALA-induced PpIX. The more than twofold increase of the fluorescence signal due to the use of h-ALA is in good agreement with the in vivo results of Kloek et al (1996).

The time course of the PpIX fluorescence intensity in neoplastic tissues shows that, following 8 mM h-ALA exposure for 2 or 4 h, synthesis of PpIX continues within almost 2 h after termination of the instillation. In this time range, the fluorescence intensity increases 400% (2 h of exposure, 2 h of resting time) and 25% (4 h of exposure, 2 h of resting time) respectively.

The significant increase of the fluorescence signal using the '(2+2)-concept' as compared to a permanent exposure to drug for 4 h, as well as the strong dependence on the instilled h-ALA concentration, can be explained by an interference of high ALA concentrations with the biosynthetic pathway of haem. This observation was confirmed by in vitro experiments made by Gaullier et al (1997) and Marti et al (1999) with several ALA esters including h-ALA. Whereas the transport of ALA across the lipid bilayer of cell membranes probably represents a bottleneck in the PpIX formation, the enhanced uptake of lipophilic h-ALA may saturate the intracellular PpIX biosynthesis. This saturation might cause a negative feedback to enzymatic activity. Furthermore, high intracellular ALA concentrations have been shown to be cytotoxic. A high cellular ALA content may induce the release of  $\text{Ca}^{2+}$  from mitochondria, mitochondria swelling and uncouple respiration (Hermes-Lima, 1995). It can also cause ferritin iron release (Berg et al, 1996) or mediate the formation of 8-hydroxy-2'-deoxyguanosine in DNA (Fraga et al, 1994).

The results presented in this study have shown that a 2 h instillation of h-ALA (8 mM) provides sufficient PpIX fluorescence for reliable photodetection of malignant and pre-malignant lesions. This reduction in instillation time to only 2 h significantly increases the patient's comfort. Moreover, this makes outpatient treatment feasible and helps to cut costs in view of the excessively increasing cost of hospitalization. Finally, the reduction of the drug dose will decrease drug cost and the potential risk of mild complications provoked by ALA, recently reported by Rick et al (1997).

While for reliable fluorescence photodetection a 2 h instillation of 8 mM h-ALA has been shown to give satisfactory results, other conditions must be fulfilled with respect to an efficient bladder cancer therapy by PDT. Among other factors, the two key parameters of high concentration of the photosensitizer and its homogeneous distribution in the target tissue play a major role for the effectiveness of PDT.

Fluorescence microscopic studies showed that, after topical application of ALA, the PpIX was restricted to the superficial layers of the bladder tumours (Steinbach et al, 1994). On the contrary, preliminary fluorescence microscopic studies on some biopsies, taken in this study (data not shown), as well as the in vitro studies of Marti et al (1999) demonstrated homogeneously distributed PpIX fluorescence over the entire urothelium after topical application of h-ALA solutions.

Considering the photobleaching of porphyrins during irradiation (Rotomski et al, 1996; Bezdetnaya et al, 1996; Moan et al, 1997), a threshold concentration of PpIX necessary for tissue destruction, and the high selectivity of h-ALA-induced PpIX, a small PpIX amount in healthy areas of the bladder, observed in this study will

probably not induce any damage in these regions. However, the twofold increase of PpIX fluorescence after 6 h in neoplastic tissues by using h-ALA may further enhance the PDT effect as compared to the use of ALA. The latter appeared insufficient as observed in recent studies (Kriegmair et al, 1996).

It can be concluded that the use of h-ALA is a promising way to improve the photodetection of neoplastic and pre-neoplastic lesions as compared to ALA. In future, h-ALA may replace the use of ALA for clinical intravesical instillation because it is easy to use, real time observation without major auxiliary devices is possible and it is relatively cheap. Finally, it looks more promising as a PDT agent than ALA itself.

## ACKNOWLEDGEMENTS

The authors are grateful to the Swiss 'Fonds National', the Common Research Program in biomedical technology between Lausanne Hospital (CHUV), the Swiss Federal Institute of Technology (EPFL), Lausanne University (UNIL), the Swiss National Priority Program in Optics, and the 'Fonds Vaud-Geneva' for their financial support. Norbert Lange thanks Patrick Gerber (ICO, University of Lausanne) for many fruitful discussions. The Deutsche Forschungsgemeinschaft (DFG), Bonn, Germany, provided the grant for Dr N Lange.

## REFERENCES

- Berg K, Anholt H, Bech O and Moan J (1996) The influence of iron chelators on the accumulation of protoporphyrin IX in 5-aminolaevulinic acid-treated cells! *Br J Cancer* 74: 688-697
- Bezdetnaya L, Zeghari N, Belitchenko I, Berberi-Heyob M, Merlin JL, Potapenko A and Guillemin F (1996) Spectroscopic and biological testing of photobleaching of porphyrins in solutions. *Photochem Photobiol* 64: 382-386
- Bridges JW, Sargent NSE and Upshall DG (1979) Rapid absorption from the urinary bladder of a series of n-alkyl carbamate: a route for the recirculation of drug. *Br J Pharmacol* 66: 283-289
- Chang SG, MacRobert AJ and Bown SG (1996) Biodistribution of protoporphyrin IX in rat urinary bladder after intravesical instillation of 5-aminolaevulinic acid. *J Urol* 155: 1744-1748
- Chang SG, MacRobert AJ, Porter JB and Bown SG (1997) The efficacy of an iron chelator (CP94) in increasing cellular protoporphyrin IX following 5-aminolaevulinic acid administration: an in vivo study. *J Photochem Photobiol B* 38: 114-122
- Cox GS, Bobillier C, Whitten DG (1982) Photo-oxidation and singlet oxygen sensitization by protoporphyrin IX and its photo-oxidation products. *Photochem Photobiol* 36: 401-407
- Dougherty TJ, Cooper MT and Mang TS (1990). Cutaneous phototoxic occurrences in patients receiving Photofrin. *Lasers Surg Med* 10: 485-488
- Fraga CG, Onuki J, Lucasoli F, Bechara EJ and Di Mascio P (1994) 5-Aminolaevulinic acid mediates the in vivo and in vitro formation of 8-hydroxy-2'-deoxyguanosine in DNA. *Carcinogenesis* 15: 2241-2244
- Fukuda H, Paredes S and Del Battle AM (1992) Tumor localizing properties of porphyrins in vivo studies using free and liposome encapsulated aminolaevulinic acid. *Comp Biochem Physiol* 102b: 433-436
- Gaullier JM, Berg K, Peng Q, Anholt H, Selbo PK, Ma LW and Moan J (1997) Use of 5-aminolaevulinic acid esters to improve photodynamic therapy on cells in culture. *Cancer Res* 57: 1481-1486
- Hanania J and Malik Z (1992) The effect of EDTA and serum on endogenous porphyrin accumulation and photodynamic sensitization of human leukemic cells. *Cancer Lett* 65: 127-131
- Hermanek P and Sobin J (1992) *UICC TNM Classification of Malignant Tumours*, 4th edn. Springer Verlag: Berlin
- Hermes-Lima M (1995) How do  $Ca^{2+}$  and 5-aminolaevulinic acid-derived oxyradicals promote injury to isolated mitochondria? *Free Radical Biol Med* 19: 381-390
- Iinuma S, Bachor R, Flotte T and Hasan T (1995). Biodistribution and phototoxicity of 5-aminolaevulinic acid-induced PpIX in an orthotopic rat bladder tumor model. *J Urol* 153: 802-806
- Jain RK (1987a) Transport of molecules in the tumor interstitium: a review. *Cancer Res* 47: 3039-3305
- Jain RK (1987b). Transport of molecules across tumor vasculature. *Cancer Metast Rev* 6: 559-593
- Jichlinski P, Forrer M, Mizeret J, Glanzmann T, Braichotte D, Wagnières G, Zimmer G, Guillou L, Schmidlin FM, Graber P, van den Bergh H and Leisinger HJ (1997) Clinical evaluation of a method for detecting superficial transitional cell carcinoma of the bladder by light-induced fluorescence of protoporphyrin IX following topical application of 5-aminolaevulinic acid: preliminary results. *Lasers Surg Med* 20: 402-408
- Kennedy JC, Pottier RH and Pross DC (1990) Photodynamic therapy with endogenous protoporphyrin IX: basic principles and present clinical experience. *J Photochem Photobiol B* 6: 143-148
- Kloek J and Beijersbergen van Henegouwen GMJ (1996) Prodrugs of 5-aminolaevulinic acid for photodynamic therapy. *Photochem Photobiol* 64: 994-1000
- Kriegmair A, Baumgartner R, Kneuchel R, Steinbach P, Ehsan A, Lumper W, Hofstaeder W and Hofstetter A (1994) Fluorescence photodetection of neoplastic urothelial lesions following intravesical instillation of 5-aminolaevulinic acid. *Urology* 44: 836-841
- Kriegmair M, Baumgartner R, Lumper W, Waidelelch R and Hofstetter A (1996) Early clinical experience with 5-aminolaevulinic acid for the photodynamic therapy of superficial cancer. *Br J Urol* 77: 667-671
- Leveckis J, Burn JL, Brown NJ and Reed MWR (1994) Kinetics of endogenous protoporphyrin IX induction by aminolaevulinic acid: preliminary studies in the bladder. *J Urol* 152: 550-553
- Levi F (1993) Incidence of infiltrating cancer following superficial bladder carcinoma. *Int J Cancer* 55: 419-421
- Loh CS, Vernon D, MacRobert AJ, Bedwell J, Bown SG and Brown SB (1993) Endogenous porphyrin distribution induced by 5-aminolaevulinic acid in tissue layers of the gastrointestinal tract. *Photochem Photobiol* 20: 47-54
- Marti A, Lange N, van den Bergh H, Sedmera D, Jichlinski P and Kuchera P (1998) Optimisation of the formation and distribution of protoporphyrin IX in the urothelium: an in vitro approach. *J Urol* (in press)
- Moan J, Streckyte G, Bagdonas S, Bech O and Berg K (1997) Photobleaching of protoporphyrin IX in cells incubated with 5-aminolaevulinic acid. *Int J Cancer* 70: 90-97
- Mostofio FK, Sobin LH and Torloni H (1973) Histological typing of urinary bladder tumors. In *International Histological Classification of Tumors*. World Health Organization Geneva
- Nagy GK, Frable WJ and Murphy WM (1982) Classification of premalignant urothelial abnormalities: A Delphi study of the National Bladder Cancer Collaborative Group A. In Sommers SC and Rosen PP (eds) pp. 219-233 Appleton: Norwalk, CT
- Novo M, Huettmann G and Diddens H (1996) Chemical instability of 5-aminolaevulinic acid used in the fluorescence diagnosis of bladder tumours. *J Photochem Photobiol B* 34: 143-148
- Orenstein A, Kostenich G, Tsur H, Roitman L, Ehrenberg B and Malik Z (1995) Photodynamic therapy of human skin tumors using topical application of 5-aminolaevulinic acid, DMSO and EDTA. *Proc SPIE* 2325: 100-105
- Ortel B, Tanew A and Honigsmann H (1993) Lethal photosensitization by endogenous porphyrins of PAM cell-modification by desferrioxamine. *J Photochem Photobiol B* 17: 273-278
- Peng Q, Moan J, Warlow T, Nesland JM and Rimington C (1992) Distribution and photosensitizing efficiency of porphyrins induced by application of endogenous 5-aminolaevulinic acid in mice bearing mammary carcinoma. *Int J Cancer* 52: 433-443
- Peng Q, Warloe T, Moan J, Heyerdahl H, Steen HB, Nesland JM and Giercksky KE (1995) Distribution of 5-aminolaevulinic acid-induced porphyrins in noduloulcerative basal cell carcinoma. *Photochem Photobiol* 62: 906-913
- Peng Q, Moan J, Warloe T, Irani V, Steen HB, Bjørseth A and Nesland JM (1996) Build-up of esterified aminolaevulinic-acid-derivative-induced porphyrin fluorescence in normal mouse skin. *J Photochem Photobiol B* 34: 96-96
- Rebeiz N, Arkins S, Rebeiz CA, Simon J, Zachary JF and Kelly KW (1996) Induction of tumour necrosis by 8-aminolaevulinic acid and 1,10-phenanthroline photodynamic therapy. *Cancer Res* 56: 339-344
- Richie JP, Shipley WU and Yagoda A (1989) Cancer of the bladder. In *Cancer Principles and Practice of Oncology*, De Vita VT, Hellmann S and Rosenberg SA (eds), pp. 1008-1020. JB Lippincott: Philadelphia
- Rick K, Sroka R, Stepp H, Kriegmair M, Huber RM and Baumgartner R (1997) Pharmacokinetics of 5-aminolaevulinic acid-induced protoporphyrin IX in skin and blood. *J Photochem Photobiol B* 40: 319-313
- Rotomski R, Bagdonas S and Streckyte G (1996) Spectroscopic studies of photobleaching and photoproduct formation of porphyrins used in tumour therapy. *J Photochem Photobiol B* 33: 61-67

- Schoenfeld N, Mamet R, Norenberg Y, Shafran M, Babuskin T and Malik Z (1994) Protoporphyrin biosynthesis in melanoma B 16 cells stimulated by 5-aminolaevulinic acid and chemical inducers: characterization of photodynamic inactivation. *Int J Cancer* 56: 106-112
- Steinbach P, Kriegsmair M, Baumgartner R, Hofstadter F and Kneuchel R (1994) Intravesical instillation of 5-aminolaevulinic acid: the fluorescent metabolite is limited to urothelial cells. *Urology* 44: 676-681
- Svanberg K, Andersson T, Killander D, Wang I, Stenram U, Andersson-Engels S, Berg R, Johansson J and Svanberg S (1994) Photodynamic therapy of non-melanoma malignant tumors of the skin using topical d-aminolaevulinic acid sensitization and laser irradiation. *Br J Dermatol* 130: 743-751
- Takeya H (1992) Preparation of 5-aminolaevulinic acid alkyl esters as herbicides. *Chem Abstr* 116: P189633
- Tyrell RM, Pourzand C and van den Bergh H (1993) Unpublished results
- Wagnière S, Hadjur C, Grosjean P, Braichotte D, Savary JF, Monnier P and van den Bergh H (1998) Clinical evaluation of cutaneous phototoxicity of 5, 10, 15, 20-tetra (m-hydroxyphenyl) chlorin. *Photochem Photobiol* 68: 382-387
- Warloe T, Peng Q, Steen HB and Gierchsky KE (1992) Localization of porphyrins in human basal cell carcinoma and normal tissue induced by topical application of 5-aminolaevulinic acid. In *Photodynamic Therapy and Biomedical Lasers*, Spinelli P, Dal Fante M and Marchesini R (eds), pp. 454-458. Elsevier Science: Amsterdam
- Warloe T, Peng Q, Heyerdahl H, Moan J, Stenn HB and Gierchsky KE (1995) Photodynamic therapy with 5-aminolaevulinic acid induced porphyrins and DMSO/EDTA for basal cell carcinoma. *Proc SPIE* 2371: 226-235

## Down-regulation of TGF- $\beta$ receptors in human colorectal cancer: implications for cancer development

M Matsushita<sup>1</sup>, K Matsuzaki<sup>1</sup>, M Date<sup>1</sup>, T Watanabe<sup>1</sup>, K Shibano<sup>1</sup>, T Nakagawa<sup>1</sup>, S Yanagitani<sup>1</sup>, Y Amoh<sup>1</sup>, H Takemoto<sup>1</sup>, N Ogata<sup>2</sup>, C Yamamoto<sup>2</sup>, Y Kubota<sup>1</sup>, T Seki<sup>1</sup>, H Inokuchi<sup>3</sup>, M Nishizawa<sup>4</sup>, H Takada<sup>5</sup>, T Sawamura<sup>1</sup>, A Okamura<sup>6</sup> and K Inoue<sup>1</sup>

<sup>1</sup>Third Department of Internal Medicine, Kansai Medical University, Moriguchi, Osaka, Japan; <sup>2</sup>Department of Ophthalmology, Kansai Medical University, Moriguchi, Osaka, Japan; <sup>3</sup>Department of Gastroenterology, Saiseikai Noe Hospital, Osaka, Japan; <sup>4</sup>Department of Medical Chemistry, Kansai Medical University, Moriguchi, Osaka, Japan; <sup>5</sup>Second Department of Surgery, Kansai Medical University, Moriguchi, Osaka, Japan; <sup>6</sup>Department of Surgical Pathology, Kansai Medical University, Moriguchi, Osaka, Japan

**Summary** Many colorectal cancer cells are resistant to the anti-proliferative effects of transforming growth factor- $\beta$  (TGF- $\beta$ ). TGF- $\beta$  also acts as paracrine factor from cancer cells on their mesenchymal cells. The aim of this study was to examine the expression of TGF- $\beta$  and its receptors in human colorectal cancer tissue and determine any relationship with cancer growth. In situ hybridization and Northern blot hybridization detection of TGF- $\beta$ , type I and type II receptor mRNA and immunohistochemical staining of TGF- $\beta$ , were performed using 11 human colorectal adenomas, 22 colorectal cancers and ten normal colorectal mucosas as control. TGF- $\beta$  receptor mRNAs were expressed mainly by normal colorectal epithelial cells and adenoma. However, mRNAs for TGF- $\beta$  receptors were only faintly, if at all, expressed in eight of 22 human colorectal cancers. In addition, intense signals of TGF- $\beta$ , mRNA and the protein were detected in all colorectal cancers. TGF- $\beta$  receptor mRNAs and TGF- $\beta$ , protein were also distributed in fibroblasts and endothelial cells in the interstitium. Moreover, Smad 4 protein was translocated to nucleus in primarily cultured adenoma cells, but not in cancer cells after TGF- $\beta$  stimulation. The escape of human colon cancer from TGF- $\beta$ -mediated growth inhibition by down-regulation of TGF- $\beta$  receptors as well as the effects of TGF- $\beta$  on stroma formation and angiogenesis indicate a possible role for TGF- $\beta$  in the progression of colon cancer in an intact host.

**Keywords:** TGF- $\beta$ ; TGF- $\beta$  receptor; Smad, colorectal cancer; colorectal adenoma

The transforming growth factor beta (TGF- $\beta$ )/activin superfamily is comprised of multifunctional and ubiquitous peptides with roles in many areas of cell biology. Three different isoforms of TGF- $\beta$ , designated as TGF- $\beta$ <sub>1</sub>, - $\beta$ <sub>2</sub> and - $\beta$ <sub>3</sub>, with similar but not identical biological activities, have been identified in various mammalian tissues and cells (Barnard et al, 1990; Sporn et al, 1992). The intracellular biological effects of TGF- $\beta$  are initiated following ligand binding to oligomeric complexes of high affinity TGF- $\beta$  type I and type II receptors (TGF- $\beta$  RI and TGF- $\beta$  RII). If one of the receptors is absent or inactivated, the cells lose their responsiveness to TGF- $\beta$ . cDNAs encoding mammalian type II receptor for TGF- $\beta$  and activin have been cloned, and each of these receptors is a transmembrane serine/threonine kinase (Mathew et al, 1991; Lin et al, 1992). Using polymerase chain reaction (PCR) cloning approaches, a series of novel serine/threonine kinase receptors (SKRs) and activin-receptor-like kinases (ALKs) have been identified (He et al, 1993; ten Dijke et al, 1993; Matsuzaki et al, 1993; Xu et al, 1994). ALK-5 has been shown to be a signalling type I receptor for TGF- $\beta$  (Franzen et al, 1993), whereas SKR1 and SKR2 have been shown to be activin type I receptors (ten Dijke et

al, 1994; Xu et al, 1995; Matsuzaki et al, 1996). The type I receptor kinase domains are more similar to each other than they are to the type II receptor kinase domains. Signalling by these receptors is mediated by the recently identified Smad protein family. Upon phosphorylation by activated receptors, Smads form complexes, move into the nucleus, associate with DNA-binding proteins and activate gene transcription (Massagué et al, 1997).

One of the most prominent effects of TGF- $\beta$  in vitro is a pronounced inhibition of epithelial cell growth (Robert et al, 1985). However, it is well known that cancers typically demonstrate resistance to the growth inhibitory effect of TGF- $\beta$  (Serra et al, 1996). In the colorectal adenoma–carcinoma sequence (Muto et al, 1975), the conversion of the non-tumorigenic phenotype of human colonic adenoma cell lines to the tumorigenic phenotype is accompanied by a reduced response to the growth inhibitory effects of TGF- $\beta$  (Manning et al, 1991). Furthermore, most colon cancer cells are resistant to the anti-proliferative effects of TGF- $\beta$  (Hoosein et al, 1989). Loss of the growth inhibitory response to TGF- $\beta$  at the cellular level is probably a more important step in the malignant progression. In addition, possible mechanisms by which TGF- $\beta$  facilitates the progression of tumour growth include immunosuppression, angiogenesis and changes in the extracellular matrix (Sporn et al, 1988).

Modulation of growth factor effects can be achieved by various mechanisms, including changes in ligand concentration, activation of latent forms of the ligand, modulation of number and affinity of

Received 30 December 1997

Accepted 26 August 1998

Correspondence to: K Matsuzaki, Third Department of Internal Medicine, Kansai Medical University, Fumizoncho 10-15, Moriguchi, Osaka 570-8506, Japan



## 5-Aminolevulinic acid and its derivatives: physical chemical properties and protoporphyrin IX formation in cultured cells

Pascal Uehlinger<sup>a</sup>, Matthieu Zellweger<sup>a</sup>, Georges Wagnières<sup>a</sup>, Lucienne Juillerat-Jeanneret<sup>b</sup>, Hubert van den Bergh<sup>a</sup>, Norbert Lange<sup>a,\*</sup>

<sup>a</sup> Institute of Environmental Engineering, Swiss Federal Institute of Technology (EPFL), CH-1015 Lausanne, Switzerland

<sup>b</sup> Institute of Pathology, CHUV Hospital, CH-1011 Lausanne, Switzerland

Received 29 March 1999; accepted 8 December 1999

### Abstract

Protoporphyrin IX (PpIX) is used as a fluorescence marker and photosensitizing agent in photodynamic therapy (PDT). A temporary increase of PpIX in tissues can be obtained by administration of 5-aminolevulinic acid (ALA). Lipophilicity is one of the key parameters defining the bioavailability of a topically applied drug. In the present work, octanol–water partition coefficients of ALA and several of its esters have been determined to obtain a parameter related to their lipophilicity. The influence of parameters such as lipophilicity, concentration, time, and pH value on PpIX formation induced by ALA and its esters is then investigated in human cell lines originating from the lung and bladder. ALA esters are found to be more lipophilic than the free acid. The optimal concentration ( $c_{opt}$ , precursor concentration at which maximal PpIX accumulation is observed) is then measured for each precursor. Long-chained ALA esters are found to decrease the  $c_{opt}$  value by up to two orders of magnitude as compared to ALA. The reduction of PpIX formation observed at higher concentrations than  $c_{opt}$  is correlated to reduced cell viability as determined by measuring the mitochondrial activity. Under optimal conditions, the PpIX formation rate induced by the longer-chained esters is higher than that of ALA or the shorter-chained esters. A biphasic pH dependence on PpIX generation is observed for ALA and its derivatives. Maximal PpIX formation is measured under physiological conditions (pH 7.0–7.6), indicating that further enhancement of intracellular PpIX content may be achieved by adjusting the pharmaceutical formulation of ALA or its derivatives to these pH levels. ©2000 Elsevier Science S.A. All rights reserved.

**Keywords:** 5-Aminolevulinic acid; 5-Aminolevulinic acid esters; Photodynamic therapy (PDT); Fluorescence; Protoporphyrin IX; ALA esters; Lipophilicity

### 1. Introduction

The exogenously stimulated formation of intracellularly generated protoporphyrin IX (PpIX), a precursor of heme, is becoming one of the fastest developing areas in the field of photodynamic therapy (PDT) and fluorescence photodetection (PD) of malignant and non-malignant diseases (see Ref. [1] and references therein). In most clinical and pre-clinical studies, systemic or topical application of 5-aminolevulinic acid (ALA) is used to temporarily increase the concentration of PpIX in the target tissues. Administration of ALA, a metabolic precursor in the biosynthetic pathway of heme, bypasses the negative feedback control exerted by heme on the enzymatic step in ALA synthesis. Although PpIX formation is present in nearly every nucleated cell, preferential formation and accumulation of this photosensitizer

have been demonstrated in tissues known to have a high cellular turnover. The main reason for a somewhat selective PpIX accumulation in the latter cell types is still not completely understood. Experimental evidence has been found that, in some tumors, the ferrochelatase activity is reduced, while the activity of the porphobilinogen deaminase is enhanced [2,3]. For historical reasons [4] and due to the ease of administration to the skin of both drug and light, the main applications of ALA-mediated PpIX therapy are in dermatology. This modality is now in Phase III trials for the treatment of actinic keratosis and has also been employed clinically for the treatment of basal cell carcinoma. Recently, other medical fields, namely pulmonology [5], urology [6–9], gastroenterology [10], ENT [11], gynecology [12], and neurosurgery [13], have implemented this technique for the improved management of cancer. In addition to its tumor selectivity, the administration of ALA prevents prolonged cutaneous photosensitivity, one of the major drawbacks of some of the earlier photosensitizers [14].

\* Corresponding author. Fax: +41-21-693-3626; e-mail: norbert.lange@epfl.ch



Despite promising results, it appears that this methodology is open to quite significant improvement, in particular in the case of topically applied ALA. Since ALA is a hydrophilic molecule, its penetration through cellular membranes and into the interstitial space of tissues is low. Hence, ALA-induced PpIX formation is often limited to superficial tissue layers. Furthermore, PpIX formation shows considerable heterogeneity when ALA is applied topically. Both inhomogeneous and limited tissue distribution result in nonefficient treatment of deeper-lying or nodular lesions, even if light in the red region of the PpIX absorption spectrum is used [15,16]. Since deeper-lying lesions are often not accessible by PDT, they are missed after topical application of ALA. Consequently, relatively high doses of ALA have to be applied over long periods of time, increasing the risk of complications [17,18].

Due to these drawbacks, PpIX-mediated PDT and diagnosis have recently been started with more lipophilic derivatives of ALA in order to enhance the poor bioavailability of ALA. Several groups have shown that using such ALA prodrugs may enhance the PpIX concentration by up to two orders of magnitude as compared with the parent molecule [19–23].

Since lipophilicity is one of the key parameters, in the present study the octanol–water partition coefficient  $P$  of some alkyl esters has been determined as a measure related to this property. With the final goal of defining clinical protocols with improved bioavailability of ALA, we investigated the impact of lipophilicity, pH value, concentration and duration of exposure of ALA and its derivatives on PpIX formation and cell viability. This was performed by means of fluorescence spectroscopy of PpIX using four different human cell lines. It was demonstrated that long-chained ALA derivatives and physiological pH values resulted in the highest relative fluorescence values. Using ALA derivatives, the choice of the optimal concentration of the PpIX precursor was shown to be of major importance for cell viability and maximal PpIX formation.

## 2. Materials and methods

### 2.1. Chemicals

ALA hydrochloride, ALA-methylester hydrochloride (m-ALA), (3-4,5-dimethylthiazol-yl)-2,5-diphenyl tetrazolium bromide (MTT), and *n*-octanol were purchased from Sigma (Fluka, Buchs, Switzerland). 0.1 N NaOH was obtained from Merck (Darmstadt, Germany). Other ALA esters (Table 1) were synthesized in our laboratories following the procedure described recently by Kloek et al. [20].

### 2.2. Determination of physicochemical properties

The apparent partition coefficients ( $P$ ) of ALA and its esters were determined in an octanol–buffer system at 21°C.

Table 1

List of hydrochlorides of ALA and esters used for in vitro experiments ( $\text{HCl} \cdot \text{R}^2\text{N}-\text{CH}_2-\text{CO}-\text{CH}_2-\text{CH}_2\text{CO}-\text{OR}^1$  = general structure)

Compound	R <sup>1</sup>	R <sup>2</sup>	Mol. mass [g/mol]	Abbreviation
ALA	H	H	167.6	ALA
ALA-methylester	CH <sub>3</sub>	H	181.6	m-ALA
ALA-ethylester	CH <sub>2</sub> CH <sub>3</sub>	H	195.6	e-ALA
ALA-butylester	(CH <sub>2</sub> ) <sub>3</sub> CH <sub>3</sub>	H	223.8	b-ALA
ALA-hexylester	(CH <sub>2</sub> ) <sub>5</sub> CH <sub>3</sub>	H	251.8	h-ALA
ALA-octylester	(CH <sub>2</sub> ) <sub>7</sub> CH <sub>3</sub>	H	279.6	o-ALA
ALA-cyclohexylester	C <sub>6</sub> H <sub>11</sub>	H	249.8	ch-ALA

The aqueous phase was a 0.1 M phosphate buffer (PBS) solution of pH 7.4. The PBS solution and the octanol were mutually saturated before use by shaking 300 ml of PBS with an equal quantity of octanol for 30 min. Twenty milligrams of the compound to be investigated were dissolved in 10 ml of the aqueous phase and an equal quantity of octanol was added. The mixtures were shaken for about 30 min and left for phase separation overnight at 4°C. Absorption of both phases was measured with a UV–Vis absorption spectrometer (Cary 5, Varian, Australia) at 269 nm (see Fig. 1(a)). The partition coefficients  $P$  were calculated according to:

$$P = c_{\text{oct}}/c_{\text{PBS}} = \text{abs}_{\text{oct}}/\text{abs}_{\text{PBS}}$$

where  $c_{\text{oct}}$  and  $c_{\text{PBS}}$  represent the solute concentrations in the organic and the aqueous phase, respectively,  $\text{abs}_{\text{oct}}$  the absorption of the compound measured in the octanol and  $\text{abs}_{\text{PBS}}$  the absorption in the PBS solution (see Fig. 1(b)). The use of low concentrations and storage at low temperatures impaired the formation of dimerization products. The absence of these products was confirmed by the absence of characteristic absorption bands in the absorption spectrum of the measured solutions.

Values of acidity constants of ALA and its esters were measured by means of potentiometric titration with a standard

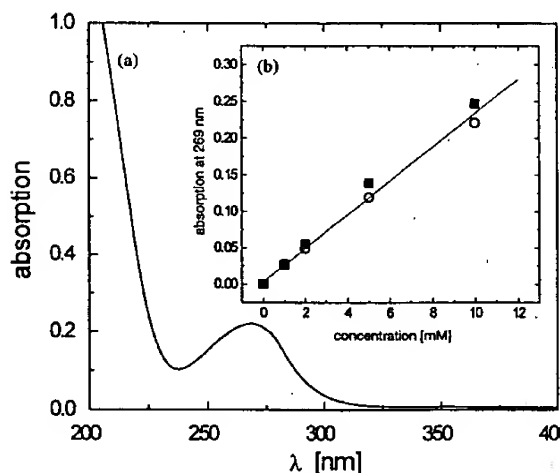


Fig. 1. (a) Absorption spectrum of b-ALA (10 mM) in PBS. (b) Absorption at 269 nm as a function of b-ALA concentration, (■) in PBS, (○) in octanol.

pH electrode (Bioblock, Frenkendorf, Switzerland). In brief, 20 mg of the corresponding drug were dissolved in 10 ml of demineralized water and titrated with 0.1 N NaOH solution. The pH of the solution was plotted against the total volume added.

### 2.3. PpIX fluorescence measurements

For fluorescence measurements, cells, subcultured in 48-well dishes, were exposed to various concentrations of the corresponding PpIX precursor and transferred into a thermostated fluorescence multiwell plate reader (CytoFluor Series 4000, PerSeptive Biosystems, Framingham, MA, USA, excitation wavelength,  $\lambda = 409 \pm 10$  nm, detection wavelength  $\lambda = 640 \pm 20$  nm). Correction for cell autofluorescence and other offset parameters was provided by five wells not exposed to the PpIX precursors. Reference was provided by 200  $\mu$ l of a Rhodamine 6G (0.1 g/l) (Lambda Physik, Göttingen, Germany) solution always present in one of the dishes.

### 2.4. Cell cultivation

All cell lines were from ATCC (Rockville, MD, USA) and grown as described. J82 and T24 cells were derived from human transitional cell carcinoma of the bladder, A549 cells from human lung carcinoma, and BEAS-2B cells were immortalized from normal human bronchial epithelium. Culture was performed in the presence in 10% fetal calf serum (FCS) and penicillin–streptomycin at 37°C and 6% CO<sub>2</sub> in a humid environment. For measurement purposes, the cells were subcultured in 48-well dishes (Costar 3548, Integra Biosciences, Cambridge, MA, USA) to give 10<sup>5</sup> cells/well 72 h prior to incubation with the ALA or one of its derivatives.

### 2.5. Determination of cell viability

The cell viability was tested by means of an MTT assay. This technique allows quantification of cell survival after cytotoxic insult by testing the enzymatic activity of the mitochondria. It is based on the reduction of the water-soluble tetrazolium salt to a purple, insoluble formazan derivative by mitochondrial enzyme dehydrogenases. This enzymatic function is only present in living, metabolically active cells. The optical density of the product was quantified by its absorption at 540 nm using a 96-well ELISA plate reader (iEMS Reader MF, Labsystems, USA). MTT, 0.5 mg/ml, was added to each well and incubated for 2 h at 37°C. The medium was then removed and the cells were washed with PBS solution. For cell lysis and dissolution of the formazan crystals formed, 250  $\mu$ l of isopropanol containing 1% 4 N HCl were added, and the absorption of each residue was determined by using the plate reader at 540 nm. Absorbance of the solution from cells incubated with ALA or its derivatives was divided by the absorption of the solution from the control cell plates to calculate the fraction of surviving cells.

### 2.6. Concentration and time dependence of PpIX formation

The influence of precursor concentration on the total amount of PpIX formed was measured by permanent incubation of the different cell lines with a given ALA derivative dissolved in PBS at pH 7.4. PpIX was measured 3 and 6 h after drug exposure. Concentration-dependent saturation of PpIX biosynthesis in A549 cell cultures was determined by using different concentrations (0.1–2 mM) of h-ALA. Cells were incubated with a medium containing 5% FCS and fluorescence measurements were carried out every 30 min during 24 h. The influence of the presence of FCS on the PpIX formation was examined by incubation of A549 cells with a 0.8 mM solution of h-ALA containing no, 1%, and 5% FCS, respectively. In order to correct all data for background autofluorescence, in each experiment six wells were incubated without any PpIX precursor.

### 2.7. Pharmacokinetic studies

PpIX formation in cells incubated with different derivatives of ALA was followed over a period of 5 h. For this purpose, the cells were incubated with the corresponding PpIX precursor at its optimal concentration (as determined according to the above-mentioned procedure). Measurements of fluorescence intensity were taken every 15 min.

### 2.8. pH Dependence of PpIX formation

The impact of initial extracellular pH was determined using solutions of ALA, h-ALA, and ch-ALA in sterile, isotonic NaCl (aq., 0.9%). The initial pH values, ranging between 5.5 and 8.5, were adjusted with 1 N NaOH for ALA and 0.1 N HCl for ALA derivatives. ALA and its derivatives were applied using concentrations lower than the optimal concentration, typically  $c_{\text{opt}}/2$ . Fluorescence intensity was measured immediately after incubation and again after 3 h. Cell viability was tested as described in Section 2.5.

## 3. Results and discussion

### 3.1. Physicochemical properties

The lipophilicity of ALA and its derivatives was assessed by measuring the apparent partition coefficient ( $P$ ) of the compounds between octanol and a PBS solution of pH 7.4. Table 2 summarizes the obtained log  $P$  values. The results plotted in Fig. 2 show that it is possible to vary the lipophilicity of ALA by more than three orders of magnitude when using ALA esters. The log  $P$  values of ALA and m-ALA are negative, representing the hydrophilic feature of these substances. Relative to ALA and m-ALA, all other esters are more lipophilic with positive log  $P$  values. Both ALA and its esters are highly protonated at pH 7.4 due to the 5-amino group. Therefore the apparent partition coefficient may be

Table 2

Log  $P$  and  $pK_a$  values for ALA and its derivatives.  $P$  is the partition coefficient between octanol and aqueous buffer solution (pH 7.4, 21°C)

Compound	log $P$	$pK_{a1}$	$pK_{a2}$
ALA	-1.51692	$4.1 \pm 0.1$	$8.7 \pm 0.2$
m-ALA	-0.94233		$8.4 \pm 0.3$
e-ALA	0.84113		$8.4 \pm 0.2$
b-ALA	1.42315		$8.3 \pm 0.1$
h-ALA	1.83883		$8.3 \pm 0.3$
o-ALA <sup>a</sup>	2.6199		
ch-ALA	1.49392		$8.3 \pm 0.2$

<sup>a</sup>  $pK_{a2}$  not measurable because of precipitation.

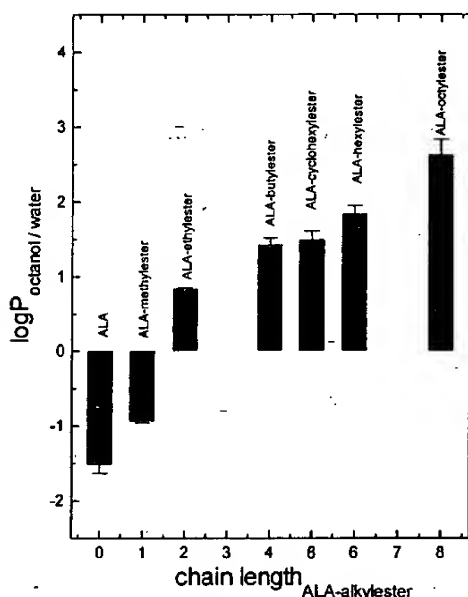


Fig. 2. Derived log  $P$  values for ALA and its derivatives.

dependent on the relative amount of uncharged molecules in the aqueous phase. The percentage of molecules with an unprotonated amino group can be calculated using the measured  $pK_a$  values (see Table 2). For the different derivatives, this percentage varies between 6 and 12%. The  $pK_{a1}$  and  $pK_{a2}$  values for ALA given in Table 2 are in good agreement with the results of Novo et al. [24]. The deprotonation of the amino group in o-ALA results in a reversible precipitation of the product in aqueous solution at pH ~ 8 and at a concentration around 20 mM. Furthermore, cleavage of some esters occurs in basic (pH > 9) solutions (data not shown) [25].

Systematic studies of Bridges et al. [26] with a series of homologue carbamates have shown a relatively constant absorption rate for compounds with log  $P$  values ranging between 0.8 and 2.8. However, carbamates with log  $P$  values less than 0.8 have shown reduced bladder-wall absorption. This suggests a higher tissue uptake for ALA esters containing two or more carbon atoms in their ester function.

Besides higher solubility of compounds with higher lipophilicity in creams and ointments, the data presented in Table

2 have additional impact for the use of ALA esters in dermatology. One of the principal functions of the skin, in particular the stratum corneum (SC), is to avoid the absorption of compounds that come in contact with the skin's surface. Using an approximation based on the analysis of 90 compounds [18], one can estimate the steady-state permeability coefficient  $K_p$  of ALA derivatives. It can be calculated that b-ALA will be transported about 50 times more efficiently into the skin than ALA while, using m-ALA, this uptake rate will only be doubled. However, the magnitude of  $P$  is important in terms of drug bioavailability. Substances that are too lipophilic may be accumulated in the SC, which consists primarily of free fatty acids, cholesterol, and ceramides. In order to obtain maximal flux across the entire skin, a balanced partition coefficient and good water and lipid solubility are required. Furthermore, the intrinsic solubility may be modified by co-diffusing formulation components.

Additionally, one should bear in mind that facilitated drug uptake does not automatically mean higher PpIX formation. Esters of ALA must be cleaved by esterases before entering the ordinary biosynthetic pathway of heme. These enzymes may have a more or less marked affinity to certain ester functions [21].

### 3.2. Influence of concentration on PpIX accumulation

The amount of porphyrin biosynthesis resulting from incubation of cells with ALA or its derivatives was determined by measuring the intensity of PpIX fluorescence.

All cell lines displayed the capability to produce PpIX when exposed to ALA or a prodrug given in Table 1. Since FCS has been shown to provoke efflux of PpIX in several cell lines [27], we incubated A549 cells with h-ALA for 5 h with and without FCS. Under our experimental conditions no influence of FCS on the total amount of PpIX generated has been found (see Table 3). The effect of concentration was assessed using ALA or ALA prodrug concentrations varying over two orders of magnitude. As shown in Fig. 3, there was a dose-dependent PpIX accumulation for each cell line and for each PpIX precursor used. The shape of the dose-response curves was similar in each case. While PpIX generation is positively correlated up to an optimal prodrug concentration ( $c_{opt}$ ) where the highest PpIX fluorescence levels occurred, PpIX generation decreases when this threshold concentration is exceeded. The absolute value of the optimal concentration varies with the type of prodrug and cell line. Except for the

Table 3

Influence of FCS on the PpIX formation in A549 cells after 5 h of incubation with 0.8 mM of h-ALA

FCS (%)	PpIX fluorescence [a.u.]
0	$680 \pm 150$
1	$670 \pm 170$
5	$680 \pm 140$

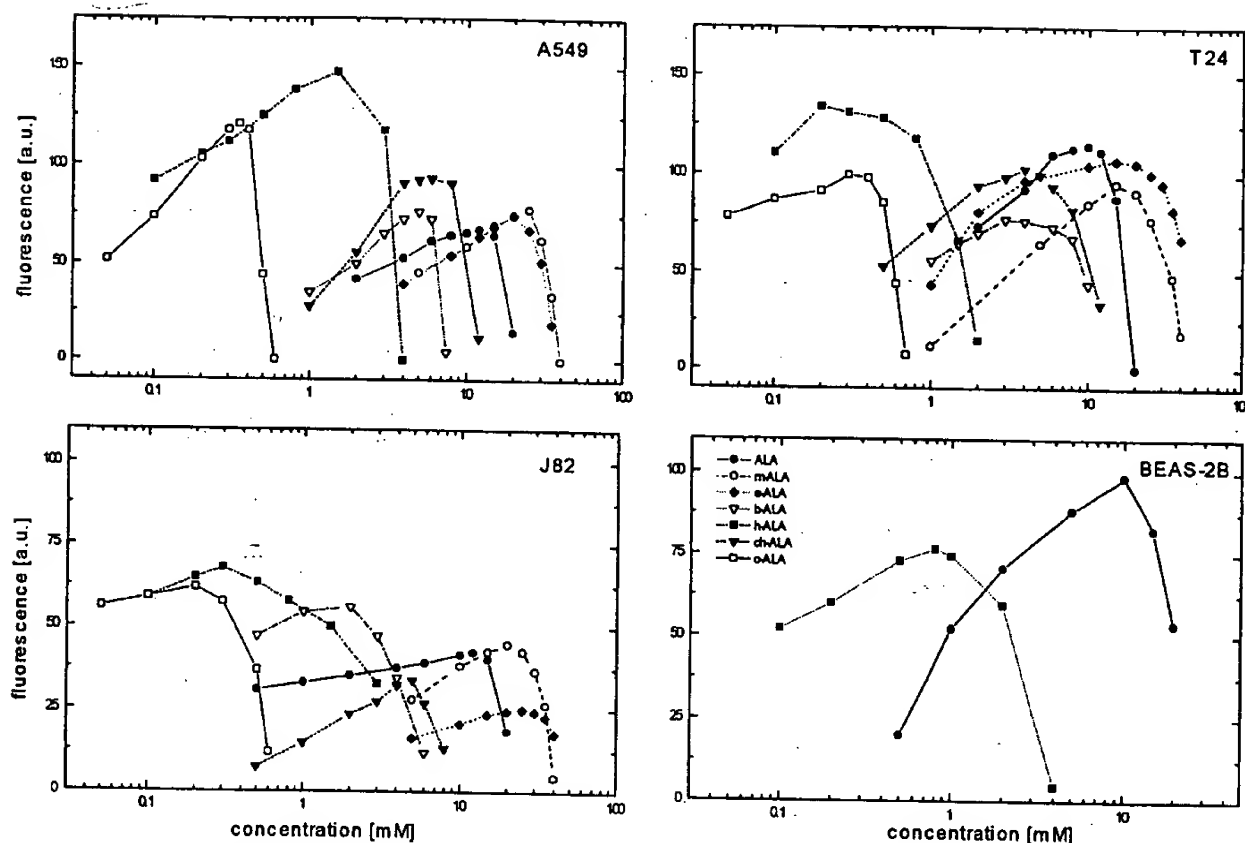


Fig. 3. Concentration dependence of PpIX accumulation for four different human cell lines after 3 h of incubation with ALA (●), m-ALA (○), e-ALA (◆), b-ALA (△), h-ALA (■), ch-ALA (▼), and o-ALA (□) (standard deviations (SD) have been omitted for the sake of clarity, see Fig. 5 for exemplary SD).

BEAS-2B cell line, incubation with h-ALA resulted in the highest fluorescence levels.

In general, the  $c_{opt}$  values for m-ALA and e-ALA were higher than for ALA. ALA esters with alkyl groups consisting of four carbon atoms or more (b-ALA, h-ALA, and o-ALA) showed their optimal PpIX formation at significantly lower  $c_{opt}$  values (Fig. 4). Furthermore, the bandwidth of the dose-response curves for these esters was always smaller than for ALA, m-ALA, or e-ALA (Fig. 3), indicating that the choice

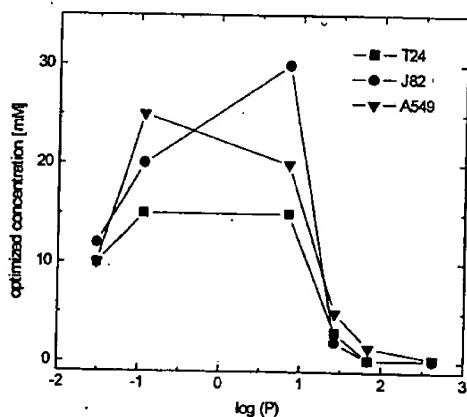


Fig. 4. Concentration of ALA and its derivatives needed to induce maximal PpIX accumulation after 3 h of incubation on A549 (▼), T24 (■), and J82 (○) cell lines. See also Table 3.

of the optimal concentration is crucial in order to guarantee an optimal PpIX generation.

Similar fluorescence intensity-concentration profiles were measured after 300 min of incubation (data not shown). Both the value of  $c_{opt}$  and the bandwidth of the dose-response curves remained unchanged. The long-term influence of permanent drug exposure on PpIX biosynthesis was tested by incubation of A549 cells with h-ALA, which has shown the most promising results under our conditions with respect to its dose-response behavior (Fig. 5). For concentrations smaller than  $c_{opt}$ , PpIX formation increases in a moderate sigmoidal way with incubation time (Fig. 5(a)). Under optimal conditions, continuously increasing PpIX accumulation can be observed for 24 h. Depending on the concentration, the linear part of these curves ends between 4 and 15 h and proceeds into a moderate plateau. For small concentrations the height of this plateau depends linearly on the concentration of h-ALA, whereas higher concentrations show a saturation of the PpIX biosynthesis (Fig. 5(b)). This might indicate a saturation of the enzymatic functions. However, higher concentrations than  $c_{opt}$  end with less PpIX formed, although no reduced cell viability has been determined under these conditions (see below).

No direct correlation between  $\log P$  and  $c_{opt}$  or the amount of PpIX produced can be noted from the data in the present work (Fig. 4). Excluding ch-ALA, however, a decrease of

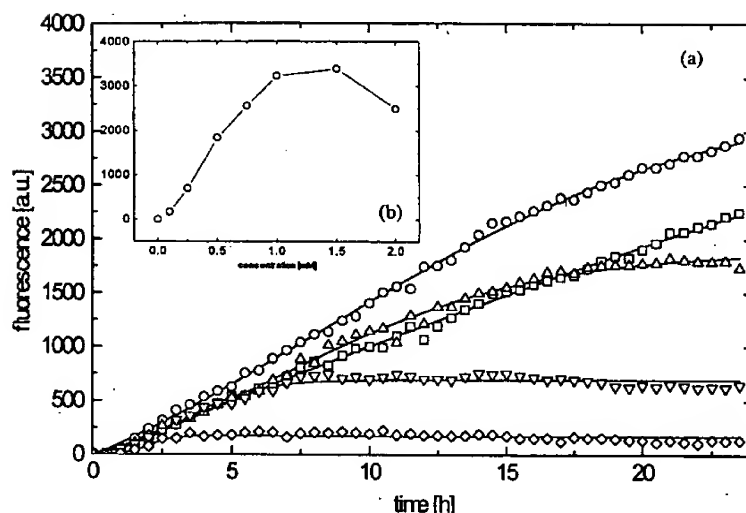


Fig. 5. (a) Pharmacokinetics of PpIX synthesis in A549 cells treated with different concentrations of h-ALA during 24 h of permanent drug exposure. Concentrations: 2 mM (□), 1.5 mM (○), 0.5 mM (△), 0.25 mM (▽), and 0.1 mM (◇). (b) PpIX formation after 24 h as a function of concentration of h-ALA solutions (for description see Section 2).

$c_{\text{opt}}$  with increasing chain length for lipophilic ALA derivatives (starting from e-ALA) can be established.

While long-chained derivatives ( $C \geq 4$ ) showed lower  $c_{\text{opt}}$  values than ALA, m-ALA as well as e-ALA seemed to be less efficient, although more lipophilic than ALA. The combination of two distinct processes may explain this behavior. While lipophilicity defines the transport of a drug across cell membranes, ALA esters must be cleaved by nonspecific esterases prior to entering the biosynthetic pathway of heme. Kloek et al. [21] have shown with cell lysates that enzymatic hydrolysis is faster for long-chained esters than for short-chained esters. This information might have an impact for further synthesis of derivatives of ALA. Such new prodrugs should have a similar lipophilicity to h-ALA or o-ALA and the enzymatic cleavage of the ester function should also be optimized. Derivatives of ALA can be adapted to specific esterases of tumor cells for further improvement of the selectivity of ALA-induced PpIX.

Similar dose-dependence characteristics have also been observed by other groups with ALA [28–32]. These groups found either a saturation of PpIX or a slight decrease of the resulting PpIX fluorescence with increasing ALA concentration. Gaullier et al. [22] observed an optimal concentration on different human and animal cell lines for long-chained ALA esters in the same order of magnitude as presented in this work. The more than twofold increase of the PpIX formation rate with ALA esters as compared with ALA is in good agreement with the results we recently obtained from measurements on an organ culture model [19]. Recently, Kloek et al. [21] compared the performance of different ALA derivatives on human lymphoma cell lines. They found that ALA pentyl ester induced the highest PpIX levels in intact cells, while h-ALA and b-ALA have shown similar fluorescence intensities after 6 h of incubation. However, in the course of their experiments, incubation was performed using

equimolar concentrations for all derivatives. Hence, it might be possible that for long-chained alkyl esters the concentration was too high to produce large amounts of PpIX.

The relative rate of PpIX generation increases with increasing lipophilicity of the corresponding ALA ester from m-ALA to h-ALA, whereas comparable rates of h-ALA and o-ALA suggest a saturation of some enzymatic functions in the biosynthetic pathway within these time ranges. Taking into account  $c_{\text{opt}}$ , which was 10–100 times lower for long-chained ALA esters than for ALA, it can be concluded that, using such compounds, the PpIX formation efficiency was enhanced by almost two orders of magnitude by simple chemical derivatization.

Since ALA is known to induce cytotoxic effects in cell culture [33–35], the PpIX accumulation observed was evaluated with respect to the cell viability after incubation with different concentrations of each PpIX precursor. It can be seen from Fig. 6 that the reduction of PpIX formation after incubation with drug doses higher than  $c_{\text{opt}}$  coincides with a reduced cell survival. This correlation was observed for all cell lines and prodrugs. Incubation with lower doses of ALA or its derivatives did not affect cell viability, as confirmed by the MTT test. From these experiments, it is obvious that only well-defined drug doses will improve the PpIX formation in clinical applications when using ALA esters instead of ALA.

### 3.3. pH Dependence of PpIX formation

It has been found that tumor tissues are generally more acidic than surrounding normal tissues. This is probably due to an overproduction of lactic acid and hydrolysis of adenosine triphosphate (ATP). Since this microenvironmental factor may influence PpIX generation, we incubated three cell lines with ALA, ch-ALA, and h-ALA solutions adjusted to pH values in the range between 5.5 and 8.5. In order to prevent

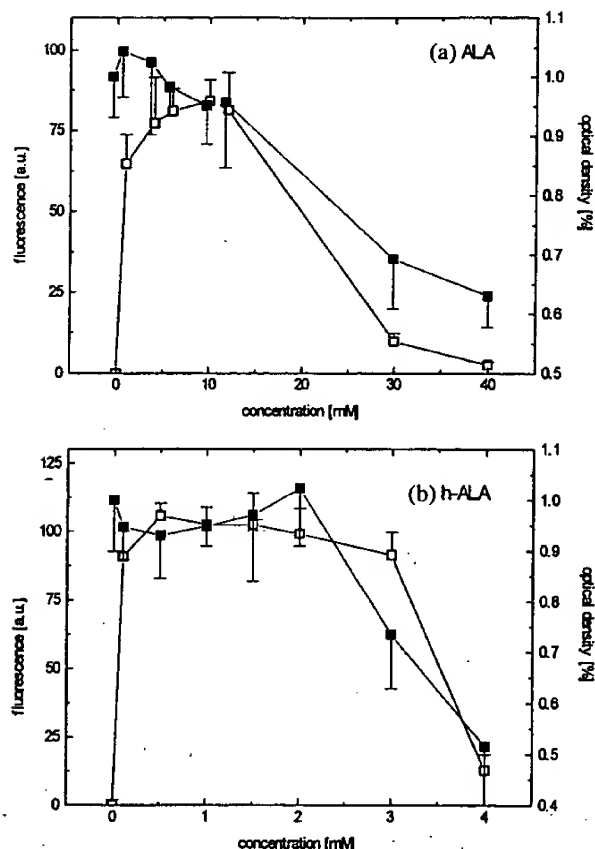


Fig. 6. Correlation of PpIX fluorescence intensity ( $\square$ ) and mitochondrial activity test by means of an MTT assay ( $\blacksquare$ ) in A549 cell for (a) ALA and (b) h-ALA (for description see Section 2).

saturation or cytotoxic effects provoked by the drug itself, concentrations lower than  $c_{\text{opt}}$  ( $c_{\text{opt}}/2$ ) were chosen. The values plotted in Fig. 7 indicate that optimal PpIX formation occurs at physiological pH values of around  $7.5 \pm 0.5$ . The total PpIX production approximately tripled at pH 7.4 compared with the production induced at pH 5.5. Due to proton release to the nonbuffered medium, the initial pH values decreased during incubation. While under alkaline conditions this effect was more marked ( $\Delta\text{pH} \sim 0.3/\text{h}$  at 8.5), the pH values under acidic conditions remained nearly unchanged ( $\Delta\text{pH} \sim 0.01/\text{h}$  at pH 6.5). Generally, PpIX production was more drastically reduced under acidic than under alkaline conditions, extending previously published results using ALA as a PpIX precursor [28,36,37]. While the decrease of PpIX formation at higher pH values can be attributed to a reduction of cell viability, the decrease under acidic conditions can be attributed to either a pH-dependent drug uptake or a reduced enzymatic activity in the biosynthesis of heme. As has been shown, ALA uptake is regulated by a pH-dependent ion pump that is more active at pH 5.0 [38]. Hence, PpIX production would be expected to increase under acidic conditions. However, it is known that intracellular pH is also downregulated when extracellular pH falls below 6.5 [39]. This might inhibit the activity of enzymes involved in the

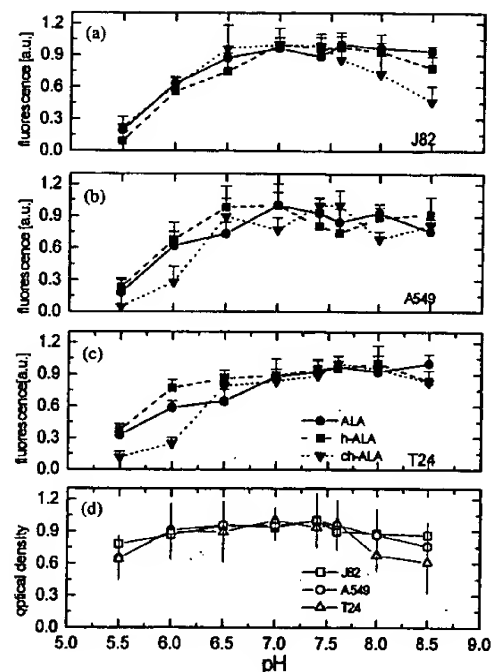


Fig. 7. PpIX formation as a function of initial pH values in (a) J82, (b) A549 and (c) T24 cell lines after 120 min of incubation with 0.1 mM h-ALA ( $\blacksquare$ ), 3.2 mM ch-ALA ( $\blacktriangledown$ ), and 5 mM ALA ( $\bullet$ ) solutions (fluorescence values are normalized to the maximum of fluorescence). (d) Mitochondrial activity test as a function of initial pH values.

biosynthetic pathway of heme, which have optimal activity between pH 7 and 7.5 [37]. A further indication for this pH-dependent intracellular process is given by the use of ALA esters, since a major part of these amphiphilic compounds will be taken up actively, as demonstrated by inhibitory tests [40].

From these experiments, it can be concluded that, for diagnostic as well as for therapeutic reasons, ALA formulations adjusted to physiological pH values should be applied. However, the instability of ALA implies the administration of ALA solution adjusted to lower pH values for the photodetection of early human bladder cancer in urology [6–9,24]. Since these are physiological pH values for urothelial cells, the uptake of ALA may not be affected by solutions buffered to a pH of 5. In contrast, the production of PpIX under these conditions may be strongly dependent on this parameter. Novo and colleagues [24] have attributed the chemical instability of ALA to an irreversible dimerization of two parent molecules followed by an oxidation of the resulting dihydropyrazine derivative. Generally, the velocity of such bimolecular reactions is proportional to the product of the concentrations of the two involved reactants. Hence, under this assumption the drastic reduction of the concentration by a factor of about 20 [22] that is used with ALA esters enhances the stability of the corresponding solution by a factor of 400. This increase of stability opens the possibility for a further increase of PpIX formation after topical application of ALA derivatives by a simple adjustment of the pharmaceutical formulation to physiological pH values.



#### 4. Conclusions

In summary, this study shows that using esters of ALA instead of ALA indicates a promising route to improve many clinical applications of PpIX-mediated PDT and fluorescence photodetection. The faster intracellular build-up of PpIX and the drastically reduced concentration relative to ALA enables treatments with significantly lower doses and shorter application times. Therefore, a significant decrease in costs should be associated with the use of such esters. Faster production of PpIX and hence shorter instillation times may play an important role for commercialization of this technique. Moreover, the enhancement of lipophilicity, which has been achieved by esterification, will result in deeper penetration of the drug into targeted lesions after topical application and possibly also in a more homogeneous distribution of the resulting photosensitizer. Therefore, more efficient PDT mediated by such prodrugs will be possible. No direct relationship between lipophilicity and total PpIX build-up has been found, indicating that two different processes, uptake and ester cleavage, are necessary for efficient PpIX formation. Moreover, long-chained esters should always be applied with lower doses than ALA. In most cell lines h-ALA has shown the most efficient PpIX formation.

A further enhancement of PpIX formation can be obtained by an adjustment of applied ALA and ALA prodrug formulations to physiological pH values.

#### Acknowledgements

The authors would like to thank John-David Aubert (Division of Pulmonology, CHUV Hospital) for providing the BEAS-2B cell cultures and Pierrette Dessous l'église Mange (Institute of Pathology, CHUV Hospital) for her assistance in maintaining the different cell lines. We gratefully thank Yann Berger and Reinhardt Neier (Institute of Chemistry, University of Neuchâtel) for the synthesis of ALA cyclohexyl ester. This work was supported in part by the Swiss 'Fonds National' (Grant 20-50691.97), the Swiss National Priority Program in Optics, the Swiss Cancer Foundation, the Swiss Society for Multiple Sclerosis, and the 'Fonds Vaud-Geneva' for their financial support. N.L. would like to thank the Schering Research Foundation for providing his grant.

#### References

- [1] Q. Peng, K. Berg, J. Moan, M. Kongshaug, J.M. Nesland, 5-Aminolevulinic acid-based photodynamic therapy: principles and experimental research, *Photochem. Photobiol.* 65 (1997) 235–251.
- [2] M. Kondo, N. Hirota, T. Takaoka, M. Kajiwara, Heme-biosynthesis enzyme activities and porphyrin accumulation in normal and hepatoma cell lines of rats, *Cell Biol. Toxicol.* 9 (1993) 95–105.
- [3] P. Hinnen, F.W.M. De Rooij, M.L.F. van Velthuisen, A. Edixhoven, R. van Hillegersberg, H.W. Tilnaus, J.H.P. Wilson, P.D. Siersema, Biochemical basis of 5-aminolevulinic acid-induced protoporphyrin IX accumulation: a study in patients with (pre)malignant lesions of the esophagus, *Br. J. Cancer* 78 (1998) 679–682.
- [4] J.C. Kennedy, R.H. Pottier, Endogenous protoporphyrin IX, a clinically useful photosensitizer for photodynamic therapy, *J. Photochem. Photobiol. B: Biol.* 14 (1992) 275–292.
- [5] R. Baumgartner, R.M. Huber, H.-J. Schulz, H. Stepp, K. Rick, F. Gamarra, A. Leberig, C. Roth, Inhalation of 5-aminolevulinic acid: a new technique for fluorescence detection of early stage lung cancer, *J. Photochem. Photobiol. B: Biol.* 36 (1996) 167–174.
- [6] P. Jichlinski, M. Forrer, J. Mizet, T. Glanzmann, D. Braichotte, G. Wagnières, G. Zimmer, L. Guillou, F.M. Schmidlin, P. Graber, H. van den Bergh, H.-J. Leisinger, Clinical evaluation of a method for detecting superficial transitional cell carcinoma of the bladder by light-induced fluorescence of protoporphyrin IX following topical application of 5-aminolevulinic acid: preliminary results, *Lasers Surg. Med.* 20 (1997) 402–408.
- [7] A. Kriegmair, R. Baumgartner, R. Knuechel, P. Steinbach, A. Ehsan, W. Lumper, F. Hofstädter, A. Hofstetter, Fluorescence photodetection of neoplastic urothelial lesions following intravesical instillation of 5-aminolevulinic acid, *Urology* 44 (1994) 836–841.
- [8] M. Kriegmair, R. Baumgartner, W. Lumper, R. Waidelich, A. Hofstetter, Early clinical experience with 5-aminolevulinic acid for the photodynamic therapy of superficial bladder cancer, *Br. J. Urol.* 77 (1996) 667–671.
- [9] M. Kriegmair, R. Baumgartner, R. Knuechel, H. Stepp, P. Steinbach, F. Hofstaedter, A. Hofstetter, Detection of early bladder cancer by 5-aminolevulinic acid induced porphyrin fluorescence, *J. Urol.* 155 (1996) 105–110.
- [10] L. Gossner, M. Stolte, R. Sroka, K. Rick, A. May, E.G. Hahn, C. Ell, Photodynamic ablation of high-grade dysplasia and early cancer in Barrett's esophagus by means of 5-aminolevulinic acid, *Gastroenterology* 114 (1998) 448–455.
- [11] K.F.M. Fan, C. Hopper, P.M. Speight, G. Buonaccorsi, A.J. MacRobert, S.G. Bown, Photodynamic therapy using 5-aminolevulinic acid for premalignant and malignant lesions of the oral cavity, *Cancer* 78 (1996) 1374–1383.
- [12] P. Wyss, M. Fehr, H. van den Bergh, U. Haller, Feasibility of photodynamic endometrial ablation without anesthesia, *Int. J. Gynec. Obstet.* 60 (1998) 287–288.
- [13] W. Stummer, S. Stocker, S. Wagner, H. Stepp, C. Fritsch, C. Goetz, A.E. Goetz, R. Kieffmann, H.J. Reulen, Intraoperative detection of malignant glioma by 5-ALA-induced porphyrin fluorescence, *Neurosurgery* 42 (1998) 518–525.
- [14] G. Wagnières, C. Hadjur, P. Grosjean, D. Braichotte, J.-F. Savary, P. Monnier, H.v.d. Bergh, Clinical evaluation of the cutaneous phototoxicity of a second generation photosensitizer for PDT: mTHPC, *Photochem. Photobiol.* 68 (1998) 382–387.
- [15] S. Grönlund-Pakkanen, K. Mäkinen, M. Talja, A. Kuusisto, E. Alhava, The importance of fluorescence distribution and kinetics of ALA-induced PpIX in the bladder in photodynamic therapy, *J. Photochem. Photobiol. B: Biol.* 38 (1997) 269–273.
- [16] A. Martin, W.D. Tope, J.M. Grevelink, J.C. Starr, J.L. Fewkes, T.J. Flotte, T.F. Deutsch, R.R. Anderson, Lack of selectivity of protoporphyrin-IX fluorescence for basal-cell carcinoma after topical application of 5-aminolevulinic acid — implications for photodynamic treatment, *Arch. Dermatol. Res.* 287 (1995) 665–674.
- [17] J. Webber, D. Kessel, D. Fromm, Side-effects and photosensitization of human tissues after aminolevulinic acid, *J. Surg. Res.* 68 (1997) 31–37.
- [18] D.M. Fiedler, P.M. Eckl, B. Krammer, Does delta-aminolevulinic acid induce genotoxic effects, *J. Photochem. Photobiol. B: Biol.* 33 (1996) 39–44.
- [19] A. Marti, N. Lange, H. van den Bergh, D. Sedmera, P. Kucera, Optimisation of the formation and distribution of Protoporphyrin IX in the urothelium: an in vitro approach, *J. Urology* 162 (1999) 546–552.

- [20] J. Klock, G.M.J. Beijersbergen van Henegouwen, Prodrugs of 5-aminolevulinic acid for photodynamic therapy, *Photochem. Photobiol.* 64 (1996) 994–1000.
- [21] J. Klock, W. Akkermans, G.M.J. Beijersbergen van Henegouwen, Derivatives of 5-aminolevulinic acid for photodynamic therapy: enzymatic conversion into protoporphyrin, *Photochem. Photobiol.* 67 (1998) 150–154.
- [22] J.-M. Gaullier, K. Berg, Q. Peng, H. Anholt, P.K. Selbo, L.-W. Ma, J. Moan, Use of 5-aminolevulinic acid esters to improve photodynamic therapy on cells in culture, *Cancer Res.* 57 (1997) 1481–1486.
- [23] N. Lange, P. Jichlinski, M. Zellweger, M. Forrer, A. Marti, L. Guillou, P. Kucera, G. Wagnières, H. van den Bergh, Photodetection of early human bladder cancer based on the fluorescence of 5-aminolevulinic acid hexylester-induced protoporphyrin IX: a pilot study, *Br. J. Cancer* 80 (1999) 185–193.
- [24] M. Novo, G. Hüttmann, H. Diddens, Chemical instability of 5-aminolevulinic acid used in the fluorescence diagnosis of bladder tumours, *J. Photochem. Photobiol. B: Biol.* 34 (1996) 143–148.
- [25] R.O. Potts, R.H. Guy, The prediction of percutaneous penetration: a mechanistical model, in: R. Gurny, A. Teubner (Eds.), *Dermal and Transdermal Drug Delivery: New Insights and Perspectives*, Wissenschaftliche Verlagsgesellschaft, Stuttgart, 1993, pp. 153–160.
- [26] J.W. Bridges, N.S.E. Sargent, D.G. Upshall, Rapid absorption from the urinary bladder of a series of n-alkyl carbamate: a route for the recirculation of drug, *Br. J. Pharmacol.* 66 (1979) 283–289.
- [27] S. Iinuma, S.S. Farshi, B. Ortel, T. Hasan, A mechanistic study of cellular photodestruction with 5-aminolevulinic acid-induced porphyrin, *Br. J. Cancer* 70 (1994) 21–28.
- [28] B. Krammer, K. Ueberriegler, In vitro investigation of ALA-induced protoporphyrin IX, *J. Photochem. Photobiol. B: Biol.* 36 (1996) 121–126.
- [29] J. Moan, G. Streckyte, S. Bagdonas, O. Bech, K. Berg, Photobleaching of protoporphyrin IX in cells incubated with 5-aminolevulinic acid, *Int. J. Cancer* 70 (1997) 90–97.
- [30] F.M. Rossi, D.L. Campbell, R.H. Pottier, J.C. Kennedy, E.F. Gudgin Dickson, In vitro study on the potential use of 5-aminolevulinic acid mediated photodynamic therapy for gynaecological tumours, *Br. J. Cancer* 74 (1996) 881–887.
- [31] D. He, S. Behar, N. Nomura, S. Sassa, H.W. Liu, The effect of ALA and radiation on porphyrin/heme biosynthesis in endothelial cells, *Photochem. Photobiol.* 61 (1995) 656–661.
- [32] S.L. Gibson, J.J. Haves, T.H. Foster, R. Hilf, Time-dependent intracellular accumulation of d-aminolevulinic acid, induction of porphyrin synthesis and subsequent phototoxicity, *Photochem. Photobiol.* 65 (1997) 416–421.
- [33] C.G. Fraga, J. Onuki, F. Lucesoli, E.J. Bechara, P. Di Mascio, 5-Aminolevulinic acid mediates the in vivo and in vitro formation of 8-hydroxy-2'-deoxyguanosine in DNA, *Carcinogenesis* 15 (1994) 2241–2244.
- [34] M. Hermes-Lima, How do  $\text{Ca}^{2+}$  and 5-aminolevulinic acid-derived oxyradicals promote injury to isolated mitochondria?, *Free Radical Bio. Med.* 19 (1995) 381–390.
- [35] K. Beerg, H. Anholt, O. Bech, J. Moan, The influence of iron chelators on the accumulation of protoporphyrin IX in 5-aminolevulinic acid-treated cells, *Br. J. Cancer* 74 (1996) 688–697.
- [36] C. Fuchs, R. Riesenberger, J. Siebert, R. Baumgartner, pH-Dependent formation of 5-aminolevulinic acid-induced protoporphyrin IX in fibrosarcoma cells, *J. Photochem. Photobiol. B: Biol.* 40 (1997) 49–54.
- [37] L. Wyld, M.W.R. Reed, N.J. Brown, The influence of hypoxia and pH on aminolevulinic acid-induced photodynamic therapy in bladder cancer cells in vitro, *Br. J. Cancer* 77 (1998) 1621–1627.
- [38] M. Bermutz, C.G.S. Moretti, C. Stella, E. Ramos, A.d.C. Battle, Delta-aminolevulinic acid transport in *Saccharomyces cerevisiae*, *Int. J. Biochem.* 25 (1993) 1917–1924.
- [39] E. Musgrove, M. Seaman, D. Hedley, Relationship between cytoplasmic pH and proliferation during exponential growth and cellular quiescence, *Exp. Cell Res.* 172 (1987) 65–75.
- [40] E. Rud, G. Glederaas, S.B. Brown, J.A. Holroyd, D. Vernon, A. Hogset, J. Moan, K. Berg, Cellular uptake mechanisms for 5-aminolevulinic acid and 5-aminolevulinic methyl ester, 8th Congress Eur. Soc. Photobiol., Granada, Spain, Book of Abstracts, S136, 1999, p. 85.

# Comparative effect of ALA derivatives on protoporphyrin IX production in human and rat skin organ cultures

A Casas<sup>1</sup>, AM del C Batlle<sup>1</sup>, AR Butler<sup>2</sup>, D Robertson<sup>2</sup>, EH Brown<sup>2</sup>, A MacRobert<sup>3</sup> and PA Riley<sup>4</sup>

<sup>1</sup>CIPYP, CONICET and University of Buenos Aires, Argentina; <sup>2</sup>School of Chemistry, University of St Andrews, St Andrews, Fife, UK; <sup>3</sup>National Medical Laser Centre and <sup>4</sup>Department of Molecular Pathology, Royal Free and University College London Medical School, 46 Cleveland Street, London W1P 6DB, UK

**Summary** Samples of human and rat skin in short-term organ culture exposed to ALA or a range of hydrophobic derivatives were examined for their effect on the accumulation of protoporphyrin IX (PpIX) measured using fluorescence spectroscopy. With the exception of carbobenzyloxy-D-phenylalanyl-5-ALA-ethyl ester the data presented indicate that, in normal tissues, ALA derivatives generate protoporphyrin IX more slowly than ALA, suggesting that they are less rapidly taken up and/or converted to free ALA. However, the resultant depot effect may lead to the enhanced accumulation of porphyrin over long exposure periods, particularly in the case of ALA-methyl ester or ALA-hexyl ester, depending on the applied concentration and the exposed tissue. Addition of the iron chelator, CP94, greatly increased PpIX accumulation in human skin exposed to ALA, ALA-methyl ester and ALA-hexyl ester. The effect in rat skin was less marked.

**Keywords:** ALA; PDT; ALA derivatives; ALA esters; iron chelators; CP94

Photodynamic therapy (PDT) is a cancer treatment involving the irradiation of tissues that have been sensitized by a photosensitizing agent. A recent approach to PDT involves the use of 5-aminolaevulinic acid (ALA) to induce the endogenous synthesis of protoporphyrin IX (PpIX); its clinical use has been recently reviewed by Peng et al (1997).

The extent to which ALA-induced photosensitization is selective depends on the rates of synthesis and metabolism of PpIX (Fukuda et al, 1992). ALA-induced PpIX accumulation has been shown in some cases to be preferentially greater in tumour cells primarily due to the reduced activity of ferrochelatase, the enzyme catalysing the incorporation of ferrous iron (Van Hillegersberg et al, 1992), and a relative enhancement of deaminase activity (Navone et al, 1990).

In vitro evidence suggests that the enzymes of the haem synthetic pathway are constitutively expressed with the exception of ALA synthase, which regulates porphyrin production by modifying the intracellular availability of ALA (Washbrook et al, 1997). Exposure of cells to an external source of ALA results in enhanced porphyrin synthesis and the accumulation of PpIX. This accumulation of porphyrin is increased by inhibition of ferrochelatase, which can be brought about by the use of iron chelators (Berg et al, 1996).

Some iron chelators such as desferrioxamine (Ortel et al, 1993), EDTA (Hanania et al, 1992) and 2,2'-dipyridyl (Walter et al, 1997) have been investigated in order to enhance the quantity of PpIX produced from ALA application with some good results. Ortho-phenanthroline has also been employed (Rebeiz et al, 1992).

It has been previously found that the hydroxypyridinone iron chelator, 1,2-diethyl-3-hydroxypyridin-4-one (CP94), enhanced porphyrin fluorescence and photosensitivity in cell lines (Bech

et al, 1997), as well as doubling the PpIX content in the urothelium of normal bladder (Chang et al, 1997) and normal colon mucosa in rats, inducing an increased area of necrosis after PDT (Curnov et al, 1998).

Uptake of ALA from extracellular sources is an important determinant of PpIX accumulation. The mechanism of cellular uptake is not clear in eukaryotic cells, but some transporter mechanisms are inferred (Washbrook et al, 1997; Correa Garcia et al, 1998). Entry by diffusion may be limited by the hydrophilic nature of ALA. Therefore, derivatives rendered more hydrophobic by the addition of lipophilic moieties which can be cleaved by intracellular enzymes have been investigated as pro-drugs.

Some lipophilic molecules, such as esterified ALA derivatives, have been used both in human basal cell carcinomas (Peng et al, 1995), in nude mouse skin (Peng et al, 1996) and in human tumour cell lines (Gaullier et al, 1997), and a higher and more homogeneous tissue distribution was produced, compared to those of free ALA-induced porphyrins. In addition, Kloeck et al (1995, 1998) demonstrated both in cell lines and in animal models that several ALA pro-drugs are capable of being taken up, de-esterified and converted into PpIX with higher efficiency than ALA itself. However, Washbrook and Riley (1997) and Gaullier et al (1997) found in vitro that ALA-methyl ester (ALA-Me) is less effective than ALA at inducing the synthesis of PpIX.

The aim of this paper is to evaluate by ex-vivo fluorescence, employing skin explants, the capacity of the chelator CP94 and several esterified ALA derivatives of enhancing PpIX synthesis.

## MATERIALS AND METHODS

### Chemicals

ALA powder, ALA-Me (Sigma Chemical Co.) and ALA-hexyl ester (ALA-He) were dissolved in saline. All other ALA derivatives were dissolved in dimethyl sulphoxide (DMSO). The iron chelator CP94 was synthesized according to the procedure of

Received 9 October 1998  
Revised 4 February 1999  
Accepted 11 February 1999

Correspondence to: PA Riley

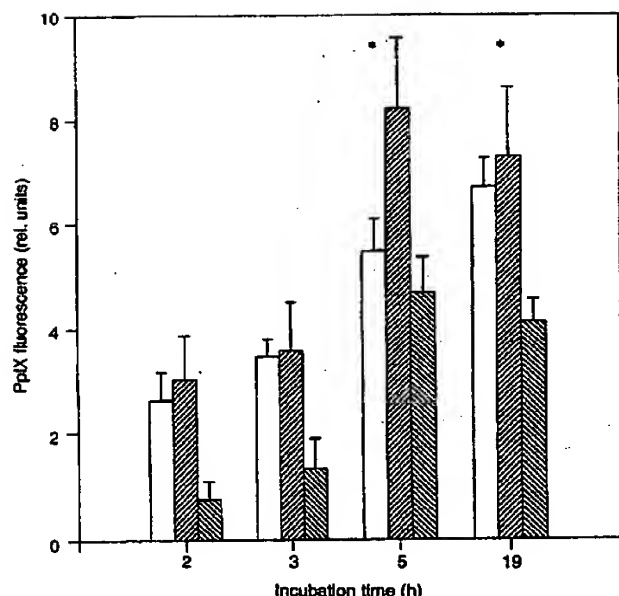


**Figure 3** PpIX fluorescence after exposure of rat skin explants to 0.6 mM ALA (□), ALA-He (▨) and ALA-Me (■) for 2, 3, 5 and 19 h. Direct skin fluorescence was measured at 410 nm excitation and 635 nm emission, and autofluorescence of explants incubated without ALA was subtracted. The bars show the means of four independent experiments performed in duplicate. Error bars show standard deviations. Asterisks denote  $P < 0.05$ .

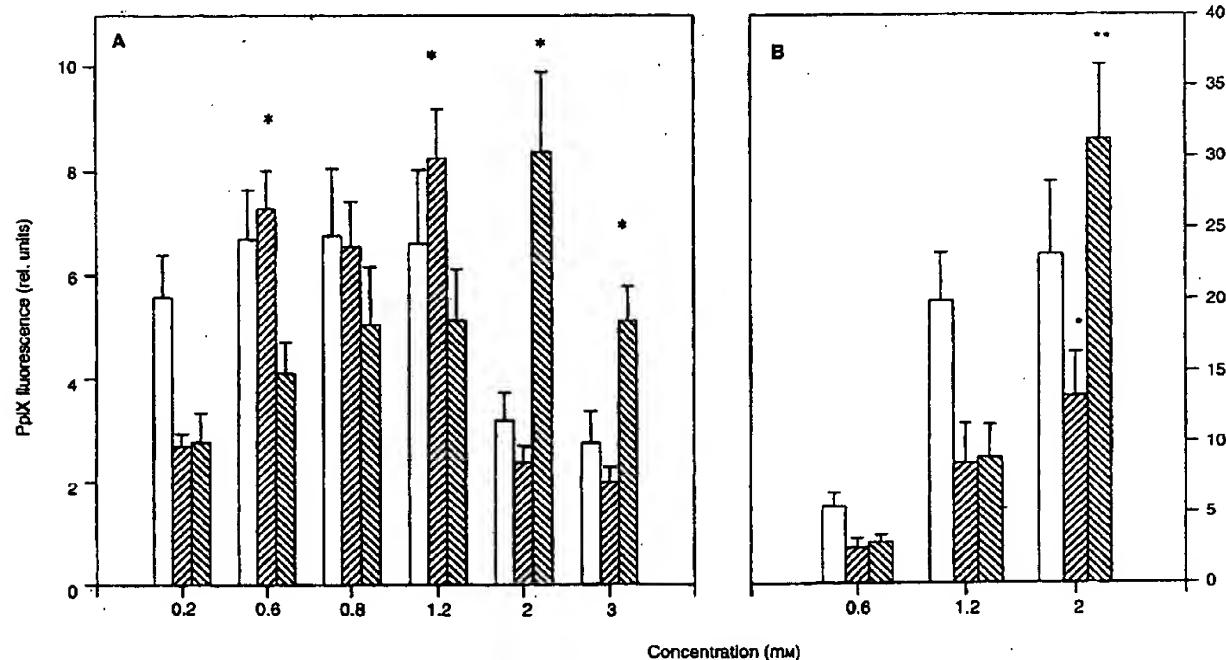
### CP94 enhancement of PpIX production

Figure 5A shows that the simultaneous exposure of rat skin explants to 0.6 mM ALA and CP94 results in a slight increase in PpIX fluorescence ( $P = 0.016$  at  $200 \mu\text{g ml}^{-1}$ ) but in human skin explants (Figure 5B) exposure to CP94 substantially increases the PpIX yield reaching a maximum of about eightfold at  $300 \mu\text{g ml}^{-1}$ . This effect was also observed at higher ALA concentrations although it was less marked, for example, using  $300 \mu\text{g ml}^{-1}$  CP94, 130% and 80% increases of PpIX were obtained on exposure of explants to 1.2 and 2 mM ALA respectively (data not shown). Moreover, CP94 elevated human skin PpIX production in presence of 1.2 mM ALA-He by sixfold and 50% on exposure to 2 mM ALA-Me.

Controls incubated in the presence of CP94 without ALA exhibited fluorescence values equal to those obtained in the absence of the iron chelator. CP94 addition to cultures did not elevate the percentage of release of hydrophilic porphyrins into the medium in any of the conditions studied.

### Fluorescence microscopy

Figure 6 shows CCD images of fluorescence in human skin explants after 19 h incubation with the hexyl ester derivative (ALA-He) at 1.2 mM with 0.6 mM CP94 and, for comparison, 1.2 mM ALA alone. In all the sections examined the fluorescence is highest in the epidermis. In rat skin a similar biodistribution was observed, although fluorescence associated with hair follicles was more evident than in the human samples. Autofluorescence was only detectable in the stratum corneum.



**Figure 4** PpIX fluorescence after 19 h exposure of rat (A) and human skin (B) to different concentrations of ALA (□), ALA-He (▨) and ALA-Me (■). Direct skin fluorescence was measured at 410 nm excitation and 635 nm emission, and autofluorescence of explants incubated without ALA was subtracted. The bars show the means of four independent experiments performed in duplicate. Error bars show standard deviations. One asterisk indicates  $P < 0.01$  and two,  $P < 0.001$  compared to the corresponding ALA concentration.



## Selective distribution of porphyrins in skin thick basal cell carcinoma after topical application of methyl 5-aminolevulinate

Qian Peng<sup>a,\*</sup>, Ana Maria Soler<sup>b</sup>, Trond Warloe<sup>b</sup>, Jahn M. Nesland<sup>a</sup>, Karl-Erik Giercksky<sup>b</sup>

<sup>a</sup>Department of Pathology, The Norwegian Radium Hospital, University of Oslo, Montebello, 0310 Oslo, Norway

<sup>b</sup>Department of Surgical Oncology, The Norwegian Radium Hospital, University of Oslo, Montebello, 0310 Oslo, Norway

Received 30 January 2001; accepted 4 July 2001

### Abstract

Topical photodynamic therapy (PDT) of superficial basal cell carcinoma (BCC) with 5-aminolevulinic acid (ALA) has achieved promising clinical results. However, the efficacy of this therapy for thick BCC is dramatically decreased by a limited diffusion of hydrophilic ALA into the tumor. Lipophilic esters of ALA may enhance their penetration into the lesion. In this randomized, open clinical study, microscopic fluorescence photometry incorporating a light-sensitive thermo-electrically cooled charge-coupled device (CCD) camera was employed to investigate the penetration of methyl 5-aminolevulinate-induced porphyrin fluorescence in thick BCC lesions. Both the distribution pattern and the amount of porphyrins in 32 lesions of 16 patients were studied after topical application of 16, 80 or 160 mg/g of methyl 5-aminolevulinate for 3 or 18 h. A highly selective and homogeneous distribution of methyl 5-aminolevulinate-induced porphyrin fluorescence was seen in all lesions studied, with much less fluorescence in the adjacent normal skin tissues. In lesions of up to 2 mm thickness the application of 160 mg/g methyl 5-aminolevulinate for 3 h showed the highest ratio of porphyrin fluorescence depth to tumor depth ( $0.98 \pm 0.04$ ), thus providing a biologic rationale for a clinical PDT trial with this regimen. © 2001 Elsevier Science B.V. All rights reserved.

**Keywords:** Basal cell carcinoma; Photodynamic therapy; Methyl 5-aminolevulinate; Porphyrin; Fluorescence; CCD camera

### 1. Introduction

Nonmelanotic skin cancer, primarily basal cell carcinoma (BCC), represents a major health concern [1,2]. BCC arises from the basal cell layer of the epidermis or its appendages. Current treatment for the disease includes Mohs' micrographic surgery, local excision, curettage and electrodesiccation, cryosurgery, radiotherapy and immunotherapy. Mohs' micrographic surgery may be suitable for large and infiltrating BCC lesions, while excisional surgery is used for small BCCs. Other modalities can be applied to patients in whom surgery is contraindicated. The goal of the treatment to be chosen is to provide patients with the safest, most cost-effective and curative therapy. However, none of the available methods are ideal with respect to convenience, cosmetic outcome and cost.

Photodynamic therapy (PDT) of cancer has developed during the past 25 years to become an important new clinical treatment modality [3]. This modality typically

involves systemic administration of a tumor-localizing photosensitizer. Subsequent activation of the photosensitizer by visible light mediates singlet oxygen-induced tumor destruction [3]. Photofrin-based PDT has recently been approved by regulatory agencies in many countries for several medical indications [3], and has also been applied successfully in dermatologic malignancies [4–6]. However, like most photosensitizers, Photofrin-PDT has a major side-effect of skin phototoxicity.

Because of the side-effects of Photofrin-PDT, considerable interest has recently been directed towards developing a new PDT regimen that relies on an endogenously synthesized sensitizer [7–9]. In the first step of the heme biosynthetic pathway, 5-aminolevulinic acid (ALA) is formed from glycine and succinyl CoA. The last step is the incorporation of iron into protoporphyrin IX (PpIX, a potent photosensitizer), which takes place in the mitochondria under the action of the enzyme ferrochelatase. By adding exogenous ALA, the naturally occurring PpIX may transiently accumulate because of the limited capacity of ferrochelatase. Furthermore, the activity of porphobilinogen deaminase, another enzyme of the heme synthesis

\*Corresponding author. Tel.: +47-2-293-5553; fax: +47-2-293-4832.  
 E-mail address: qian.peng@labmed.uio.no (Q. Peng).

Table 2  
Specific porphyrin fluorescence at different depths of the lesion (mean  $\pm$  S.E.)<sup>a</sup>

Depth ( $\mu$ m)	3 h			18 h		
	16 mg/g	80 mg/g	160 mg/g	16 mg/g	80 mg/g	160 mg/g
0–200	146 $\pm$ 19 (4) <sup>b</sup>	144 $\pm$ 20 (4)	228 $\pm$ 21 (6)	146 $\pm$ 14 (5)	456 $\pm$ 44 (5)	171 $\pm$ 15 (6)
201–400	318 $\pm$ 20 (4)	354 $\pm$ 27 (4)	345 $\pm$ 32 (6)	490 $\pm$ 8 (2)	695 $\pm$ 94 (5)	441 $\pm$ 43 (6)
401–600	460 $\pm$ 37 (4)	355 $\pm$ 18 (4)	324 $\pm$ 29 (6)	404 $\pm$ 6 (2)	658 $\pm$ 110 (5)	543 $\pm$ 38 (3)
601–800	177 $\pm$ 2 (4)	202 $\pm$ 11 (4)	262 $\pm$ 25 (6)	188 $\pm$ 14 (2)	635 $\pm$ 96 (4)	640 $\pm$ 99 (3)
801–1000	12 $\pm$ 1 (3)	189 $\pm$ 13 (4)	382 $\pm$ 31 (6)	163 (1)	381 $\pm$ 55 (4)	332 $\pm$ 32 (3)
1001–1200	°	230 $\pm$ 16 (3)	373 $\pm$ 15 (5)	30 (1)	461 $\pm$ 242 (3)	164 $\pm$ 85 (3)
1201–1400	°	74 $\pm$ 3 (3)	262 $\pm$ 4 (4)	°	822 (1)	177 (1)
1401–1600	°	°	116 $\pm$ 3 (2)	°	°	39 (1)
1601–1800	°	°	114 $\pm$ 4 (2)	°	°	40 (1)
1801–2000	°	°	46 (1)	°	°	108 (1)

<sup>a</sup> Background (740) of tissue autofluorescence was subtracted from all data.

<sup>b</sup> Number of measurements.

<sup>c</sup> No porphyrin fluorescence or no deeper lesions measurable.

time [3]. PDT with systemic application of Photofrin is an effective modality for treating superficial cutaneous tumors [9]. However, the main disadvantage of using Photofrin-PDT is the risk of prolonged skin phototoxicity. PDT based on topically applied ALA has recently shown promising results in the treatment of superficial skin disorders [9]. It is an easy and cheap procedure with no risk of cutaneous photosensitization. Topical ALA-PDT is, however, inefficient at treating thick BCC, with only about 50% cure rates achieved [9]. The reason for this is not entirely known, but our previous study has shown a very limited penetration of ALA-induced porphyrins into thick BCC lesions after topical application of 20% ALA for 3 h [12]. Similar results were also reported by others [24].

The present study demonstrates that porphyrin fluorescence induced by methyl 5-aminolevulinate is selectively and homogeneously distributed in thick BCC lesions with little fluorescence seen in the dermis (Fig. 1). Furthermore,

topical treatment with 160 mg/g methyl 5-aminolevulinate for 3 h or 80 mg/g for 18 h produced an adequate depth of porphyrin fluorescence throughout the thick tumors. The relative depth of porphyrin fluorescence for the two regimens was 98 and 88%, respectively, indicating an apparent improvement in the penetration depth of porphyrins into thick tumors compared with the other treatment regimens studied. This is also supported by our recent finding that a complete response rate of 82.4% was obtained after a 3-month follow-up in a group of 273 thick BCC lesions that had been PDT-treated with a 3-h topical application of 160 mg/g methyl 5-aminolevulinate following surface removal.

The normal epidermis showed much less methyl 5-aminolevulinate-induced porphyrins than the surrounding BCC lesions. This selectivity of methyl 5-aminolevulinate-induced porphyrins in the tumor is of clinical importance since it can reduce the phototoxic reactions of local healthy tissue to PDT. In addition, the production of porphyrins induced by methyl 5-aminolevulinate in normal epidermis is also dependent upon the application time. Application for 3 h induced much less porphyrins in normal epidermis than for 18 h, demonstrating a possibly reduced tumor selectivity of the porphyrins with a longer application time.

In conclusion, the application of 160 mg/g methyl 5-aminolevulinate for 3 h can induce porphyrin formation throughout the depth of thick BCC lesions (up to 2 mm) with high selectivity. This regimen should thus be explored for the photodynamic treatment of thick BCC in clinical trials.

#### Acknowledgements

We thank T. Stanescu and E. Angell-Petersen for excellent assistance and PhotoCure ASA for providing the Metvix cream.

Table 3  
Depth of porphyrin fluorescence in lesions

	3 h	18 h
<i>Lesion depth (mm) per dose of methyl 5-aminolevulinate: mean <math>\pm</math> S.E. (range)</i>		
16 mg/g	1.5 $\pm$ 0.26 (0.7–2.2)(5) <sup>a</sup>	1.0 $\pm$ 0.09 (0.8–1.2)(5)
80 mg/g	1.6 $\pm$ 0.21 (1.0–2.0)(5)	1.1 $\pm$ 0.07 (0.9–1.3)(5)
160 mg/g	1.4 $\pm$ 0.22 (0.6–2.0)(6)	1.2 $\pm$ 0.16 (0.9–1.9)(6)
<i>Depth of porphyrin fluorescence (mm) mean <math>\pm</math> S.E. (range)</i>		
16 mg/g	0.7 $\pm$ 0.18 (0.0–1.0)(5)	0.5 $\pm$ 0.19 (0.2–1.1)(5)
80 mg/g	1.0 $\pm$ 0.26 (0.0–1.4)(5)	1.0 $\pm$ 0.11 (0.6–1.3)(5)
160 mg/g	1.3 $\pm$ 0.21 (0.6–2.0)(6)	0.8 $\pm$ 0.24 (0.4–1.9)(6)
<i>Relative depth of porphyrin fluorescence (%) mean <math>\pm</math> S.E. (range)</i>		
16 mg/g	55.7 $\pm$ 16.4 (0–100)(5)	52.0 $\pm$ 19.7 (16.7–100)(5)
80 mg/g	61.5 $\pm$ 17.5 (0–100)(5)	88.2 $\pm$ 9.7 (50–100)(5)
160 mg/g	98.3 $\pm$ 1.7 (90–100)(6)	66.9 $\pm$ 14.9 (25–100)(6)

<sup>a</sup> Number of subjects measured.





## ON THE PHARMACOKINETICS OF TOPICALLY APPLIED 5-AMINOLEVULINIC ACID AND TWO OF ITS ESTERS

Johan MOAN\*, Li Wei MA and Vladimir IANI

Institute for Cancer Research, Oslo, Norway

The kinetics of protoporphyrin IX (PpIX) production in normal tissues and WiDr tumors of mice were studied after topical application of 5-aminolevulinic acid (ALA) and its methyl ester and hexyl ester. ALA and ALA esters were applied on a spot of 1.0 cm diameter on normal skin and on skin overlaying tumors. PpIX production was studied by fluorescence measurements. ALA induced PpIX not only on the spot of application but also on remote skin areas. This was not found for the ALA esters. They produced PpIX only on the spot of application. Thus, ALA, but neither its esters nor PpIX, is passing into the circulation. The time needed for ALA to enter the circulation through normal skin was about 5 hr. Even when looking normal, the skin overlaying tumors was more permeable to ALA than normal skin. Thus, when applied on the tumor, ALA induced PpIX on remote skin areas without any lag phase. Mainly, PpIX was found in all tissues although small amounts of a porphyrin with an excitation peak at about 400 nm, supposedly uroporphyrin and/or coproporphyrin, were found, notably in remote skin areas. An altered stratum corneum of the skin overlaying tumors probably contributes to the tumorselectivity, although in the present tumor system less PpIX was found in tumors than in muscles. This is probably related to biochemical and physiological conditions in this particular tumor, since i.p. injection of ALA also leads to less PpIX formation in the tumor than in skin/muscle tissue. Nevertheless, it seems evident that ALA can diffuse more easily from the skin surface and down to the vasculature in the tumor than in the normal tissue and that this leads to a higher concentration of PpIX in the tumor than would have been found if the physiological factors relevant for drug diffusion were the same for tumors as for skin/muscles.

© 2001 Wiley-Liss, Inc.

**Key words:** 5-aminolevulinic acid; protoporphyrin IX; photodynamic therapy; 5-aminolevulinic acid esters; pharmacology; transcutaneous penetration

5-aminolevulinic acid (ALA) is being topically applied for photodynamic therapy (PDT) of skin malignancies. Such ALA-PDT is based on the ALA induced production of the photosensitizer protoporphyrin IX (PpIX) in tumors. Several reports on pharmacokinetics, fluorescence and spectroscopy of PpIX induced by ALA, both in animal experiments and in humans, have been published.<sup>1–4</sup> In some cases, the ALA-induced PpIX production is tumor selective and in other cases it is not. It seems that the tumor selectivity is related to a number of factors such as high concentrations of the rate-limiting enzyme uroporphobilinogen desaminase (PBGD), low concentrations of ferrochelatase (FeC) and iron in tumors.<sup>5</sup> Physiological factors, such as a large interstitial space, a compromised blood flow and a poor lymphatic drainage, may also play roles. Finally, the skin barrier is certainly important for the penetration of ALA into tumors. It is likely that the stratum corneum constitutes the main barrier. Since the skin penetration of molecules of similar size increases with increasing lipophilicity,<sup>6,7</sup> ALA esters, which are more lipophilic than ALA itself, were introduced for ALA-PDT of skin tumors.<sup>8,9</sup> These esters seem to be more selectively producing PpIX in some tumors than ALA.<sup>10</sup>

In the present work, we have studied the PpIX production in normal tissues and in tumors of mice after topical application of ALA and ALA-esters. Their penetration through the skin and into the circulation was investigated by measuring PpIX formation at remote skin sites.

### MATERIAL AND METHODS

#### Chemicals

5-aminolevulinic acid (ALA) hydrochloride, 5-aminolevulinic acid methylester hydrochloride and 5-aminolevulinic acid hexylester hydrochloride were obtained from PhotoCure AS (Oslo, Norway).

#### Animals and tumor line

Female Balb/c athymic nude mice were obtained from Bomholtgaard (Ry, Denmark). At the start of the experiments, the mice were 7 to 8 weeks old, with an average body weight of 20–25 g. Three mice were housed per cage with autoclaved filter covers in a room with subdued light at constant temperature (24–26°C) and humidity (30–50%). Food and bedding were sterilized and the mice were given tap water ad libitum in sterilized bottles. Approximately  $5 \times 10^6$  WiDr cells (a human colon adenocarcinoma cell line) suspended in 0.04 ml of phosphate-buffered saline (PBS) were implanted subcutaneously on the flank of each mouse. The animals were anesthetized with subcutaneous injection of hypnorm dormicum (approximately 4 ml/kg body weight) to facilitate proper application of the cream. The animals woke up within 1 hr and appeared normally active during the ALA application.

#### ALA application

A cream was prepared using 20% wt/wt ALA, ALA methylester or ALA hexylester in an ointment (Unguentum, Merck, Darmstadt, Germany). Approximately 0.2 mg of the freshly prepared cream was applied on a single spot of 1 cm diameter on each mouse either on the tumor or on normal skin, and covered with adhesive dressing (opSite Flexigrid, Smith & Nephew Medical, Ltd., Hull, England). Measurements of PpIX were performed after different times of the creams application.

#### Fluorescence measurements

Fluorescence was measured by means of a Perkin Elmer LS50B luminescence spectrometer (Norwalk, CT). The fluorescence measurements were carried out through the transparent adhesive dressing. Spectra were recorded using a front-surface set-up, which gave a high *in vivo* fluorescence signal. A thin glass plate was gently applied on the site of examination of the mouse skin in order to avoid any movements of the skin surface. In some cases an optical fibre standard accessory was used. The fluorescence excitation wavelength was set at 407 nm, corresponding to the maximum of the Soret band of PpIX in cells. The excitation and emission slits were set at 5 and 10 nm, respectively. Scattered

**Abbreviations:** ALA, 5-aminolevulinic acid; PpIX, protoporphyrin IX; PDT, photodynamic therapy

Grant sponsor: The Norwegian Cancer Society.

\*Correspondence to: Department of Biophysics, Institute for Cancer Research, ullemkjausveien 70, 0310 Montebello, Oslo, Norway. Fax: +47 22 93 42 70. E-mail: johan.moan@labmed.uio.no

Received 11 September 2000; Revised 3 November 2000; Accepted 20 November 2000

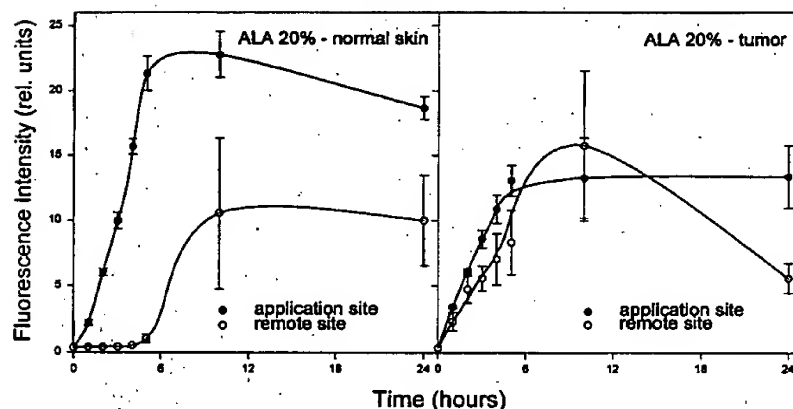


FIGURE 1 - PpIX formation after application of a 20% ALA cream on a spot of diameter 1.0 cm on either normal skin (left panel) or on tumors (right panel). The fluorescence was measured on the spot of ALA application and on a spot on the opposite flank of the mice. Data from 3 mice for each panel. The bars correspond to the standard error of the measurements.

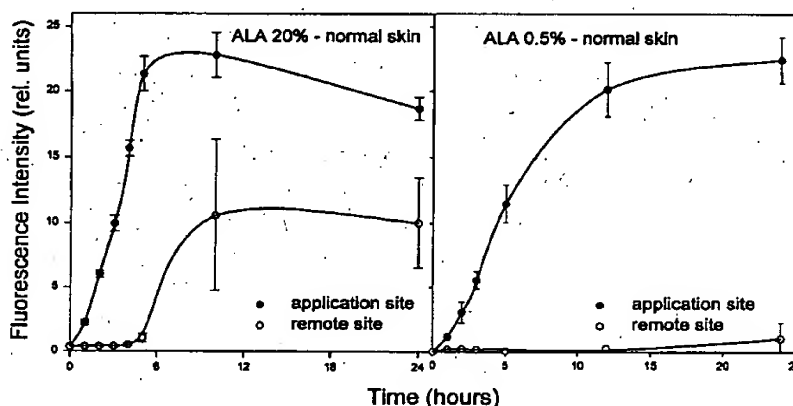


FIGURE 2 - PpIX formation after application of a 20% ALA or a 0.5 % ALA cream on a spot of diameter 1.0 cm of normal skin. The fluorescence was measured on the spots of ALA application and on the spots on the opposite flank of the mice.

excitation light was removed from the detected light with a 530 nm cut-off filter. Skin autofluorescence background was subtracted from all fluorescence spectra.

## RESULTS

When ALA was topically applied, either on control skin on the flank of the mice, or on a tumor localized on the flank, PpIX was produced not only on the spot of application, but also on the opposite flank of the mice (Fig. 1). The skin overlaying the tumors looked completely normal. During the first 5 hr of ALA application, PpIX was produced in the tumor as well as in normal tissue. Somewhat less was produced in the tumor, and the maximum was reached a few hours later (Fig. 1). After i.p. injection of 200 mg ALA per kg, PpIX was produced both in tumors and in normal tissues, reaching a maximum at 2 to 3 hr, and about half as much PpIX was produced in the tumor as in normal skin/muscle (data not shown). The kinetics of PpIX production on the flank opposite to that of ALA application were significantly different for tumors and normal tissues. For ALA application on normal tissue there was a delay of about 5 hr before PpIX started to appear on the opposite flank, and after that significantly less was produced on the

opposite flank than on the site of application. For application on the tumor, however, there was no delay and similar amounts of PpIX was produced on the opposite flank as on the tumor where ALA was applied (Fig. 1). Furthermore, interestingly, a low concentration of ALA (0.5 %) applied on control skin resulted in much less production of PpIX on the remote skin spot as compared with the application of 20 % ALA (Fig. 2).

When the methyl ester of ALA (ALA-Me) was applied, there was no PpIX production of the flank opposite to that on which ALA-Me was applied (Fig. 3). Application of ALA-Me gave rise to less PpIX than application of ALA did, but the tumor to normal tissue ratio was slightly, but not significantly, larger for ALA-Me than for ALA, i.e., 0.85 vs. 0.59 for ALA. Similar data were obtained for the hexyl ester of ALA (ALA-Hex) as for ALA-Me (Fig. 4), although application of ALA-Hex gave some more PpIX than application of ALA-Me did. For ALA-Hex the tumor to normal tissue ratio of PpIX fluorescence was 0.85, i.e., similar to that for ALA-Me.

The fluorescence excitation spectra were recorded 5 and 7 hr after ALA application. There was a slight difference, manifested as a more pronounced shoulder at about 400 nm, between the spectra at the site of application and those at the opposite flank (Fig. 5).

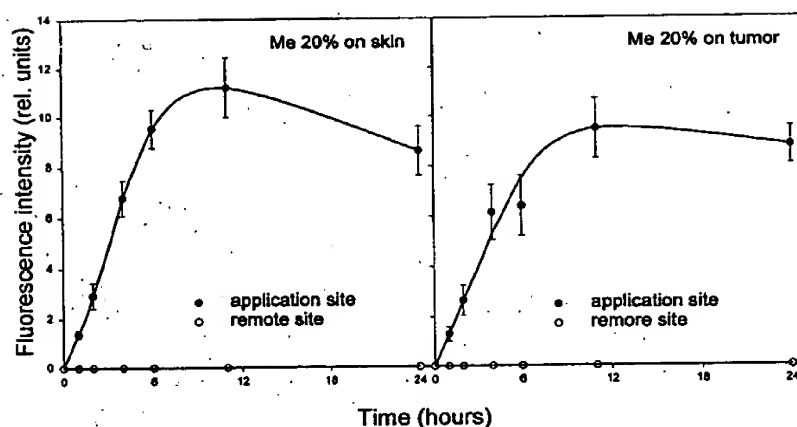


FIGURE 3 - PpIX formation after application of a cream containing 20% ALA-methylester (Me). For details, see the legend of Figure 1.

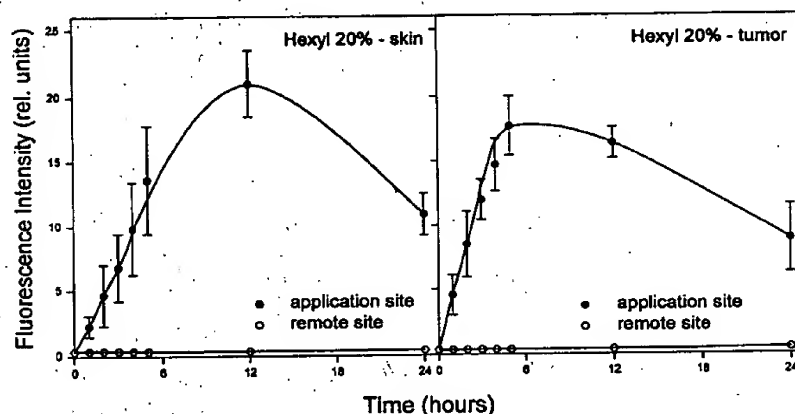


FIGURE 4 - PpIX formation after application of a cream containing 20% ALA-hexylester (Hexyl). For details, see the legend of Fig. 1.

#### DISCUSSION

The present work clearly shows that topical application of ALA leads to PpIX formation not only on the spot of application but also on remote skin areas of mice. There is a striking difference between ALA and the ALA esters in that the latter produce PpIX only on the spot of application. It is therefore clear that it is ALA that is transported via circulation and not PpIX nor any of its intermediate precursors in the heme synthesis from ALA. The same intermediates are likely to be formed also from the ALA esters. It is also clear that the ALA esters are not carried to remote sites by the circulation. These findings are in agreement with our earlier observations.<sup>10</sup>

Most likely the difference between ALA and the ALA esters is related to the differences in lipophilicity, the esters being more lipophilic than ALA. Thus, the octanol/water partition coefficients are about 0.03, 0.11 and 70 for ALA, ALA-Me and ALA-Hex, respectively.<sup>12</sup> According to a model for skin permeability,<sup>7</sup> the corresponding fluxes through the stratum corneum can be estimated to be 1, 5.3, and 2,700 in relative values, respectively. Apparently, the opposite is observed in the present work, namely,

that ALA goes more easily to the circulation than the esters do. This indicates that the esters bind to molecules in the supravascular tissue or become trapped in the tissue before they reach the circulation. It has been proposed that an optimal penetration depth relies on an intermediate lipophilicity: too low lipophilicity makes the penetration through the stratum corneum difficult, while too high lipophilicity leads to binding to the membranes and other lipid structures in tissues and therefore prevents a deep penetration.<sup>12</sup> It is not known if esterases need to act on ALA esters before they enter the heme cycle. Neither is the concentration and stability of such esterases in mice known.

The next surprising finding is that the skin overlaying the tumors, which looks normal, constitutes a much lower barrier for ALA penetration than the skin overlaying healthy tissue (Fig. 1). When applying ALA on tumors, similar amounts of PpIX were produced on remote skin spots as on the spots of ALA application. Furthermore, there was no significant delay in PpIX formation on the remote spots (Fig. 1). This, again, indicates an easy and rapid passage of ALA through skin and tumor tissue to the circulation. At 24 hr, however, the PpIX concentration on the remote spots was

## Topical Application of 5-Aminolevulinic Acid Hexyl Ester and 5-Aminolevulinic Acid to Normal Nude Mouse Skin: Differences in Protoporphyrin IX Fluorescence Kinetics and the Role of the Stratum Corneum<sup>†</sup>

Johanna T. H. M. van den Akker<sup>\*1</sup>, Vladimir Iani<sup>1</sup>, Willem M. Star<sup>2</sup>, Henricus J. C. M. Sterenborg<sup>2</sup> and Johan Moan<sup>1</sup>

<sup>1</sup>Department of Biophysics, Institute for Cancer Research, The Norwegian Radium Hospital, Oslo, Norway and

<sup>2</sup>Photodynamic Therapy and Optical Spectroscopy Programme, Subdivision of Clinical Physics, Department of Radiation Oncology, Daniel den Hoed Cancer Center/University Hospital Rotterdam, The Netherlands

Received 12 April 2000; accepted 10 August 2000

### ABSTRACT

An important limitation of topical 5-aminolevulinic acid (ALA)-based photodetection and photodynamic therapy is that the amount of the fluorescing and photosensitizing product protoporphyrin IX (PpIX) formed is limited. The reason for this is probably the limited diffusion of ALA through the stratum corneum. A solution to this problem might be found in the use of ALA derivatives, as these compounds are more lipophilic and therefore might have better penetration properties than ALA itself. Previous studies have shown that ALA hexyl ester (ALAHE) is more successful than ALA for photodetection of early (pre)malignant lesions in the bladder. However, ALA pentyl ester slightly increased the *in vivo* PpIX fluorescence in early (pre)malignant lesions in hairless mouse skin compared to ALA. The increased PpIX fluorescence is located in the stratum corneum and not in the dysplastic epidermal layer. In the present study, ALA- and ALAHE-induced PpIX fluorescence kinetics are compared in the normal nude mouse skin, of which the permeability properties differ from the bladder. Application times and ALA(HE) concentrations were varied, the effect of a penetration enhancer and the effect of tape stripping the skin before or after application were investigated. Only during application for 24 h, did ALAHE induce slightly more PpIX fluorescence than ALA. After application times ranging from 1 to 60 min, ALA-induced PpIX fluorescence was higher than ALAHE-induced PpIX fluorescence. ALA also induced higher PpIX production than ALAHE after 10 min of application with concentrations ranging from 0.5 to 40%. The results of experiments with the penetration enhancer and tape stripping indicated that the stratum corneum acts a bar-

rier against ALA and ALAHE. Use of penetration enhancer or tape stripping enhanced the PpIX production more in the case of ALAHE application than in the case of ALA application. This, together with the results from the different application times and concentrations indicates that ALAHE diffuses more slowly across the stratum corneum than ALA.

### INTRODUCTION

Administration of 5-aminolevulinic acid (ALA)<sup>†</sup> to cells and tissues results in the production of protoporphyrin IX (PpIX) which can be used clinically as a photosensitizer for photodetection or photodynamic therapy (PDT) of cancer (1–3). Since ALA is a small molecule, it can penetrate through the skin and into tumors after topical application. However, an important drawback of topical application of ALA is that the bioavailability of ALA is limited by diffusion of ALA through biological barriers such as the stratum corneum. Therefore, high ALA doses have to be applied in order to achieve sufficiently high PpIX levels suitable for PDT (4–6). A solution to this problem might be the use of esterified ALA, which is more lipophilic than ALA itself. This higher lipophilicity might result in better penetration into the skin, higher PpIX levels and a more uniform and deeper PpIX distribution.

Several ALA esters have been synthesized and tested *in vitro* in different cell lines (7–10). The long chained ALA esters were more efficient than the short ones in improving PpIX production in cells (9,10). In human and rat skin explant cultures, ALA hexyl ester (ALAHE) proved to be successful in increasing PpIX production after incubation times of 5 and 19 h (11). In this set-up, ALA and its derivatives are absorbed from the medium through the dermis to reach the epidermis, thus resembling more the systemic delivery

<sup>†</sup>Posted on the website on 6 September 2000.

\*To whom correspondence should be addressed at: Center for Photobiology and Photodynamic Therapy, School of Biochemistry and Molecular Biology, University of Leeds, Leeds LS2 9JT, UK. Fax: 44-113-2333017; e-mail: hanneke@bmb.leeds.ac.uk

© 2000 American Society for Photobiology 0031-8655/00 \$5.00+0.00

<sup>†</sup>Abbreviations: ALA, 5-aminolevulinic acid; ALAHE, 5-aminolevulinic acid hexyl ester; ALAME, 5-aminolevulinic acid methyl ester; ANOVA, analysis of variance; HPE-101, 1-[2-(decylthio)ethyl]azacyclopentan-2-one; PDT, photodynamic therapy; PpIX, protoporphyrin IX; SNK, Student–Newman–Keuls.

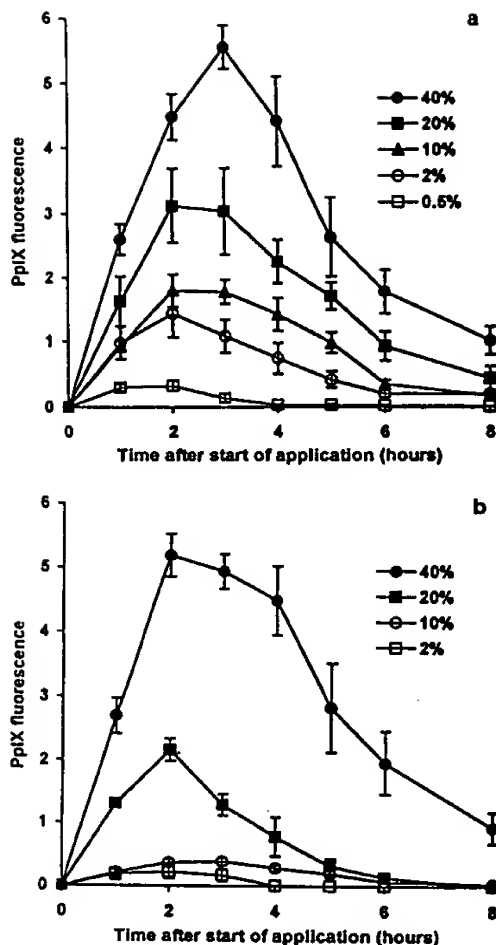


Figure 3. *In vivo* PpIX fluorescence kinetics in nude mouse skin after 10 min (a) ALA or (b) ALAHE application. The concentration of ALA or ALAHE in the cream was 0.5 (open squares), 2 (open circles), 10 (solid triangles), 20 (solid squares) or 40% (solid circles). PpIX fluorescence units are arbitrary, but comparable between all curves. Error bars indicate standard error of the mean.

and ALAHE, possibly slightly earlier for ALAHE than for ALA.

No ALA/ALAHE ratio of the PpIX fluorescence can be calculated for the 0.5 and the 2% application concentration because the PpIX fluorescence levels are zero or too small after application of 0.5 or 2% ALAHE. Table 2 shows the ALA/ALAHE ratios of the PpIX fluorescence for 10, 20 and 40% application. The 10% ALAHE-induced PpIX fluorescence levels are small, which results in a relatively large ALA/ALAHE ratio of the PpIX fluorescence. The ALA/ALAHE ratio of the PpIX fluorescence for the 10% concentration is larger (SNK,  $P < 0.01$ ) than the 20 and the 40% which are not significantly different from each other (SNK).

#### Continuous application

The PpIX fluorescence kinetics during continuous application of ALA and ALAHE up to 14 h after start of the application are shown in Fig. 4. At 24 h after start of the

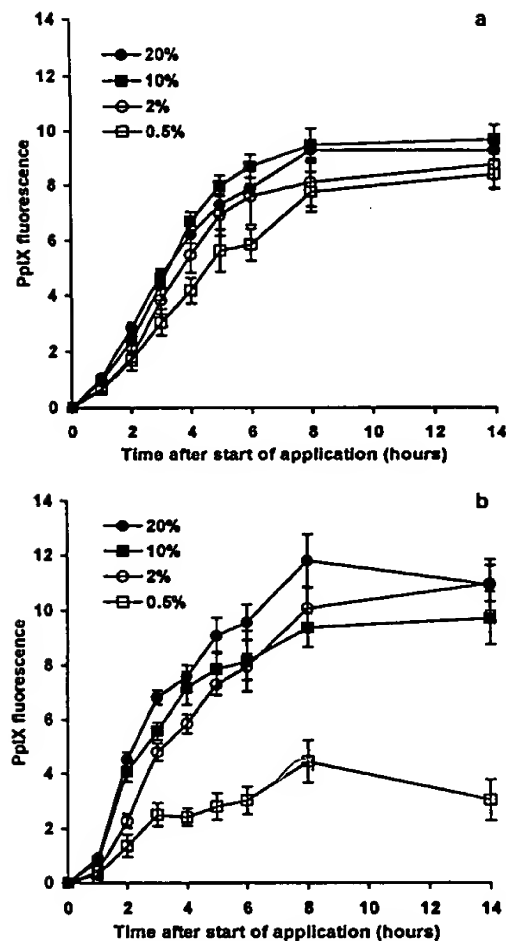


Figure 4. *In vivo* PpIX fluorescence kinetics in nude mouse skin during continuous application of (a) ALA or (b) ALAHE. The concentration of ALA or ALAHE in the cream was 0.5 (open squares), 2 (open circles), 10 (solid squares) or 20% (solid circles). PpIX fluorescence units are arbitrary but comparable among all curves. Error bars indicate standard error of the mean.

application, the PpIX fluorescence has decreased for all concentrations of ALA and ALAHE (data not shown). Only the 0.5% ALAHE-induced PpIX fluorescence is lower than the PpIX fluorescence after 0.5% ALA. For the other concentrations, the ALAHE-induced PpIX levels are slightly higher than the corresponding ALA-induced PpIX levels.

The ALA/ALAHE ratios are shown in Table 2 and the ALA/ALAHE ratio for 0.5% application is significantly higher than the other ratios (SNK,  $P < 0.01$ ). The 2, 10 and 20% ALA/ALAHE ratios are the same (SNK).

#### Addition of penetration enhancer

Figure 5 shows that the penetration enhancer HPE-101 changes the kinetics of ALA- and ALAHE-induced PpIX. When ALA is applied for 60 min in the presence of HPE-101, the maximum fluorescence is reached at the same time point (3 h after start of application) and has the same level as with ALA application alone (Fig. 5a). However, HPE-101

# ALA and ALA hexyl ester-induced protoporphyrin synthesis in chemically induced skin tumours: the role of different vehicles in improving photosensitization

A Casas<sup>1</sup>, C Perotti<sup>1</sup>, H Fukuda<sup>1</sup>, L Rogers<sup>2</sup>, AR Butler<sup>2</sup> and A Batlle<sup>1</sup>

<sup>1</sup>Centro de Investigaciones sobre Porfirinas y Porfirias (CIPYP), CONICET and Department of Biochemistry, School of Sciences, University of Buenos Aires, Argentina; and <sup>2</sup>School of Chemistry, University of St Andrews, St Andrews, Fife, UK

**Summary** Exogenous administration of 5-aminolevulinic acid (ALA) is becoming widely used to enhance the endogenous synthesis of Protoporphyrin IX (PpIX) in photodynamic therapy. We analysed porphyrin formation in chemically induced squamous papillomas, after topical application of ALA and ALA hexyl ester (He-ALA) administered in different formulations, as well as the pattern of distribution in the internal organs, and the synthesis of porphyrins in distant tumoural and normal skins. A lotion formulation containing DMSO and ethanol was the best vehicle for topical ALA delivery to papillomas, whereas cream was the most efficient formulation for He-ALA application. Similar porphyrin concentration can be accumulated in the skin tumours employing either ALA or He-ALA delivered in their optimal formulations. The use of cream as a vehicle of both ALA and He-ALA, induces highest porphyrin tumour/normal skin ratios. The main advantage of using He-ALA is that porphyrins synthesized from the ester are more confined to the site of application, thus inducing low porphyrin levels in normal skin, liver, blood and spleen, as well as in papillomas distant from the point of application, independently on the vehicle employed, so reducing potential side effects of photodynamic therapy. © 2001 Cancer Research Campaign <http://www.bjcancer.com>

**Keywords:** ALA; ALA esters; photodynamic therapy; squamous papillomas

Photodynamic therapy (PDT) is a very promising antineoplastic treatment, specially for superficial skin tumours, based on the preferential accumulation of a photosensitizer in malignant tissue after its administration. Light of an appropriate wavelength illumination excites the photosensitizer and subsequent photoactivation results in the release of cytotoxic substances such as singlet oxygen or free radicals which are responsible for the destruction of PDT treated tissue (Dougherty et al, 1984).

At the beginning of the 1990s 5-aminolevulinic acid (ALA), a precursor of the endogenous photosensitizer protoporphyrin IX (PpIX), began to be used to induce the selective accumulation of tetrapyrroles endogenously synthesized in the tumour tissue (Kennedy and Pottier, 1990; Fukuda et al, 1992).

ALA-mediated photodynamic therapy (ALA-PDT) shows promise in skin precancerous stages such as solar keratoses, Bowen's disease, and tumours including basal cell carcinomas, Paget's disease and squamous cell carcinomas (Kurwa and Barlow, 1999). Nonmalignant skin pathologies such as psoriasis (Boehncke et al, 1994) and actinic keratoses, among others, have also been treated by ALA-PDT (Fritsch et al, 1998).

However, the fact that ALA is a zwitterion at physiological pH and therefore has low lipid solubility, limits its clinical application. ALA poorly passes through biological barriers such as stratum corneum of the skin and cellular membranes. Hence, ALA-induced PpIX formation is often restricted to superficial tissue

layers because of both inhomogeneous and partial tissue distribution in deeper-lying or nodular lesions (Peng et al, 1995).

It is expected that more lipophilic ALA prodrugs can cross cellular membranes more easily than ALA. After reaching the site of action, the prodrug is enzymatically converted to ALA, which in turn is converted into PpIX. Kloek et al (1996, 1998), Gaullier et al (1997) and Casas et al (2001) found that long chain ALA esters are taken up, hydrolysed to the free acid and transformed into PpIX with higher efficiency than ALA, leading to higher photosensitizer levels both in vivo and in vitro.

Some ALA esters have been used in normal mouse skin (Peng et al, 1996) and in human basal cell carcinomas (Peng et al, 1995), and a higher and more homogeneous tissue distribution was produced when compared to that of free ALA-induced porphyrins.

Van den Akker et al (2000a) using hairless mice showed that ALA pentyl ester produces only slightly more PpIX than ALA in UVB-induced (pre)cancerous skin lesions, while in normal skin, porphyrin levels were equal from both ALA compounds. The same authors (Van den Akker et al, 2000b), found in normal mice skin that ALA hexyl ester was not better than ALA in synthesizing PpIX. In both studies, ALA and ALA esters were delivered in a cream formulation.

Another approach aimed at improving the pro-drug skin penetration is the use of different vehicles and enhancers for their administration (Casas et al, 1999a, 2000a).

The aim of this work was to modulate and optimize porphyrin accumulation and tumoural selectivity, employing different vehicles and the penetration enhancer DMSO, in the delivery of ALA and ALA hexyl ester using a murine skin tumour model.

Due to the scarcity of appropriate animal models to study the effectiveness of ALA-PDT, we employed skin tumours induced in SENCAR mice by two-stage initiation/promotion protocol.

Received 6 June 2001

Revised 17 August 2001

Accepted 17 September 2001

Correspondence to: A Batlle, Viamonte 1881 10A, 1056 Buenos Aires, Argentina

Initiation of tumorigenesis by the carcinogen 7,12-dimethylbenz[a]anthracene (DMBA), followed by continuous treatment with phorbol ester promoters, such as 12-*o*-tetradecanoylphorbol-13-acetate (TPA), results in the formation of premalignant papillomas (Burns et al, 1983).

In this paper we have analysed porphyrin formation in chemically induced squamous papillomas, after topical application of ALA and He-ALA administered in different formulations, as well as the pattern of porphyrin distribution in the internal organs, and the synthesis of porphyrins in distant tumoural and normal skins.

## MATERIALS AND METHODS

### Animals and drugs

Six- to eight week-old female SENCAR mice were provided by the Comisión Nacional de Energía Atómica Argentina (CNEA). Animals were housed separately, acclimatized before use, subjected to a 12 h light/ 12 h dark cycle and fed with mice chow (Molinos Río de la Plata, Argentina), and water *ad libitum*.

ALA, 7,12-dimethylbenz[a]anthracene (DMBA) and 12-*o*-tetradecanoylphorbol-13-acetate (TPA), were purchased from SIGMA Chem Co., St Louis, MO, USA. ALA hexyl-ester (He-ALA) was synthesized according to the method previously described by Casas et al (1999b). All other chemicals were of analytical grade.

### Induction of tumours in SENCAR mice skin

Chemical carcinogen-induced benign squamous papillomas were developed employing the following protocol: 6–8-week-old female SENCAR mice were shaved. Only those animals in resting phase of the hair cycle were used in the tumour protocol and treated topically on the dorsal shaved area with a single topical application of DMBA (20 µg in 0.2 ml acetone/mouse). One week later, animals were treated once a week during 4 months with TPA (2 µg in 0.2 ml acetone/mouse) to obtain papillomas. Using this protocol, after 16 weeks, about 50% of the mice treated had an average of three to four tumours per mouse. Few tumours were randomly verified histopathologically as squamous papillomas. Only animals with closely matched tumour size were employed.

Animals were treated in accordance with guidelines established by the Animal Care and Use Committee of the Argentine Association of Specialists in Laboratory Animals (AADEALC), in full accord with the UK Guidelines for the Welfare of Animals in Experimental Neoplasia (UKCCCR, 1988).

### Preparation and administration of ALA formulation

Saline solution: the hydrochloric salt of ALA and He-ALA were dissolved in saline at a concentration of 150 and 225 mg/ml respectively immediately before use. Saline/ethanol: 40% ethanol in saline. Saline/DMSO: 10% dimethylsulfoxide in saline. Saline/DMSO/ethanol: 10% DMSO and 40% ethanol in saline. Cream: ALA and He-ALA were daily prepared at 20% and 30%, respectively, in an oil in water emulsion cream (Genargen, Argentina). A total amount of 15 mg ALA and 22.5 mg He-ALA per mouse was applied in order to obtain an equimolar free ALA concentration for all formulations. In tumour bearing mice, ALA and He-ALA in different formulations were topically applied over a single papilloma surface (weighing approximately 100 mg) plus a 3 mm peritumoural

margin rubbing in the surface during a period of 5 min, time at which no vestiges of either cream or lotion are visible. Before any application, mice received mild anaesthesia (Fentanyl and Diazepam). All formulations were applied under occlusive dressing to avoid distribution of the compounds.

For porphyrin determinations in both skin and internal organs, mice having 3–4 papillomas were employed. The peritumoural skin (3 mm margin of skin surrounding the treated papilloma) was carefully removed from the tumour itself. The rest of the non-treated papillomas were pooled for porphyrin extraction. Samples of distant normal skin were excised from the ventral area of the mice.

In experiments aimed at studying porphyrin distribution as a function of the distance of ALA application, 7–8 tumour-bearing mice were employed. In this case, a single papilloma was topically treated as explained above and the distant papillomas were processed separately for porphyrin measurement. In tumour-free mice, ALA or He-ALA was applied and rubbed in over an area of 1.76 cm<sup>2</sup> in diameter of normal skin, and another three distant normal skins were excised from different consecutive zones. All the skins were shaved before processing.

Optimal time and precursor concentrations were chosen from previous work (Casas et al, 2000b).

### Tissue porphyrin extraction

After 3 hr of ALA or He-ALA topical application, animals were sacrificed. Before killing, mice were injected with heparin (0.15 ml, 1000 UI) and after sacrifice, they were perfused with 200 ml of sterile saline. The tissue samples were homogenized in a 4:1 solution of ethyl acetate: glacial acetic acid mixture. Blood samples were heparinized and vigorously vortexed with the same extraction solvents. The mixtures were centrifuged for 30 min at 3000 g, and the supernatants were added with an equal volume of 5% HCl. Extraction with HCl was repeated until there was no detectable fluorescence in the organic layer. The aqueous fraction was used for the determination of porphyrins. For fluorometric determination, a Shimadzu RF-510 spectrofluorometer was used, with an emission wavelength of 604 nm and an excitation wavelength of 406 nm, employing a PpIX reference standard.

### Statistical analysis

The unpaired *t*-test was used to establish the significance of differences between groups. Differences were considered statistically significant when *P* < 0.05. Three mice per group were employed.

## RESULTS

Figures 1 and 2 show porphyrin synthesis in treated papillomas, distant papillomas, normal skin surrounding papillomas and normal distant skin after topical application of ALA and He-ALA respectively, applied in different formulations. The cream vehicle is twice as efficient as saline lotion at inducing porphyrin synthesis in papillomas treated with ALA (Figure 1). However, by adding ethanol, or DMSO and ethanol to the saline formulation, but not DMSO alone, tetrapyrrole accumulation can be significantly increased when compared with saline lotion (*P* = 0.001 and *P* = 0.0007 respectively). Saline/DMSO/ethanol vehicle induces 3.5 times more porphyrin accumulation than saline alone. A completely different pattern is observed in papillomas treated with He-ALA



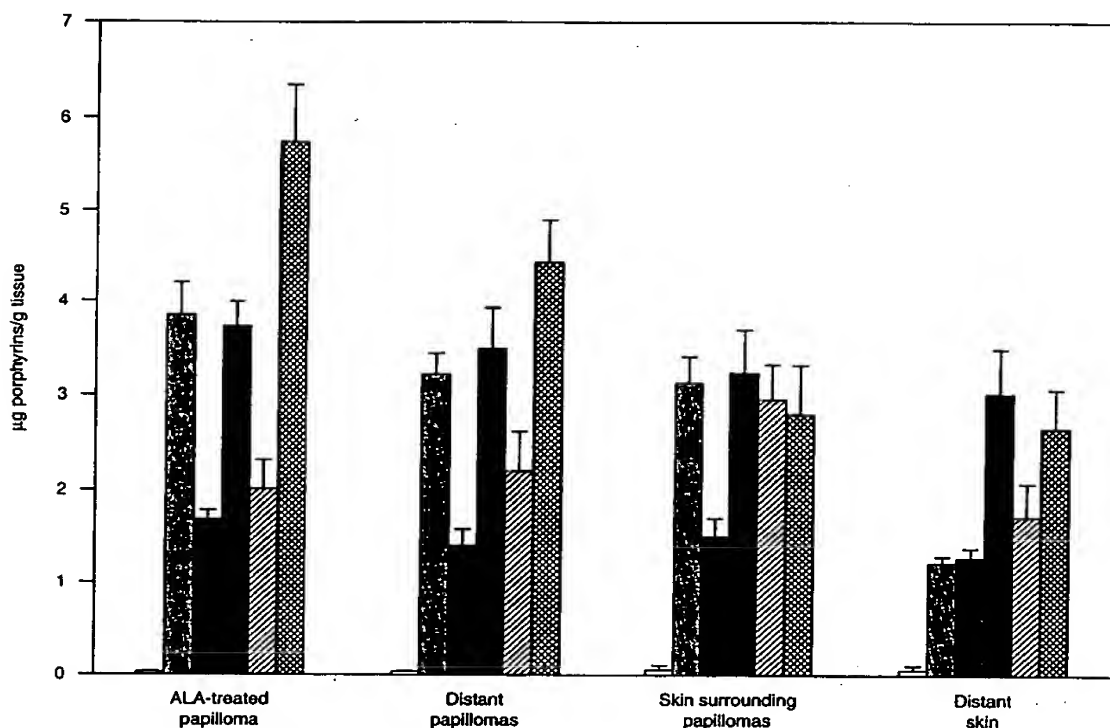


Figure 1 Porphyrin synthesis in skin of tumour-bearing mice after topical application of ALA. Porphyrins were determined 3 h after ALA application in different vehicles: (□) control without any treatment, cream (■), saline lotion (▤), saline/ethanol (▨), saline/DMSO (▧) and saline/DMSO/ethanol (▩). Bars represent porphyrin values (mean  $\pm$  SD)

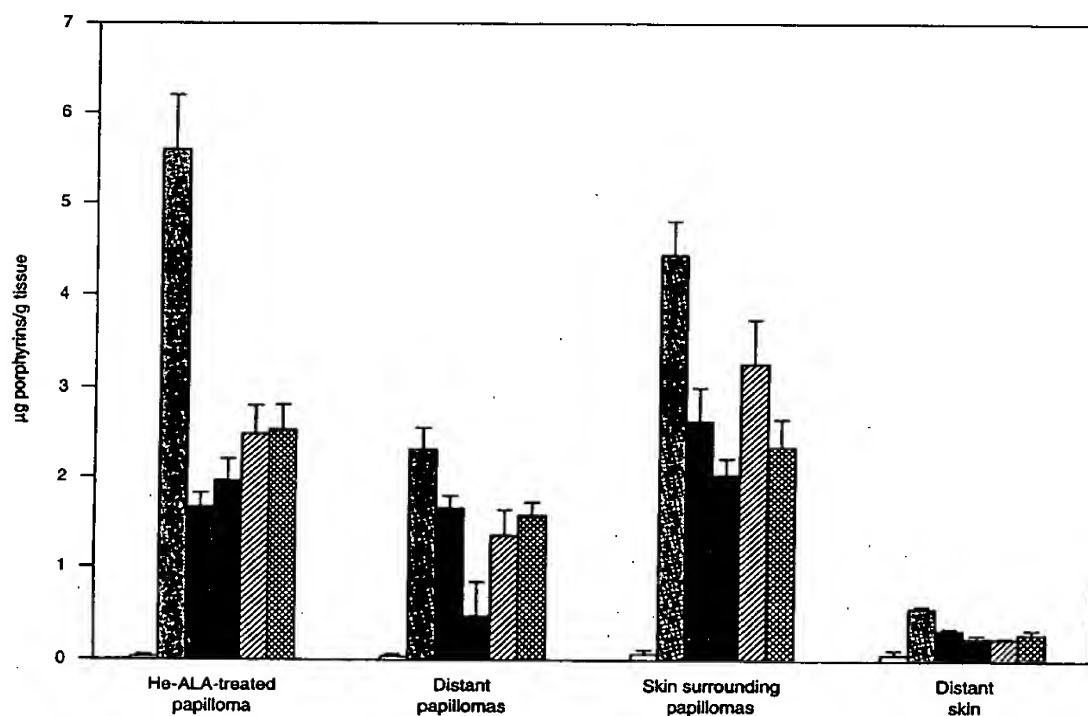


Figure 2 Porphyrin synthesis in skin of tumour-bearing mice after topical application of He-ALA. Porphyrins were determined 3 h after He-ALA application in different vehicles: (□) control without any treatment, cream (■), saline lotion (▤), saline/ethanol (▨), saline/DMSO (▧) and saline/DMSO/ethanol (▩). Bars represent porphyrin values (mean  $\pm$  SD)